ANALYSIS OF SEDIMENT DYNAMICS IN INTENSIVELY MANAGED LANDSCAPES

BY

MINGJING YU

DISSERTATION

Submitted in partial fulfillment of the requirements
for the degree of Doctor of Philosophy in Geography
in the Graduate College of the
University of Illinois at Urbana-Champaign, 2018

Urbana, Illinois

Doctoral Committee:

Professor Bruce Rhoads, Chair and Director of Research
Professor Murugesu Sivapalan
Professor Thanos Papanicolaou, University of Tennessee, Knoxville
Associate Professor Alison Anders

ABSTRACT

The flux of fine sediment within agricultural watersheds is an important factor determining the environmental quality of streams and rivers. Human activity has significantly altered the hydrological and biogeochemical cycles within terrestrial and aquatic environments through agricultural intensification, tile drainage installation, and urban development. The study of watershed-scale sediment dynamics is of great value for understanding and predicting the response of sediment dynamics to intensive human impact and is crucial to developing management strategies for reducing the vulnerability of the ecosystem to future changes. The primary objective of this dissertation is to investigate sediment sources, sediment transport, and sediment yield in an intensively managed agricultural landscape. This objective was accomplished by combining of field sampling and measurements, laboratory analysis, sediment fingerprinting study, statistical analysis and modeling exploration in the Upper Sangamon River Basin, Illinois.

The relative contributions from cropland, grassland, forested floodplain, upper grazed floodplain, and lower grazed floodplain to the suspended sediment in the stream are evaluated by sediment fingerprinting techniques. The grazed areas of the floodplain are identified as the primary source of fine suspended sediment within the headwaters of the Sangamon River. Erosion of the floodplain both by surface runoff and by streambank erosion contribute to the production of almost all fine sediment sampled within the stream system. The results are consistent both for event and aggregated samples and for large and small events. The fingerprinting results are also consistent with visible and historical evidence of active erosion of grazed areas of floodplain upstream from the in-stream sampling location. Evidence from field

reconnaissance and inspection of aerial photography supports the conclusion that cattle grazing plays an important role in accelerating floodplain and streambank erosion.

The relationships between rainfall, discharge, and suspended sediment concentration are examined by sediment rating curve approach and hysteresis analysis. Sediment rating curves developed for three sites along the Sangamon River all have a peaked pattern with a transition point at geometric mean of discharge, indicating suspended sediment load in the stream is far below the stream transport capacity during high flows. Spatially, suspended sediment concentrations tend to become more coincident with the seasonality of rainfall and discharge with increasing watershed size and the mean suspended sediment concentration decreases as drainage area increases. Temporally, the SRCs developed for the rising and falling limbs of hydrographs and the four sampling seasons also exhibit the same trends, suggesting that these trends are not scale-dependent. The peaked pattern of sediment rating curve is most apparent in sediment rating curve developed on discharge and sediment data collected in summer, which means the limitation of sediment supply is most significant in summer.

Sediment fluxes in modern times and before European settlement is investigated by using a semi-distributed, coupled hydrologic and sediment model. Intensive agricultural activities since European settlement have increased sediment supply and enhanced suspended sediment load in stream, and also influence re-distribution of detached sediment within the system. The percent of sediment supply from each source to the total amount of mobilized sediment significantly changed from 1840s to 2000s, and the agricultural uplands have become the major source of suspended sediment in the stream. The model estimates that sediment supply from uplands increased 11-fold from the 1840s to 2000s, and sediment yield in 2000s is 9 times of that in 1840s. A higher percent of sediment is transported out of the system and deposited in the channel

in 2000s than in 1840s. Suspended sediment load has increased more rapidly than floodplain sedimentation. The re-distribution of detached sediment is also influenced by the presence of built levees and extended channel network. With the increased sediment supply and decreased percent of floodplain sedimentation, sediment delivery ratio for the entire watershed only increased 4%.

In conclusion, the integrated results from field, statistical and modeling studies advance the knowledge and understanding of sediment supply, delivery, and export in intensively managed landscapes. The findings also inform management strategies aimed at reducing the vulnerability of this landscape to ongoing human impact.

ACKNOWLEDGEMENTS

The work leading toward the completion of my dissertation has been a journey unlike any other in my lifetime. There have been many people who have helped and supported me.

I would first like to thank my advisor, Dr, Bruce Rhoads for his insight to the design of this dissertation study, careful guidance through all stages of my research, and support and encourage. He enabled me to think critically and taught me how to be a researcher. His passion for research inspired me and his knowledge helped me throughout my PhD study over the past four years.

I gratefully acknowledge my Ph.D. committee members, Prof. Murugesu Sivapalanan, Prof. Thanos Papanicolaou and Prof. Alison Anders for serving on my doctoral committee and providing valuable feedback on my research.

I owe gratitude to the many that have helped me collect the data presented herein: Quinn Lewis, Umar Muhammad, Laura Keefer, Donald Keefer, Conor Neal, Kimberly Attig, and Andrew Stumpf. I would like to thank Hongyi Li and Sopan Patil for their help in modeling. I would also like to thank Susan Etter and Matthew Cohn for their help in my study and research in the University of Illinois.

Special thanks to my parents Liping and Yonghua for their unending love and support. Thanks to my husband Hao for 10-years happiness and joy. Thanks to my parents-in-law Haiyan and Xueping for your support and help. Thank you my baby Heather, never have I felt one year could be so long and also so short. Thank you my baby Heidi, I am so looking forward to seeing you. I dedicate my dissertation to the memory of my grandfather — I miss you so much.

This research is partially supported by the NSF Grant # EAR-1331906 for the Critical Zone Observatory for Intensively Managed Landscapes (IML-CZO), a multi-institutional collaborative effort.

To my family, with love

TABLE OF CONTENTS

CHAPTER 1

INTRODUCTION

1.1 Motivation

As the awareness of water pollution, eutrophication and other water-related environmental concerns grows, the significance of sediment in the transport of nutrients and contaminants from agricultural areas to streams has received increasing attention. Human agency has been introduced as a flux in sediment budgets that can alter regimes of sediment transport, and causing dramatic morphodynamic changes (Urban and Rhoads, 2003). Human activity has significantly altered the hydrological and biogeochemical cycles within terrestrial and aquatic environments through agricultural intensification, tile drainage installation, and urban development. In intensively managed landscapes (IMLs), human activity has profound impact on sediment dynamics by disturbing soil structure, increasing nutrient loadings, and reducing storage and residence time of sediment (Gregory, 2006). Sediment generation and transport processes, which influence the mass and energy distribution within a watershed, are often accelerated under profound human impact. This human-triggered acceleration of sediment flux affects the capacity of landscapes to adapt to future changes associated with ongoing human activity or with extreme weather events caused by global climate change. A broad range of sustainable ecosystem services on which human populations depend are also impaired by elevated sediment fluxes. Therefore, the study of watershed-scale sediment dynamics is of great value for understanding and predicting the response of sediment dynamics to intensive human impact.

The need for understanding watershed-scale sediment dynamics is not new. However, a complete, predictive understanding of how a suite of physical, chemical, biological and human

factors that govern the rates of generation and transport and the interactions among these factors have yet to be achieved (de Vente et al., 2013; Belmont et al., 2014). The effect of human impact on sediment dynamics in IMLs at the watershed level is not well quantified (Maalim, et al., 2013): characterization of spatial and temporal distribution of human-modified sediment sources and transport pathways in IMLs is incomplete and linking sediment dynamics to human impact still remains a challenge. There is also a critical gap in predicting temporary storage and re-suspension within the channel–floodplain complex (Belmont et al., 2014; Pizzuto et al., 2014). Moreover, a challenging task in the study of sediment dynamics is to translate the general understanding of processes into predictive models.

This dissertation investigates sediment dynamics in an intensively managed agricultural landscape to provide insight into the factors that control sediment generation, transport and yield at the watershed scale. Through field measurements and monitoring, statistical analysis, a sediment rating curve approach, hysteresis analysis, sediment fingerprinting techniques, and simulation modeling, this dissertation reveals the controlling factors that govern sediment generation, transport, and yield at the watershed scale.

1.2 Research questions/objectives

The primary objective of this dissertation is to estimate and predict the dynamics of fine sediment flux at the watershed scale in an intensively managed landscape. The research questions in this dissertation are

R1) Where does fine (< 0.063 mm) suspended sediment in the headwater of IMLs come from, and how do land use and channel morphology influence the contributions from various sediment sources?

R2) How does the flux of fine sediment vary temporally and spatially within an IML watershed, and what factors control the spatial and temporal heterogeneity of fine-sediment export?

R3) How did watershed-scale fine sediment dynamics change under human impact and how will watershed-scale fine sediment dynamics change under ongoing human impact?

The research questions are addressed using a combination of methods including the use of sediment fingerprinting techniques, statistical analysis, sediment rating curve approach, hysteresis analysis and coupled hydrologic and sediment modeling approach. By examining these questions, this dissertation provides insight into the dynamics of sediment within intensively managed agricultural landscapes. Theoretically, exploring watershed-scale sediment dynamics enriches understanding of sediment movement within intensively managed landscapes and the response of sediment systems to human modification of landscapes. Practically, by producing a predictive understanding of sediment dynamics in IMLs, this dissertation provides information for mitigating environmental impacts of human activity.

1.3 Scientific background

To provide proper context for this dissertation, it is important to outline the key components comprising the current conceptual understanding of watershed-scale sediment dynamics. A suite of physical, chemical, biological and human factors govern rates of sediment generation and transport. The use of sediment fingerprinting techniques, statistical analysis and modeling approach provides a suitable framework for characterizing and predicting watershed sediment dynamics.

1.3.1 Watershed-scale sediment dynamics

The movement of sediment influences the mass and energy distribution within a watershed and thus provides the basic process-form link in fluvial geomorphology. The movement of sediment from hillslopes to the watershed outlet involves the various mechanisms of erosion, transport, and deposition. Sediment mobilization, transport, storage and yield within a watershed are characterized by considerable spatial and temporal variability (Walling, et al., 1998). The dominant processes vary with climate, topography, soil type, land use, bedrock, vegetation, and management practices.

The two most important watershed sources of sediment are typically upland hillslope erosion and stream bank erosion, when the material is eroded by flow or introduced into suspension after bank collapse (Gellis and Walling, 2011). On hillslopes, rill and sheet erosion are important, and affected by climate, topography, soil erodibility and transportability, vegetation cover, land use, subsurface effects, tillage roughness and tillage pattern (Foster, 1982). Four major processes accomplish sediment removal and transport on hillslopes: detachment by raindrop impact, detachment by runoff, transport by raindrop splash, and transport by runoff (Aksoy and Kavvas, 2005). For the sediment entrained by flow, the inception of motion was found to be dependent on both the slope and the Reynolds number of the flow over the slope (Lau and Engel, 1993). On floodplains, migration of headcuts into material that was deposited from overbank events is a primary erosion process (Fox and Papanicolaou, 2007). In the channel, erosion consists of streambed and stream-bank erosion. The entrainment of sediment from the channel bed depends on the physical properties of particles and flow condition. Sediment is entrained from channel bed when the shear stress exerted by the flow exceeds the critical value for a given size of particle. Bank erosion involves bank failure and

hydraulic action (Thorne and Tovey, 1981; Rinaldi and Darby, 2007; Simon et al., 2000; Wilson et al., 2012). Bank failure often occurs during recessional stages of flow events, when water drains out of previously inundated banks, thereby creating positive pore pressure. The bank erosion initiated by hydraulic action in meandering rivers tends to be concentrated at the outer bank downstream of the bend apex where velocities are highest, while point bars develop at inner bank with material supplied by longitudinal and transverse currents. Progressive erosion at cutbanks and deposition at point bars lead to lateral and downstream migration of meandering river channels.

Two major factors control sediment transport in the rivers: sediment supply and transport capacity of the flow (Gao et al., 2013; Gran et al., 2013). For a given flow, a maximum amount of sediment can be transported by the flow. The maximum amount is referred to as the sediment carrying capacity. Streams adjust to accommodate the sediment load and discharge. When the capacity of flow decreases, shear velocity falls below the setting velocity of a particle and deposition of particles begins (Vanoni, 1975). Generally, the amount of material transported by flow is less than its capacity and most of fine particles supplied to the streams can be carried in suspension. Therefore, the transport of the fine particles is mostly controlled by sediment supply rate rather than transport capacity of the flow (Asselman, 2000). However, the transport of coarse material is capacity-limited and intermittent; they are usually transported during transport-effective events that exceed the threshold for entrainment of this material.

Sediment is routed through landscapes and river network in a non-uniform manner, and erosion and deposition of sediment across a watershed are temporally and spatially variable processes (Fox and Papanicolaou, 2007). Many watershed variables such as climate, vegetation, topography, soil type, and human disturbances determine the sources, fate, and transport

processes of sediment. The precise link between upstream erosion, sediment mobilization and downstream sediment yield involves many uncertainties due to the nonlinearity and discontinuous nature of sediment processes. Spatially, erosion may occur on the soil with high edibility. Temporally, the erosion process is episodic, including first flushing of loose surface material at the beginning of a storm. Intermediate storages also increase the uncertainties of sediment mobilization and yield (Walling and Collins, 2008).

Human activities such as intensive agriculture and land drainage have significant impact on watershed-scale sediment dynamics. Sediment studies conducted in various human-modified watersheds show that agricultural practices disturb soil structure, accelerate soil erosion, and reduce storage and residence time of sediment (Costa, 1975; Trimble, 1983; Gregory, 2006; Belmont et al., 2011). Human agency has therefore been introduced as a flux in sediment budgets causing altered regimes of sediment generation and transport, and dramatic morphodynamic changes (Urban and Rhoads, 2003). The characterization of sediment dynamics under human impact at the watershed scale requires an understanding of the connectivity between sediment generation within the watershed and its transport within the river channel network (Verstraeten et al., 2007; Medeiros et al., 2010).

1.3.2 Sediment fingerprinting techniques

Information concerning sediment provenance has been identified as an essential prerequisite for understanding watershed-scale sediment dynamics, particularly for fine (< 0.063 μm) sediment (Walling et al., 1993). Sediment fingerprint techniques are a valuable alternative to traditional direct monitoring for identifying sediment sources in a watershed and allocating the amount of sediment contributed by each source through the use of natural tracer technology with a combination of field data collection, laboratory analyses of sediments, and statistical modeling

techniques (Davis and Fox, 2009). The science of sediment fingerprinting has been evolving rapidly over the past decade. It has been poised to improving the understanding of sediment sources, as well as the routing of sediment through watersheds since 1980s (Rhoton et al., 2005; Walling, 2005; Collins et al., 1998; Mukundan et al., 2010; Belmont et al., 2014). The use of sediment fingerprinting approach can generate valuable information on the relative importance of individual potential sources contributing to the suspended sediment flux of a river. Such information is valuable not only for linking upstream sediment sources and downstream sediment yield but also for assessing sediment control projects (Walling and Collins, 2008).

Sediment fingerprint techniques are based on the premise that the variations in sediment properties directly reflect spatial and temporal variations in the contributions of sediment from distinguishable sources (Collins et al. 1998). The fingerprints in the potential sources are expected to vary as a function of soil, vegetation and land use. Thus the suspended sediment collected at the basin outlet can be considered as a linear combination of the contributions from different sediment sources. Therefore, the potential sediment sources can be reliably distinguished by their 'fingerprints', the provenance of the sediment can be established by comparing its properties with those of the sources, using a mixing model coupled with uncertainty analysis. The sediment fingerprinting procedures include statistical verification of the discrimination based on tracer properties and the use of multivariate mixing models to estimate the relative contributions of individual sources (Collins et al., 1998; Walling et al., 2001; Gellis and Walling, 2011; Smith and Blake, 2014).

The first area of development in sediment fingerprint techniques involved the selection of diagnostic properties that can discriminate a number of potential sources (Walling, 2005). The fingerprints are physical or chemical properties of sediment. Those fingerprints can be generally

categorized as conservative and non-conservative tracers. The conservative tracers' defining characteristic does not change appreciably over sediment routing timescales (Belmont et al., 2014); while the non-conservative tracers' distinguishing characteristics change during sediment transport, deposition, and re-suspension processes. Conservative tracers are usually used to identify sediment sources throughout the watershed geographically. Various conservative tracers have been used as sediment fingerprints to quantify the magnitude of erosion and partition suspended sediment: trace elements, organic matter content, and stable isotope geochemistry (Collins et al., 1998; Walling and Amos, 1999; Wilson et al., 2003; Walling, 2005; Fox and Papanicolaou, 2008) Other properties that are related to different sediment sources have also been used as sediment fingerprints: magnetic susceptibility (Yu and Oldfield, 1989; Slattery et al., 1995), clay mineralogy (Gingele and De Deckker, 2005), particle size (Walling and Amos, 1999), and colorimetric properties (Grimshaw and Lewin, 1980).

Non-conservative tracers are usually used to distinguish sediment derived from surface and subsurface sources (Walling and Woodward, 1992). Temporal storage of sediment in floodplain during flood events may convolute the sediment fingerprinting signature of alluvial floodplain sources. The suspended sediment derived from floodplain can be deposed sediment that eroded from hillslopes in previous flood events. Fallout radionuclides (137Cs, 210Pb, and 210Pbe) have often been used to differentiate sediment derived from surface soil erosion from that of near-channel fluvial erosion, which can aid in the understanding of channel-floodplain processes (Belmont et al., 2014). Fallout radionuclides are commonly rapidly and strongly adsorbed by soil particles upon reaching the watershed surface as fallout, thus their subsequent redistribution proves a means of tracing sediment mobilization, transfer and deposition (Ritchie and Mchenry, 1990; Zapata, 2012). Assessment of the post-fallout redistribution of the

radionuclides offers a basis for documenting time-integrated rates and patterns of sediment redistribution and storage within the watershed system, especially for floodplain intermediate storage and retention of sediment in floodplain.

Sediment tracing approaches are most applicable where fine sediment is a problem (Gellis and Walling, 2011). Fine suspended sediment dominates the flux of solid material eroded from hillslope, transported by streams, and deposited in sinks (Meade, et al., 1990), and it is also a vector for the transport of nutrients and organic contaminants, such as phosphorus (P), pesticides, PCBs, heavy metals and pathogens (Walling, 2005). Thus fine sediments are disproportionately responsible for degradation of surface waters (Whiting et al., 2005). Therefore, understanding the provenance of fine sediment is a prerequisite for determining the fate of nutrients and other pollutants in the environment (Whiting et al., 2005). Reduction of fine sediment load is critical to reducing contaminants and nutrient transport (Gellis and Walling, 2011).

1.3.3 Watershed sediment dynamics modeling

With the rapid developments in numerical methods for fluid mechanics and sediment transport, computational modeling has become an effective tool for studying sediment in various environments (Papanicolaou, et al., 2008). Over the past three decades, a large number of computational sediment transport models have been developed and used to determine upland erosions or estimate the in-channel processes (Fan, 1988; Papanicolaou et al., 2008).

By predicting sediment sources, fluxes and sinks, watershed-scale sediment transport models provide a potentially powerful tool for estimating sediment supply and yield. Various watershed-scale sediment transport models have been developed for diagnosing and predicting the sediment movement within watersheds: SEDNET (Prosser et al., 2001), USLE (Wischmeier

and Smith, 1965), ANSWERS (Beasley et al., 1980), KINEROS (Smith, 1981), WEPP (Nearing et al., 1989), EUROSEM (Morgan et al., 1998), AGNPS (Young et al., 1989), and SHETRAN (Ewen et al., 2000). The choice of a certain model for solving a specific problem depends on the nature and complexity of the problem itself, the chosen model capabilities to simulate the problem adequately, data availability for model calibration, data availability for model verification, and overall available time and budget for solving the problem (Wu, 2008). Modeling approaches have faced several challenges when applied to a range of watershed scales. Nature of sediment processes is dependent upon watershed size and time scales. Due to the large variability of environmental variables over spatial and temporal scales, the source, flux, and sinks are difficult to predict and model precisely. As watershed area increases, the opportunity of storage also increases, so the accurate estimation of rate and flux is limited to small watersheds. In response to these challenges, watershed sediment models can be modified to incorporate independent information on sediment sources and sinks, dominant mechanism, and rates of sediment erosion and deposition.

1.4 Outline of this dissertation

Understanding watershed-scale sediment transport is a prerequisite for implementing best management practices for watersheds. To answer the research questions, field measurements and monitoring, statistical analysis, sediment rating curve approach and hysteresis analysis, fingerprinting techniques, and modeling approach are combined as study framework. It includes a top-down approach by analyzing hydrological and sediment data and a bottom-up approach by simulating watershed-scale sediment dynamics. Chapter 2 explores the suspended sediment provenance of Saybrook watershed, IL, through using sediment fingerprinting techniques. It illustrates the identification of potential sediment sources in an agricultural landscape and the

process of evaluating the relative contributions from potential sediment sources to the suspended sediment through a two-step statistical process. It also discusses the how agricultural activities, especially cattle grazing, impact the provenance of suspended sediment. Chapter 3 is aimed at exploring the relationship between precipitation, water discharge and suspended sediment concentration for three sediment sampling sites Saybrook, Mahomet, and Monticello along a lowland agricultural river in an intensively managed agricultural landscape at seasonal, intra-event and event scales and revealing the complex interaction between sediment transport and storm patterns. With the results of sediment source tracing and suspended sediment data analysis, chapter 4 applies a semi-distributed hydrologic and sediment model, THREW model, to simulate and compare pre-settlement and modern times sediment dynamics at Upper Sangamon River Basin, IL. It focuses on comparing sediment generation on hillslope and channel, entrainment and deposition processes in channels, floodplain sedimentation, and suspended sediment yields between pre-settlement and modern times. Through a model-based evaluation of scaling issues related to sediment flux, it reveals the impact of human activities, especially agricultural activities and channelization, on sediment dynamics at watershed scale. Chapter 5 is the concluding chapter which summaries the major findings from this dissertation and outlines future opportunities for extensions of this work.

1.5 References

Asselman, N. E. M. (2000). Fitting and interpretation of sediment rating curves. *Journal of Hydrology*, *234*(3–4), 228–248. http://doi.org/10.1016/S0022-1694(00)00253-5

Beasley, D. B., L. F. Huggins, & E. J. Monke (1980). ANSWERS: A model for watershed planning, Trans. ASAE, 23(4), 938–944.

Belmont, P., Willenbring, J. K., Schottler, S. P., Marquard, J., Kumarasamy, K., & Hemmis, J. M. (2014). Toward generalizable sediment fingerprinting with tracers that are conservative and nonconservative over sediment routing timescales. *Journal of Soils and Sediments*, *14*(8), 1479–1492. http://doi.org/10.1007/s11368-014-0913-5

Ewen, J., G. Parkin, and P. E. O'Connell (2000). SHETRAN: Distributed River Basin Flow and Transport Modeling System, J. Hydrol. Eng., 5(3), 250–258, doi:10.1061/(ASCE)1084-0699(2000)5:3(250).

Gao, P., Borah, D. K., & Josefson, M. (2013). Evaluation of the storm event model DWSM on a medium-sized watershed in central New York, USA. *Journal of Urban and Environmental Engineering*, *7*(1), 1–7. http://doi.org/10.4090/juee.2013.v7n1.001007

Gellis, A.C., &Walling, D.E. (2011). Sediment source fingerprinting (tracing) and sediment budgets as tools in targeting river and watershed restoration programs. *Geophysical Monograph Series 194*, 263–291. http://doi.org/10.1029/2010GM000960

Gran, K. B., Finnegan, N., Johnson, A. L., Belmont, P., Wittkop, C., & Rittenour, T. (2013). Landscape evolution, valley excavation, and terrace development following abrupt postglacial base-level fall. *Bulletin of the Geological Society of America*, *125*(11–12), 1851–1864. http://doi.org/10.1130/B30772.1

Medeiros, P. H. A., Güntner, A., Francke, T., Mamede, G. L., & Carlos de Araújo, J. (2010). Modelling spatio-temporal patterns of sediment yield and connectivity in a semi-arid catchment with the WASA-SED model. *Hydrological Sciences Journal*, *55*(4), 636–648. http://doi.org/10.1080/02626661003780409

Morgan, R. P. C., Quinton, J. N., Smith, R. E., Govers, G., Poesen, J. W. A., Auerswald, K., … Styczen M. E. (1998). The Euro- pean Soil Erosion Model (EUROSEM): A dynamic approach for predicting sediment transport from fields and small catchments. *Earth Surf. Processes Landforms, 23*(6), 527–544, doi:10.1002/(SICI)1096-9837(199806)23:6<527::AID-ESP868>3.0.CO;2-5.

Nearing, M. A., Foster, G. R., Lane, L. J., & Finkner, S. C. (1989). A process- based soil erosion model for USDA - Water Erosion Prediction Project technology, *Trans. ASAE, 32*(5), 1587–1593.

Papanicolaou, A. N. T., Krallis, G., & Edinger, J. (2008). Sediment transport modeling review—current and future developments. *Journal of Hydraulic Engineering, 134*(1), 1-14.

Simon, A., Curini, A., Darby, S. E., & Langendoen, E. J. (2000). Bank and near-bank processes in an incised channel. *Geomorphology*, *35*(3–4), 193–217. http://doi.org/10.1016/S0169-555X(00)00036-2

Smith, H. G., & Blake, W. H. (2014). Sediment fingerprinting in agricultural catchments: A critical re-examination of source discrimination and data corrections. *Geomorphology*, *204*, 177–191. http://doi.org/10.1016/j.geomorph.2013.08.003

Thorne, C. R., & Tovey, N. K. (1981). Stability of composite river banks. *Earth Surface Processes and Landforms*, *6*(5), 469–484. http://doi.org/10.1002/esp.3290060507

Verstraeten, G., Prosser, I. P., & Fogarty, P. (2007). Predicting the spatial patterns of hillslope

sediment delivery to river channels in the Murrumbidgee catchment, Australia. *Journal of Hydrology*, *334*(3–4), 440–454. http://doi.org/10.1016/j.jhydrol.2006.10.025

Walling, D. E., Collins, a. L., Sichingabula, H. M., & Leeks, G. J. L. (2001). Integrated assessment of catchment suspended sediment budgets: A Zambian example. *Land Degradation and Development*, *12*(5), 387–415. http://doi.org/10.1002/ldr.461

Walling, D. E., Woodward, J. C., & Nicholas, A. P. (1993). A multi-parameter approach to fingerprinting suspended-sediment sources. *Tracers in Hydrology*, *215*(215), 329–338. http://doi.org/10.2489/jswc.66.5.323

Wilson, C. G., Papanicolaou, a. N. T., & Denn, K. D. (2012). Partitioning fine sediment loads in a headwater system with intensive agriculture. *Journal of Soils and Sediments*, *12*, 966–981. http://doi.org/10.1007/s11368-012-0504-2

Wischmeier, W. H., & D. D. Smith (1965), Predicting rainfall erosion losses from croplands east of the Rocky Mountains, USDA, Agric. Handb. 282, U.S. Gov. Print. Off., Washington, D. C.

Young, R. A., Onstad, C. A., Bosch, D. D., & Anderson, W. P. (1989). AGNPS: A nonpoint-source pollution model for evaluating agricultural watersheds, *J. Soil Water Conserv.*, *44*(2), 168–173.

CHAPTER 2

TRACING SUSPENDED SEDIMENT USING FINGERPRINTING TECHNIQUES

Abstract[1]

The flux of fine sediment within agricultural watersheds is an important factor determining the environmental quality of streams and rivers. Despite this importance, the contributions of sediment sources to suspended sediment loads within intensively managed agricultural watersheds remain poorly understood. This study assesses the provenance of fine suspended sediment in the headwater portion of a river flowing through an agricultural landscape in Illinois. Sediment source samples were collected from five sources: croplands, forested floodplains, grasslands, upper grazed floodplains, and lower grazed floodplains. Event-based and aggregated suspended sediment samples were collected from the stream at the watershed outlet. Quantitative geochemical fingerprinting techniques and a mixing model were employed to estimate the relative contributions of sediment from the five sources to the suspended sediment loads. To account for possible effects of small sample sizes, the analysis was repeated with only two sources: grazed floodplains and croplands/grasslands/forested floodplains. Results based on mean values of tracers indicate that the vast majority of suspended sediment within the stream (>95%) is derived from erosion of channel banks and the soil surface within areas of grazed floodplains. Uncertainty analysis based on Monte Carlo simulations indicates that mean values of tracer properties, which do not account for sampling variability in these properties, probably overestimate contributions from the two major sources. Nevertheless, this analysis still supports

[1] This chapter contains previously published material from,
Yu, M., & Rhoads, B. L. (2018). Floodplains as a source of fine sediment in grazed landscapes: Tracing the source of suspended sediment in the headwaters of an intensively managed agricultural landscape. *Geomorphology*, *308*, 278-292. https://doi.org/10.1016/j.geomorph.2018.01.022.

the conclusion that floodplain erosion accounts for the largest percentage of instream sediment (≈55-75%). Although grazing occurs over only a small portion of the total watershed area, grazed floodplains, which lie in close proximity to the stream channel, are an important source of sediment in this headwater steam system. Efforts to reduce fluxes of fine sediment in this intensively managed landscape should focus on eroding floodplain surfaces and channel banks within heavily grazed reaches of the stream.

2.1 Introduction

As awareness of water pollution, eutrophication and other water-related environmental concerns grows, the importance of sediment in the transport of nutrients and contaminants from agricultural areas to streams has received increasing attention (Haan et al., 2003; Smith and Blake, 2014; Lamba et al., 2015; Neal and Anders, 2015). Both the physical and the geochemical properties of suspended sediment are strongly controlled by sediment sources (Walling and Amos, 1999; Wilson et al., 2008; Williamson et al., 2014). Human activity, such as intensive agriculture and land drainage, has significantly altered the hydrological and biogeochemical cycles within terrestrial and aquatic ecosystems, particularly within agricultural landscapes in the midwestern United States (Rhoads et al., 2016). In intensively managed landscapes (IMLs), human activity has a substantial impact on sediment dynamics through disturbance of soil structure, seasonal variations in vegetation cover, and reduced storage and residence time of sediment (Gregory, 2006). The provenance of suspended sediment in the streams has been altered by human activities as well. Changes in river dynamics, channel morphology, land use patterns, and agricultural activities induced by humans in IMLs are reflected in the relative contributions from various sediment sources to suspended sediment loads.

Information concerning sediment provenance has been identified as an essential prerequisite for understanding watershed-scale sediment dynamics, particularly for fine (<0.063 μm) sediment (Walling et al., 1993; Collins et al., 1997; Koiter et al., 2013; Smith and Blake, 2014). Sediment fingerprinting techniques are valuable alternatives to direct monitoring for identifying the provenance of suspended sediment (Gellis and Walling, 2011; Collins et al., 2017) These techniques are based on the premise that variations in sediment properties directly reflect spatial and temporal variations in the contributions of sediment from distinguishable sources (Walling and Amos, 1999; Gellis and Noe, 2013; Wilkinson et al., 2013). Suspended sediment collected at the basin outlet can be considered a linear combination of contributions from different sediment sources, and the potential sediment sources can be reliably distinguished by their 'fingerprints' using a mixing model coupled with uncertainty analysis. Sediment fingerprinting procedures include statistical verification of the discrimination based on tracer properties and the use of mixing models to estimate the relative contributions of individual sources (Peart and Walling, 1986; Collins et al., 1996, 1997; Walling and Amos, 1999; Fox and Papanicolaou, 2007; Wilson et al., 2008; Gellis and Walling, 2011; Belmont et al., 2014; Lamba et al., 2015).

Sediment fingerprinting techniques generate valuable information on the relative importance of individual potential sources contributing to the suspended sediment flux of a river. Such information is crucial not only for linking upstream sediment sources to downstream sediment yields, but also for assessing sediment control projects (Walling and Collins, 2008). The science of sediment fingerprinting has evolved rapidly over the past two decades (Collins et al., 1998; Walling, 2005; Rhoton et al., 2006; Mukundan et al., 2010; Belmont et al., 2014) and fingerprinting techniques have been used in a variety of sediment tracing studies within

watersheds of various sizes (Collins et al., 1998; Olley and Caitcheon, 2000; Walling, 2005; Mukundan et al., 2010; Belmont et al., 2011). Combinations of multiple chemical properties—the composite fingerprints—have been developed for identifying and partitioning sources. Rigorous quantitative procedures for sediment tracing have also been developed, including statistical verification of source discrimination based on tracer properties and the use of multivariate mixing models to estimate the relative contributions of individual sources (Collins et al., 1998; Walling, 2005).

Sediment fingerprinting techniques involve the selection of diagnostic properties that can discriminate a number of potential sources (Walling, 2005; Davis and Fox, 2009; Collins et al., 2017). The fingerprints are physical or chemical properties of sediment. Those fingerprints can be generally categorized as conservative and non-conservative tracers. Conservative tracers have defining characteristics that do not change appreciably over sediment routing timescales (Belmont et al., 2014), while the non-conservative tracers have distinguishing characteristics that change during sediment transport, deposition, and re-suspension processes. Conservative tracers are usually used to identify sediment sources throughout the watershed geographically. Various conservative tracers have been used as sediment fingerprints to quantify the magnitude of erosion and partition suspended sediment: trace elements, organic matter content, and stable isotope geochemistry (Collins et al., 1998; Walling and Amos, 1999; Wilson et al., 2003; Walling, 2005; Fox and Papanicolaou, 2008). Other properties that are related to different sediment sources have also been used as sediment fingerprints: magnetic susceptibility (Yu and Oldfield, 1989; Slattery et al., 1995), clay mineralogy (Gingele and De Deckker, 2005), particle size (Walling and Amos, 1999), and colorimetric properties (Grimshaw and Lewin, 1980).

The distinctiveness of tracers from various sources is of central importance in sediment fingerprinting studies. Distinctive conservative tracers that do not change during transport from source to sampling location are preferred so that concentrations of tracers at the sampling location represent a mixture of tracer material contributed to the stream by each source. However, for depositional environments like floodplains, stored sediments represent mixtures from different sources that contribute sediment to floodplains. If tracer properties are conservative over the timescale of floodplain storage, eroded floodplain material can be difficult to trace because, like instream sediment, it is a mixture of material from various sources. In many cases, concentrations of conservative tracers for floodplain materials have intermediate values relative to concentrations for upstream sources, indicating that indeed this material is a mixture of other source material (Belmont et al., 2014). Under these conditions, tracer concentrations of floodplain material are not distinctive from concentrations associated with a mixture of other source material. Although tracer concentrations of floodplain material may match well those for instream sediment, apportionment of sediment sampled within the stream to erosion of the floodplain is problematic because erosion of a mixture of upland sources could produce the same concentrations. The extent to which tracers remain conservative within geochemically active floodplain environments has yet to be resolved (Koiter et al., 2013; Collins et al., 2017). Where tracers are believed to act conservatively over storage timescales, non-conservative tracers, particularly fallout radionuclides with known rates of radioactive decay, have been used to document time-integrated rates and patterns of sediment redistribution and storage within the watershed system, especially for floodplain intermediate storage and retention of sediment in the floodplain (Ritchie and McHenry, 1990; Walling and Woodward, 1992, Zapata, 2012; Belmont et al., 2014).

Tracing sources of suspended sediment in watersheds is important for the design of management practices to reduce sediment loads and contributions of sediment-adsorbed nutrients from agricultural areas to streams. However, contributions of different sediment sources to suspended sediment loads within intensively managed agricultural landscapes in the midwestern United States are still poorly understood. To improve understanding of sediment dynamics in such landscapes, this study assesses the provenance of suspended sediment in a headwater agricultural watershed and evaluates the influence of land use and channel geomorphology on suspended sediment load. Quantitative geochemical fingerprinting techniques and a mixing model are used to estimate the relative contributions of sediment from croplands, forested floodplains, ungrazed grasslands, upper streambanks/grazed floodplains, and eroding channel banks within areas of grazed floodplains to the suspended sediment loads at the watershed outlet. Uncertainty associated with the fingerprinting results is explored through Monte Carlo simulation.

2.2 Study area

The study area is the most headwater portion of the upper Sangamon River basin (USRB) in Illinois, USA (Figure 2.1). The portion of the USRB examined in the present study is located near the town of Saybrook, IL and therefore is referred to as the Saybrook watershed. The drainage area of the watershed is 84.3 km^2. Land use is dominated by row-crop agriculture (>90% of total land use), mainly the cultivation of corn and soybeans. The watershed has been carved into a complex assemblage of terminal and recessional moraines deposited by the Lake Michigan lobe of the Laurentide Ice Sheet during the Wisconsin glacial episode. The topography of the watershed is relatively flat with an average watershed slope of 3.24° and a standard deviation of 2.69°. Soils within the watershed have developed on loess, except floodplain soils,

which have formed on alluvium.

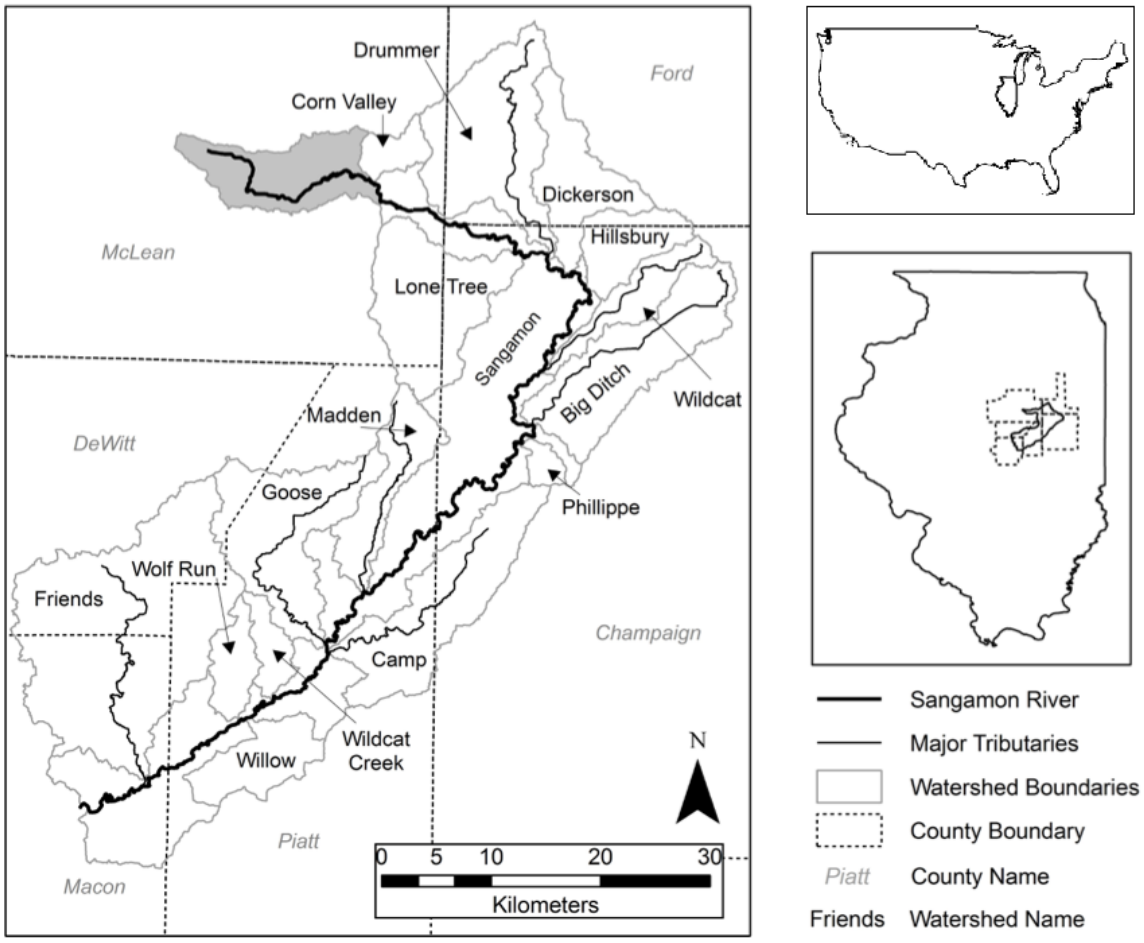

Figure 2.1: The Upper Sangamon River basin showing the location of the Saybrook watershed (shaded).

The USRB, which is part of the Intensively Managed Landscapes Critical Zone Observatory (IML-CZO), lies within one of the most intensively managed landscapes in the world (Pimentel, 2012). Many streams in this landscape have been channelized and extended headward for the purpose of agricultural land drainage (Rhoads and Herricks, 1996; Urban and

Rhoads, 2003). In the USRB, available data indicate that the total length of channels within the drainage network is three times greater than the total length prior to European settlement (Rhoads et al., 2016).

The USRB drains into Lake Decatur, an artificial reservoir established in the early 1920s. As a result of enhanced incoming fluxes of fine sediment, the 12 km^2 reservoir has lost more than one-third of its original volume since the 1920s (Fitzpatrick et al., 1987; Bogner, 2002), necessitating repeated dredging to maintain this municipal water supply. The influx of this sediment has been attributed to farming activities (Bogner, 2002), but apportionment of sediment among potential sources remains uncertain. The human perturbed sediment dynamics in the USRB are consistent with global transformations of sediment dynamics under human impact (Gregory, 2006), providing an opportunity to advance understanding of sediment dynamics in IMLs.

2.3 Methods

2.3.1 Field sampling and monitoring

Potential sediment sources in sediment tracing studies typically are defined based on differences in geology, vegetation, geomorphology, and human disturbance. Geochemical characteristics of sediments and organic material should vary in conjunction with variation in these landscape-scale factors (Walling, 2005). To identify potential categories of sediment sources, land use within the Saybrook watershed was evaluated using the National Land Cover Database 2011. Land use categories within the watershed in this classification scheme include croplands, grasslands, forests, pastures, and urban areas (Figure 2.2; Table 2.1). Croplands consist of corn, soybeans, and winter wheat, whereas the pasture category includes grazed areas of floodplains.

Table 2.1: Land use categories for the Saybrook watershed.

Land use	Area (km^2)	Percentage (%)
Cropland	77.24	91.60
Grassland	1.56	1.85
Forest	0.44	0.52
Developed/urban	4.84	5.74
Grazed floodplain	0.24	0.29

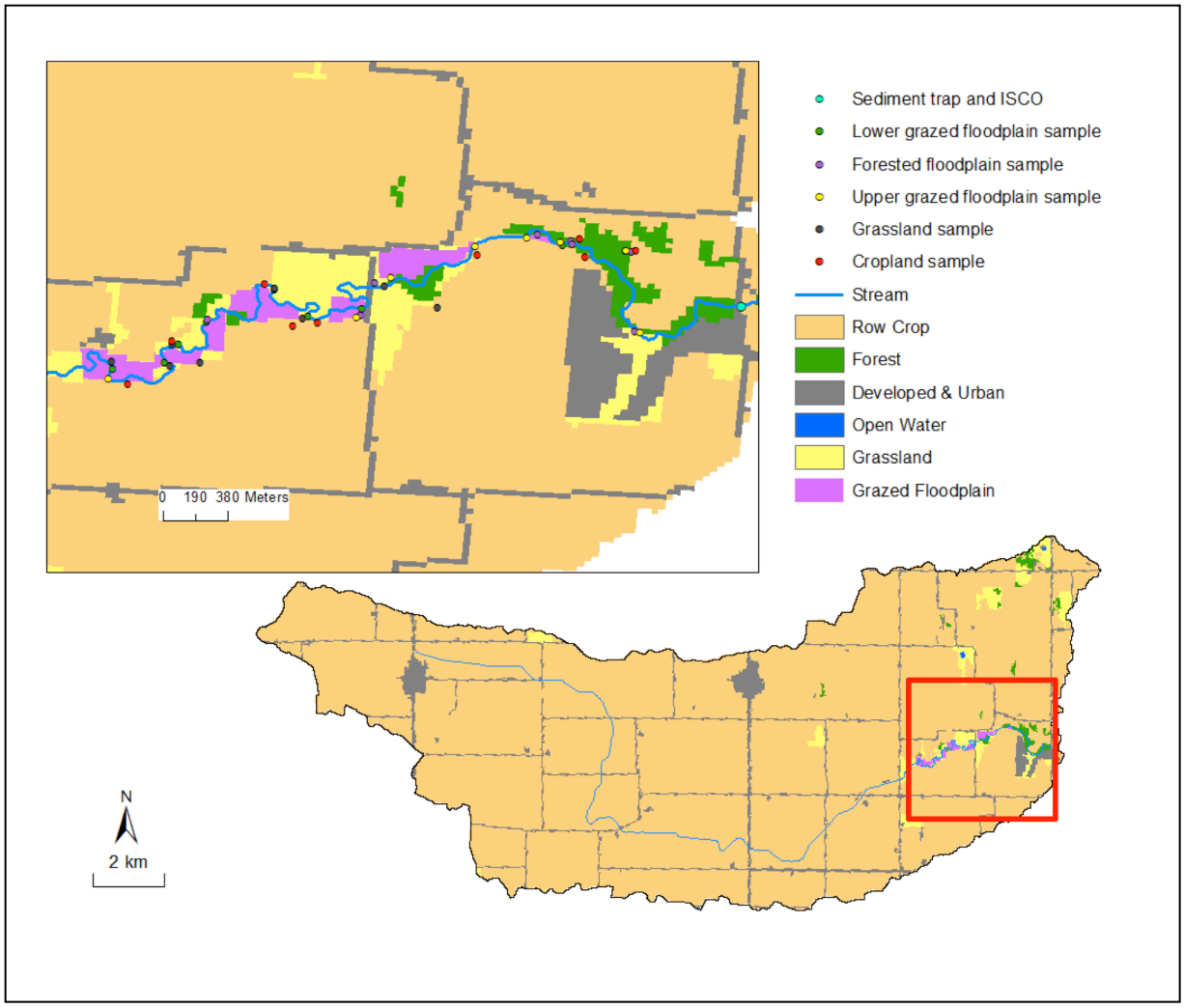

Figure 2.2: Land use and sampling locations in the Saybrook watershed. Gray lines represent paved roads.

For the purposes of sediment sampling, the land-use classification scheme was refined to focus on potential sources of sediment. Sampling sites were chosen based on land use, field reconnaissance and inspection of aerial photography. The proximity and potential connectivity to streams, the accessibility, and the possible evidence of erosion were three criterions for selecting sampling sites (Smith and Blake, 2014). Sediment samples representative of potential source areas were collected across the watershed from croplands, forested floodplains, grasslands, upper

streambanks and the soil surface within areas of grazed floodplains (upper grazed FP), and lower parts of eroding streambanks within areas of grazed floodplains (lower grazed FP) (Figure 2.2). Grazed floodplains were distinguished from grasslands by the presence of cattle or cattle pathways determined from both field observations and interpretation of recent aerial photographs. Although the streambanks constitute the margins of the floodplain, lower portions of streambanks within grazed areas of the floodplain were sampled separately from the floodplain surface, including the upper 5 cm of the streambanks, to determine if the eroding lower banks have a distinct tracer signature and, if so, are contributing substantially to fine sediment production. The samples from the floodplain surface represent recently deposited overbank materials, whereas the lower bank samples represent older alluvium deposited either through vertical or lateral accretion. Although urban areas may in highly urbanized settings introduce substantial amounts of sediment into streams (Kim and Sansalone, 2008), developed/urban areas in the Saybrook watershed, which represent small, rural residential areas, were not sampled because these areas are not serviced by storm-sewer systems connected to the stream network that would be expected to deliver fine sediment to the Sangamon River. Roads in the watershed are paved with asphalt and also should not be a major source of fine sediment. All sample sites were located within close proximity to the Sangamon River to eliminate effects associated with differences in distance of the sources from the stream channel. Distal sources are dominated by croplands and it is assumed that cropland samples collected near the river are representative of croplands throughout the watershed.

Field campaigns in June 2014 and April 2015 produced 52 source samples – ten to eleven samples from each source. All samples were collected in active erosional areas, such as rills in the grassland and cropland areas, eroding upper streambanks within grazed floodplains, exposed

surface soil in the forested floodplains, and vertical faces of unvegetated stream banks. A coated trowel was used to collect samples from either the upper 5 cm of the soil or from the face of eroding channel banks.

Aggregate and continuous sampling techniques were used to collect suspended sediment from the stream at the watershed outlet. Suspended sediment samples were collected throughout individual runoff events using an ISCO 6712 automatic pump sampler. The ISCO sampler was installed at the watershed outlet with an intake tube mounted above the normal flow height. Event-based samples of water and suspended sediment were obtained at specific time intervals when the water level exceeded a critical value or at irregular time intervals based on variations in the rate of change in water stage. In addition to the event-based sampling, an in situ tube sampler was deployed at the same location. The sampler consisted of an intake tube positioned at 60% of the mean flow depth connected to a large vented tube (Figure 2.3). Abrupt changes in cross-sectional area between the small inlet tube and the large body of the sampler cause the sediment to settle out as flow moves through the device (Phillips et al., 2000). Deployment of the sampler in the late spring and early summer of 2014 and 2015 yielded two aggregate sediment samples.

A rating curve was constructed to determine the relationship between stage and discharge at watershed outlet. Water discharges were measured using a Swoffer current meter during low, wadeable flows and an acoustic Doppler current profiler (ADCP) during high, unwadeable flows. Stage was monitored at 15-min intervals using a pressure transducer installed within the river at the discharge measurement location.

To characterize the relation between suspended sediment concentration (SSC) and water discharge, sediment rating curves were developed for rising and falling limbs of events. The most commonly used sediment rating curve is a power function (Asselman, 2000):

$$SSC = aQ^b \quad (2.1)$$

where *SSC* is suspended sediment concentration (mg/l), Q is the water discharge (m^3/s), a is a dimensional coefficient and b is a dimensionless exponent. Log-transformed discharge and suspended sediment concentration data were fitted with a linear regression (Horowitz, 2003).

Total amounts of sediment derived from storm events were calculated to quantify the sediment fluxes of events. The total amount of sediment from an event was calculated as:

$$q_s = \sum_{i=1}^{n-1} Q_{w,\, t_i+\Delta t_i/2} \times \left(\frac{(SSC_{t_i}+SSC_{t_{i+1}})\times 10^{-6}}{2}\right) \times \Delta t_i \quad (2.2)$$

where q_s is the total amount of sediment (tons), $Q_{w,\, t_i+\Delta t_i/2}$ is the water discharge (m^3/s) at time $t_i + \Delta t_i/2$ (s), SSC_{t_i} is the suspended sediment concentration (mg/l) at time t_i, Δt_i is the time interval from t_{i+1} to t_i, and n is number of samples.

Figure 2.3: Deployment of tube sampler (white tube near bottom of photo) within the Sangamon River at the outlet of the Saybrook watershed.

2.3.2 Laboratory processing

Suspended sediment samples were returned to the laboratory and settled at room temperature. Suspended sediment concentrations were measured using the standard gravimetric method. Source samples and suspended samples were dried at 40ºC. The dried samples were gently disaggregated using a mortar and pestle and sieved using stainless steel sieves to 63 μm. Although it is possible that sieving using stainless steel sieves could affect concentrations of Cr, Fe, or Ni in the samples, any potential introduction of trace elements by the sieves, were it to occur, should be relatively uniform across the various samples.

For the metal concentration analysis, 1 g of each sample was sent to Activation laboratories in Ontario, Canada for trace element geochemistry analysis with ICP/OES after aqua regia digestion. This leaching procedure involved treating the sample in a solution of three parts HCl to one part HNO_3 to dissolve most oxides, many silicates (including trace-element rich micas and clays), all sulfides and carbonates, and many organic substances (Neal and Anders, 2015). Material remaining after aqua regia digestion is mostly quartz and other phases that tend to contain few trace elements. For the organic content analysis (%C, %N) and stable isotopic composition ($\delta^{13}C$ and $\delta^{15}N$) analysis, 30±2 mg of each sample were analyzed on a CE Instruments NC 2500 elemental analyzer in series with a ConFlo IV universal interface coupled to a Delta V Advantage Isotope Ratio Mass Spectrometer at the Illinois State Geological Survey.

2.3.3 Sediment fingerprinting procedures

Quantitative sediment fingerprinting techniques and a mixing model were employed to estimate the relative contributions of sediment from potential sources to the suspended sediment loads at the basin outlet. Organic matter content, stable isotopic composition and trace metals of soil samples were used as potential tracers. To assess the conservative behavior of each tracer

property, the range in source tracer concentrations was compared to the range of concentrations of the corresponding elements in the suspended sediment concentrations. Those tracers with ranges of concentrations in the suspended sediment that fell outside the ranges of concentrations of tracers in the source materials were removed from subsequent analysis.

A two-step statistical model was used to identify fingerprints from chemical properties. Tracer concentrations of source materials were aggregated to provide a single mean value for each potential source. Each chemical property was analyzed individually using Kruskal-Wallis *H* test to determine the capability of differentiating among different sediment sources. The null hypothesis assumes that the samples are from identical populations and the alternative hypothesis assumes that the samples come from different populations. Chemical properties with *p*-values less than the significance level (0.05) for the *H* test were considered potential tracers. Once sets of potential tracers were identified, stepwise discriminant function analysis (DFA) involving stepwise minimization of Wilks' lambda (Collins et al., 1998) was used to determine the optimal combination of tracer properties that pass the Kruskal-Wallis *H* test (Collins and Walling, 2002). The composite fingerprint (Collins et al., 1998; Walling, 2005) is a suite of tracers that generate low Wilks' Lambda.

A mixing model (Collins et al., 1996) was used to estimate the relative contributions of the potential sources to the suspended sediment load. The mixing model is based on a set of linear equations where each tracer has an equation relating the tracer concentration in the suspended sample to the sum of tracer concentrations for each source multiplied by the respective unknown percentage of source contributions (Smith and Blake, 2014). The composite fingerprint was incorporated into the mixing model to generate the percentage of contributions.

The mixing model is solved by using an optimization procedure that selects values for source contributions by minimizing the sum of the squares of the residuals (*SSE*):

$$SSE = \sum_{i=1}^{n}[(C_i - \sum_{s=1}^{m} P_s C_{i,s})/C_i]^2 \quad (2.3)$$

where C_i is the concentration of tracer *i* in suspended sediment, P_s is the percentage contribution from source *s*; $C_{i,s}$ is the mean concentration of tracer *i* in source sample *s*, *n* is the number of fingerprint properties comprising the optimum composite fingerprint, and *m* is the number of sediment source categories. The mixing model seeks to satisfy the constraints that contributions of each source to the suspended sediment at the watershed outlet must lie between 0 and 1, and the sum of contributions of the sources to the suspended sediment at the watershed outlet must be unity (Collins et al., 1998).

A controversial issue in sediment fingerprinting studies is whether corrections should be performed to account for differences in grain size and organic matter content between samples. Although some studies employ such corrections (Collins et al., 1997; Gellis and Walling, 2011), others have not either because no differences occur in source materials and in-stream sediment (Evrard et al., 2011, 2013) or to avoid the risk of over-correction (Martínez-Carreras et al., 2010). Smith and Blake (2014) re-examined the need for corrections and argued that inconsistent relationships among particle size, organic matter content, and tracer property concentrations undermined the basis for corrections. Their sensitivity analysis also showed that correcting source tracer data for differences in organic matter could lead to significant over-correction and produce large changes to source contribution estimates that could not be justified. They

recommended that such corrections not be used. Based on their recommendation, corrections for grain and organic differences were not performed in this study.

2.3.4 Uncertainty Analysis

The uncertainty surrounding source and sediment sampling was quantified using a Monte Carlo routine that repeatedly solves the mixing model using random samples drawn from the original datasets on elemental concentrations of each sample from each sediment source. The mean values of tracer concentrations for sets of samples from each source are usually used in the mixing model to estimate the relative contributions of sediment from each source. However, uncertainty arises in small samples where mean values may not accurately reflect variability in values of concentrations among individual samples collected from a particular source. A Monte Carlo approach can complement the mixing model and test uncertainty associated with the sampling strategy and tracer property selection. Through this approach, values of tracer concentrations were selected randomly from distributions of tracer values associated with each source. Eq. (2.1) was then optimized r = 10,000 times by adjusting P_S to minimize SSE, with each run using a separate set of values $C_{i,s}$ in Eq. (2.1) randomly selected from the tracer distributions. The mean percentage contribution of the estimates was reported and compared with that estimated using mean values of tracer concentration. This method also yields standard deviations of the percentage contributions.

2.4 Results

To provide a context for interpreting the sediment fingerprinting results, hydrological characteristics of the Sangamon River during the sampling events are first analyzed to illustrate the dynamics of the river when suspended sediment was sampled within the river. The sediment fingerprinting results is used to evaluate the relative contribution from each potential source.

Uncertainties associated with sediment fingerprinting processes are explored through Monte Carlo simulation.

2.4.1 Hydrological Characteristics of Sediment Sampling Conditions

The ISCO sampler collected event samples on July 12-15 and September 10-12, 2014. The precipitation totals for the two events, as determined from nearby rain gages, were 84 and 79 mm, respectively (Figure 2.4). Due to equipment problems, the ISCO sampler operated only at the peak and falling limb of an initial subevent during July 2014, but sampled throughout a subsequent subevent that occurred immediately after the initial subevent (Figure 2.4). The peak discharges of the initial subevent and subsequent subevent were about 47 and 42 m^3/s, respectively. Based on field measurements of stage and channel bank heights at the gaging site, the bankfull stage is about 98.75 m (arbitrary datum), which corresponds to a discharge of about 42 m^3/s. Thus, the two peaks were close to or slightly exceeded the bankfull discharge. Both subevents attained peak discharge in about six hours, with the initial high flow not fully subsiding before the rise in discharge occurred in the subsequent flow. The event in September 2014 was less flashy than the two July subevents. The peak discharge was 23 m^3/s, and it took 22 h for the flow to reach peak stage.

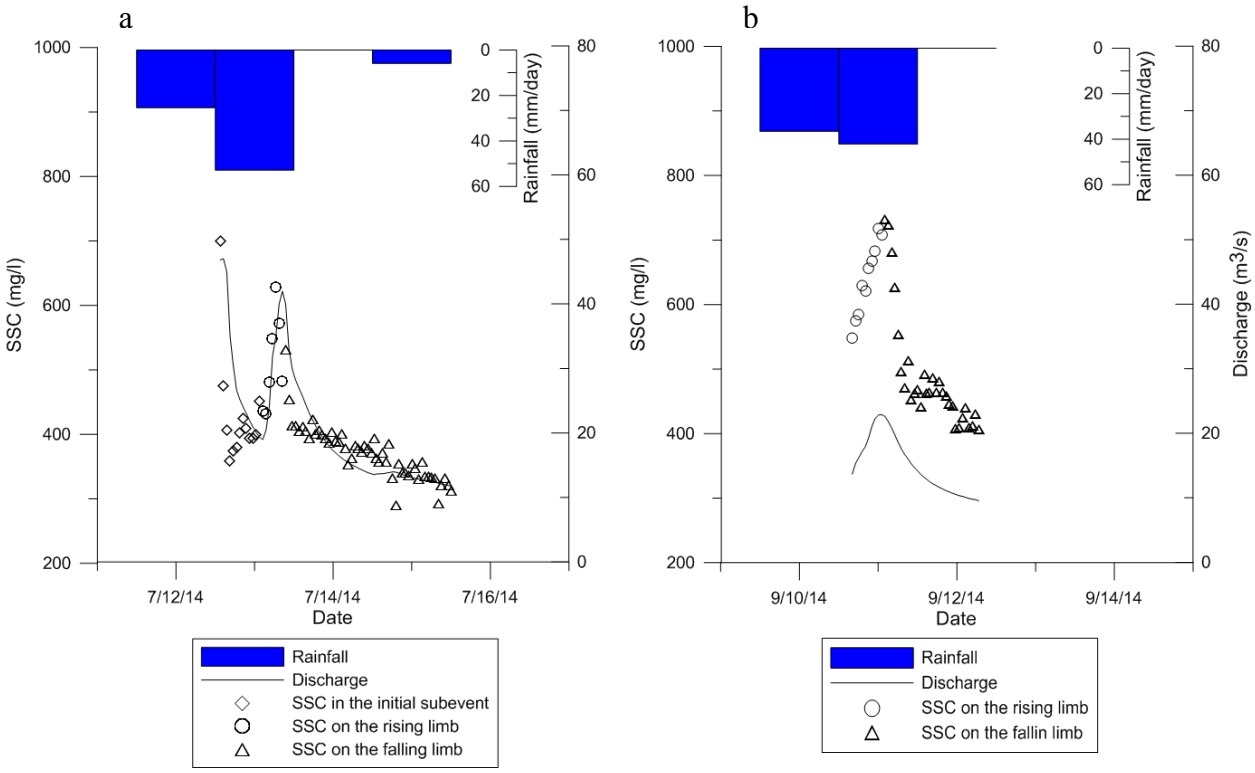

Figure 2.4: Water discharge and SSCs for (a) first event and (b) second event.

Two aggregated samples that included multiple high and low flows were collected using the tube sampler – one in 2014 and another in 2015 (Figure 2.5). The tube sampler was deployed for about 2.5 months in 2014 and 3.5 months in 2015. During the first period of deployment, peak discharges did not exceed 20 m^3/s and generally were less than 10 m^3/s. Thus, all flows were sub-bankfull. By contrast, discharge frequently exceeded 10 m^3/s during the second period of deployment and two overbank events occurred during this sampling interval.

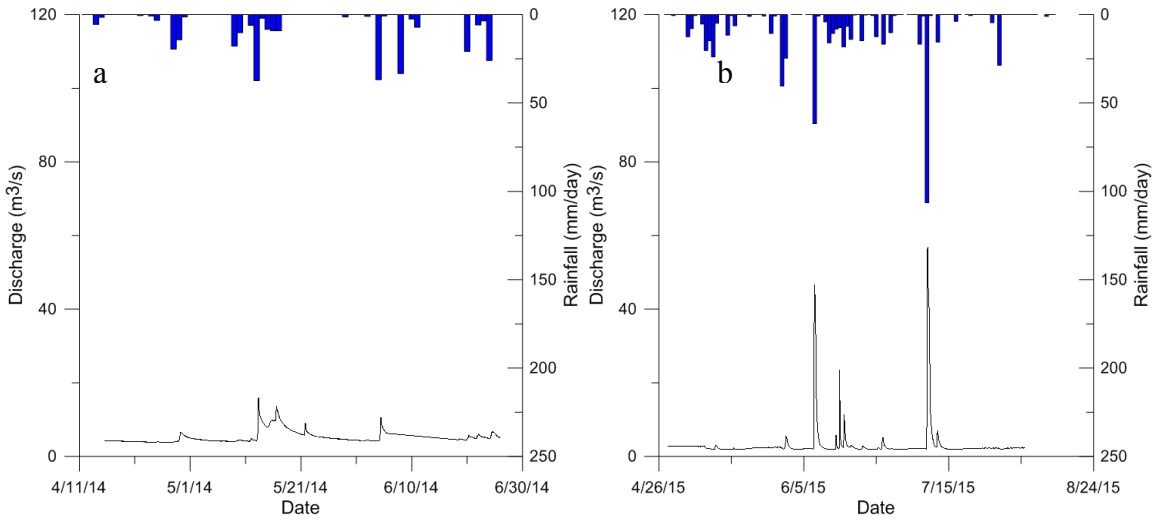

Figure 2.5: Daily precipitation and discharge during the sampling period for tube samples obtained in (a) 2014 and (b) 2015.

2.4.2 Suspended sediment concentration and fluxes

Temporal patterns of SSC during the July and September 2014 events basically mirror patterns of discharge (Figure 2.4). SSC decreased with decreasing discharge during the initial subevent in July 2014, before reaching a fairly steady value of about 350 mg/l immediately prior to the subsequent subevent, even though discharge continued to decrease. The pattern of data suggest that a small, secondary peak in SSC occurred immediately prior to the subsequent subevent, with SSC increasing and then decreasing by about 75-100 mg/l. This secondary peak may reflect a pulse of sediment from a discrete input of fine material to the river system. During the subsequent subevent SSC increased at a slightly faster rate and declined at a slower rate than discharge. As a result, the peak in SSC occurred about two hours prior to the peak in discharge, when flow was still well below the bankfull stage. Despite the occurrence of a larger peak discharge immediately prior to the subsequent peak, the delivery of fine sediment appears to be a supply-limited process whereby eroded material was moved readily into the stream during initial

stages of the storm-event runoff. No substantial exhaustion effect was immediately apparent, but the SSC corresponding to the peak Q of the initial subevent does exceed the peak SSC during the subsequent subevent. Thus, the supply of sediment during the subsequent subevent appears to be at least slightly less than the supply during the initial subevent. Moreover, because no SSC data are available for the rising limb of the initial subevent, the peak SSC during this subevent is unknown; this peak may have been much larger than the peak SSC during the subsequent subevent. The value of SSC at peak Q during the subsequent subevent was less than the SSC for the first sample of the falling limb, but this disparity may reflect sampling variability. On the falling limb, values of SSC decreased to about 350 mg/l and then declined gradually over time even though discharge continued to decline relatively rapidly.

During the event in September 2014, values of SSC increased less rapidly than discharge on the rising limb, but decreased more rapidly than discharge on the falling limb. The SSC peaked one hour after the peak in discharge and then fell rapidly over a 4-5 h period to a value of about 450 mg/l. Thereafter, SSC declined only about 50 mg/l over the next 24 h. Overall, values of SSC during this event were about 100 mg/l higher than those during the July event.

Differences in the relations between SSC and Q for the two events can be examined quantitatively by developing sediment rating curves for rising and falling limbs of the hydrographs. Only the complete hydrograph of the subsequent subevent on July 13-14, 2014 is considered. Falling limb of the initial subevent on July 12-13 is not included. Sediment rating curves have the form of Eq. (2.1). Differences among the coefficient *a* tend to be indicative of material erodibility and transportability, whereas differences among the exponent *b* represents how readily new source material becomes available with increasing runoff or how much the erosive power of the river increases with increasing flow rate (Asselman, 2000). The July event

includes seven samples on the rising limb and 52 samples for the falling limb. SSCs for this hydrograph ranged from 290 to 627 mg/l. Analysis for the September event was based on 10 samples for rising limb and 30 samples for falling limb with SSCs ranging from 407 to 718 mg/l.

The larger value of *b* on the rising limb than on the falling limb of the July 13-14 event confirms the more rapid rate of increase in SSC with increasing Q on the rising limb than decreasing SSC with decreasing Q on the falling limb. Likewise, the larger value of *b* on the falling limb of the September 10-12 event than on the rising limb substantiates the more rapid decrease in SSC with falling Q compared to increasing SSC with increasing Q. The larger values of *b* for the September event compared to the July event indicate that sediment was more readily mobilized with increasing Q in September compared to July. Exhaustion of sediment supply during the initial event in July (12-13) may have contributed to relatively low values of *b* for the July 13-14 hydrograph. Surprisingly, values of *a* were higher for the July event compared to the September event, suggesting that baseline sediment availability was greater in July, even though SSCs were generally higher in September than in July.

The rating curves, along with the relation between discharge and concentration (Eq. (2.2)), were used to estimate the total amount of sediment by weight transported by the July 12-13 and Sept 10-12 events. This analysis yields estimates of 49 tons for the July event and 10.4 tons for the September event. Thus, although SSCs were higher in the September event than in the July event, the July event, which had much larger discharges, moved five times the mass of sediment transported in the September event.

Sediment rating curves developed for July events have a higher exponent *b* and lower coefficient *a* than the sediment rating curves developed for September event (Figure 2.6; Table 2.2). Although the coefficient *a* and exponent *b* in Eq. (2.1) have no physical meaning, their

values often reflect the alteration of sediment supply, the power of the stream to erode and transport sediment, and the spatial scale of the watershed (Asselman, 2000; Warrick, 2015). Coefficient *a* reflects erosion severity and exponent *b* represents the erosive power of the river and the extent to which new sediment sources become available when discharge increases (Asselman, 2000). Higher *a* and lower *b* in the July event indicates, that compared to the September event, the availability of easily transported material was greater during this event and that the erosive power of the river was relatively low or that fewer new sediment sources became available as discharge increased.

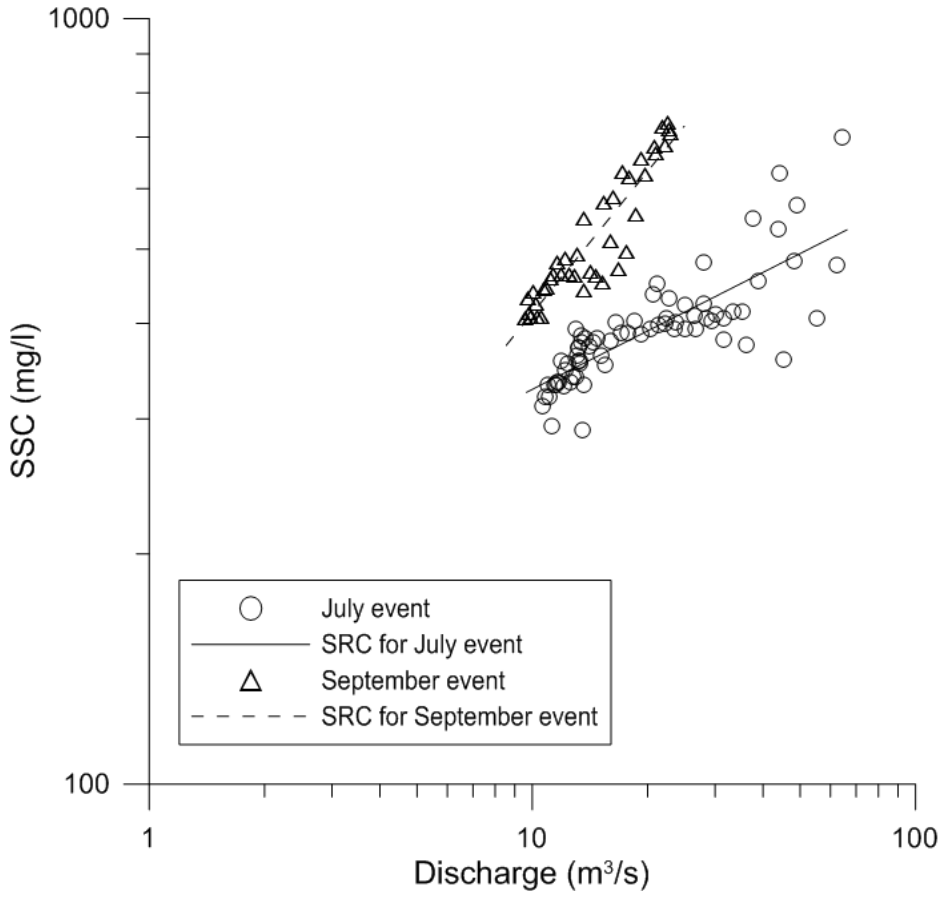

Figure 2.6: Sediment rating curve for the July and September events.

Table 2.2: Sediment rating curves for runoff events.

Event	Sediment rating curve	R^2
Jul. 13-14, 2014 rising limb	$SSC = 172.2Q^{0.3063}$	0.61202
Jul. 13-14, 2014 falling limb	$SSC = 188.22Q^{0.2423}$	0.69913
Sep. 10-12, 2014 rising limb	$SSC = 149.36Q^{0.4961}$	0.96957
Sep. 10-12, 2014 falling limb	$SSC = 117.71Q^{0.5455}$	0.79573

Sediment rating curves derived from log-transformed sediment and discharge data exhibit linear relationships between SSC and Q (Figure 2.6); however, the relations between SSC and Q during the events in July and September are highly nonlinear. This nonlinearity of sediment is evident in plots of SSC versus Q, which define hysteresis loops (Figure 2.7). The July 13-14 event produced a clockwise hysteresis loop, which indicates that the C/Q ratios for a given Q were greater on the hydrograph's rising limb than on the falling limb. The clockwise loop usually is interpreted as a first flush phenomenon, whereby sediment is supplied to the in-stream sampling location by a source close to this location (Seeger, 2004; Gao and Josefson, 2012; Vaughan et al., 2017). It may also indicate exhaustion of source material during the falling limb (Williams, 1989; Wilson et al., 2012). The second event produced a figure-eight loop combining a clockwise loop at low flow with a counterclockwise loop at high flow – a pattern typical of a delay in peak concentration relative to discharge followed by a rapid decline in concentration with decreasing discharge. This pattern may reflect delayed input of sediment from a proximal or distal source followed by rapid exhaustion of sediment supply (Vercruysse et al., 2017).

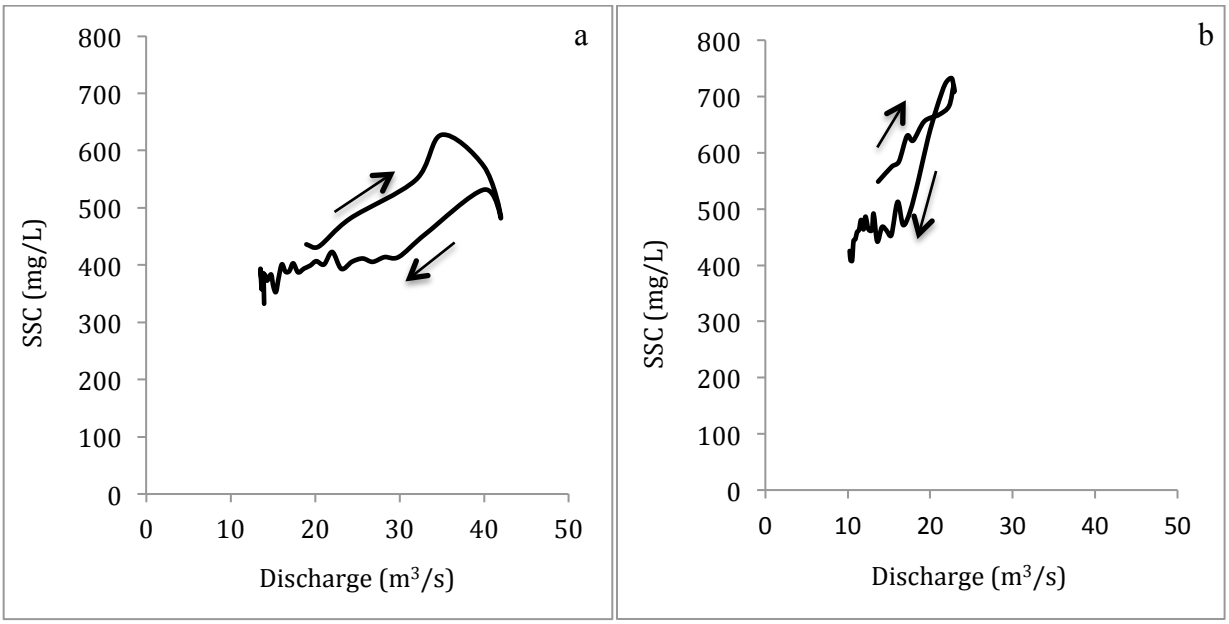

Figure 2.7: Relationship between suspended sediment concentration and discharge, as well as the associated hysteresis for (a) the first event and (b) the second event.

2.4.3 Suspended sediment fingerprinting

Thirty element potential tracers were evaluated for the sediment fingerprinting analysis (Table 2.3).

Table 2.3: Tracer properties included at each step.

Step	Tracer properties included
Tracer	Cu, Mn, Ni, Pb, Zn, Al, As, B, Ba, Be, Ca, Co, Cr, Fe, K, La, Mg, Na, P, Sc, Sr, Ti, V, Y, Zr, S, %N, %C, δ^{15}N, δ^{13}C
Range examination	Cu, Mn, Ni, Pb, Zn, Al, As, B, Ba, Be, Ca, Co, Cr, Fe, K, La, Mg, P, Sc, Ti, V, Y, Zr, S, %N, δ^{15}N, δ^{13}C
Kruskal-Wallis *H* test	Al, Ba, Be, Ca, Cr, Fe, La, Mg, Sc, Ti, V, Y, S, %N
DFA	Ca, Sc, Be, S

The Kruskal-Wallis *H* test was used to determine the capability of those chemical properties to distinguish different sources. The tests returned *p*-values for each tracer. Among the 30 tracers, *p*-values for 14 chemical properties were statistically significant at the 0.05 level. These 15 tracer properties were then entered into the step-wise minimization of Wilkes' lambda procedure to define the composite fingerprint. The combination of ^{10}Be, Ca, Sc, and S, which generates the minimum Wilks's Lambda, emerged as the optimal composite fingerprint for sediment tracing. This composite fingerprint differs significantly among the potential sediment sources based on the mean, median and standard deviation of tracer concentrations for each source sediment sample (Table 2.4).

Although the statistical analysis indicates that the five sources have significantly different tracer properties, inclusion of floodplain sources in fingerprinting analysis can still be problematic. Floodplain materials are a mixture of sediment from other sources, which in the USRB include cropland and grassland sources, with cropland constituting the major source (> 90% of the watershed area – Table 2.1). If the tracers are truly conservative over the timescale of floodplain storage or are not preferentially amassed within the floodplain, mean values of tracer properties for floodplain sediment should be intermediate between those for croplands and grasslands (Belmont et al., 2014). In such cases, the tracer properties for floodplain material may differ statistically from properties from other sources, but are not distinctive because these values cannot be discriminated from values associated with mixtures of upland sources. However, mean values of some of the tracers for forested floodplains, upper grazed floodplains, and lower grazed floodplains greatly exceed corresponding means for croplands or grasslands. In particular, the means of Be and Sc for the lower grazed floodplains are much greater than the means of these tracers for grasslands and croplands and the means of Ca and S for upper grazed

floodplains are much greater than the means of these two tracers for croplands and grasslands. These results suggest that either the tracers are not truly conservative over the timescale of floodplain storage or that some process tends to concentrate conservative tracers within the floodplain. In any case, the tracer properties for the floodplain sources not only differ significantly from tracer properties for upland sources, but have distinctive properties based on considerations of mixing. This assessment of tracer properties warrants mixing analysis of instream samples based on the five different sources.

Table 2.4: Mean and median values for tracer properties.

	Be (ppm)			Ca (%)			Sc (ppm)			S (%)		
	Mean	Median	SD	Mean	Median	SD	Mean	Median	SD	Mean	Median	SD
Lower grazed floodplains	0.85	0.8	0.17	0.82	0.66	0.46	4.45	4	1.81	0.02	0.02	0.01
Forested floodplains	0.72	0.7	0.11	1.22	1.11	0.62	3.20	3	0.63	0.03	0.03	0.01
Croplands	0.72	0.7	0.09	0.79	0.62	0.57	3.64	4	0.67	0.02	0.02	0.01
Grasslands	0.66	0.65	0.07	0.82	0.49	0.66	3.00	3	0.00	0.03	0.03	0.01
Upper grazed floodplains	0.66	0.7	0.05	2.14	2.22	0.79	3.10	3	0.32	0.05	0.045	0.02

Results of the mixing model analysis based on mean values of tracer concentrations for each source indicate that eroding channel banks within grazed floodplains contribute the overwhelming majority of suspended sediment within the stream at the watershed outlet (Table 2.5). Together these two sources account for 97% of the in-stream sediment. The results are the same for event and aggregated samples, confirming that the delivery of fine sediment from these

two sources is consistent over all types of events. Source signals of forested floodplains, croplands, and grasslands are minor or essentially absent.

Table 2.5: Estimated contributions of sediment sources to in-stream suspended sediment based on mean tracer concentrations from source samples.

	Lower Grazed Floodplains (%)	Forested floodplains (%)	Croplands (%)	Grasslands (%)	Upper grazed floodplains (%)	Sum of the squares of the residuals
Aggregated, 2014	1	1	1	1	96	0.50
Aggregated, 2015	48	1	1	1	49	0.44
Rising limb, Jul. 13-14, 2014	58	1	1	1	39	1.56
Falling limb, Jul. 13-14, 2014	61	1	1	1	36	1.69
Rising limb, Sep. 10-12, 2014	55	1	1	1	42	1.64
Falling limb, Sep. 10-12, 2014	52	1	1	1	45	1.92

2.4.4 Monte Carlo analysis

Sediment fingerprinting methods include a variety of sources of uncertainty (Martinez-Carreras et al., 2008), including effects associated with source–stream connectivity, the assumption of perfect mixing conditions, the extent to which tracer behavior is conservative, and the representativeness of source samples (Collins and Walling, 2004; Walling, 2005; Gellis and Landwehr, 2006; Martinez- Carreras et al., 2008; Gellis and Walling, 2011; D'Haen et al., 2012; Koiter et al., 2013; Wilkinson et al., 2013). Another source of uncertainty when sources are represented by a small number of samples is the extent to which the use of mean values for tracer properties adequately captures inherent variability in tracer values among individual samples (Small et al., 2002). One way to explore this uncertainty is to apply the mixing model repeatedly to values of the tracers sampled randomly from underlying distributions using a Monte Carlo sampling routine (Martinez-Carreras et al., 2008; Collins et al., 2010; Hancock et al., 2014; Smith and Blake, 2014). The mixing-model analysis based on mean concentrations of tracer properties indicates that contributions from forested floodplains, croplands, and grasslands are negligible; however, such as analysis does not consider variations in tracer properties among individual samples of sediment obtained from each source. To consider this effect, tracer properties were randomly selected through a Monte Carlo sampling routine from the sets of individual samples from each source, rather than using the mean concentrations from these sources. Because individual samples exhibit different degrees of tracer-concentration similarity with the suspended sediment samples, the results of the mixing model analysis based on Monte Carlo simulation analysis illustrates how inherent variability in the tracer concentrations among sources affects the estimated contributions of each source to the suspended sediment.

The Monte Carlo sampling routine generates distributions for the contributions from each

source sample to suspended sediment loads. Mean contributions for each source are average values derived from individual estimates of contributions obtained by applying the mixing model to 10,000 randomly sampled values of the tracer properties. In general, distributions of tracer values for the sets of source samples tend to be rather flat, indicating high variability among samples for a particular source. As a result, Monte Carlo sampling of these distributions results in frequent inclusion of extreme values in the simulations, producing distributions of contributions for each source that include widely varying estimates of contributions (Table 2.6).

The Monte Carlo analysis results in mean estimates of contributions from each source that differ rather markedly from the estimates based on mean tracer concentrations (Tables 2.4 and 2.5). Although grazed floodplains and channel banks remain the dominant sources, the estimated contributions from these two sources decrease from 97% to between 66 and 77%. The Monte Carlo results also change somewhat the relative importance of upper grazed floodplains versus lower grazed floodplains for the event samples. Estimated percentage contributions from upper grazed floodplains now exceed the estimated contributions by lower grazed floodplains. Grasslands and croplands, the two upland sources of sediment, are each estimated to contribute between about 4% and 15% to the instream sediment load. Moreover, estimated contributions from croplands, which are distal to the river in relation to the grazed floodplains, are greater both during events with greater runoff (July 13-14 versus Sept 10-12, 2014) and during aggregated sampling periods with greater runoff (2015 versus 2014, Figure 2.5). These results, which include the effect of variability in sampled values of tracers on estimates of source contributions, seem more realistic than the extreme percentage contributions to instream sediment by grazed floodplains derived from mean tracer values.

Table 2.6: Estimated mean contributions of sources samples to suspended sediment concentration based on Monte Carlo sampling routine (10,000 random sampling repetitions) for the five sources.

	Lower grazed floodplains (%)	Forested floodplains (%)	Croplands (%)	Grasslands (%)	Upper grazed floodplains (%)
Aggregated, 2014	8.08	16.63	3.91	13.14	58.24
Aggregated, 2015	26.66	10.78	12.75	8.55	41.26
Rising limb, Jul. 13-14, 2014	28.55	10.88	13.51	5.10	41.96
Falling limb, Jul. 13-14, 2014	30.03	10.87	14.33	4.69	40.08
Rising limb, Sep. 10-12, 2014	31.45	12.47	9.05	6.02	41.01
Falling limb, Sep. 10-12, 2014	30.88	13.35	7.30	5.69	42.77

Table 2.7: Estimated mean contributions of sources samples to the suspended sediment concentration based on Monte Carlo sampling routine (10,000 random sampling repetitions) for two groupings of the five sources.

	Uplands/grasslands/ forested floodplains (%)	Grazed floodplains (%)
Aggregated, 2014	45.4	54.7
Aggregated, 2015	47.5	52.5
Rising limb, Jul. 13-14, 2014	36.6	63.4
Falling limb, Jul. 13-14, 2014	36.2	63.8
Rising limb, Sep. 10-12, 2014	36.3	63.7
Falling limb, Sep. 10-12, 2014	33.7	66.4

Recent recommendations on sediment fingerprinting suggest that source sample sizes less than 20 can introduce considerable uncertainty into apportionment modeling results (Collins, 2017). Another way to deal with the small sample size problem is to analyze the data using fewer categories to increase the number of samples per category. Although the upper grazed floodplain and lower grazed floodplain sources can be discriminated statistically based on differences in tracer signatures, both are part of the floodplain and the fingerprinting results using five sources indicate that both are major sources of sediment to the stream. To reduce uncertainty that might arise from a limited number of samples, the upper grazed floodplain and lower grazed floodplain samples were combined into one grouping. The other three sources, croplands, forested floodplains, and ungrazed grasslands were also combined into a single grouping. Apportionment

analysis was then performed for these two groupings using the four tracers. Results of this alternative analysis based on mean values of the tracers indicate that almost 95% of the suspended sediment for both aggregated and event-based samples came from group one containing the two original grazed floodplain sources (upper bank/floodplain surface and lower streambanks). Monte Carlo analysis of source apportionment using the mixing model indicates that 53-55% of the instream sediment for the aggregated samples was derived from the grazed floodplains and that 63-67% of the event-based instream sediment came from the grazed floodplains. Although these estimates of grazed floodplain contributions are less than derived from Monte Carlo analysis for the five separate sources (Table 2.6), they still support the conclusion that most of the fine sediment in the stream consists of eroded material from the grazed floodplains.

2.5 Discussion

The results of this study suggest that grazed areas of the floodplain are the primary source of fine suspended sediment within the headwaters of the Sangamon River. Erosion of the floodplain both by surface runoff and by streambank erosion contribute to the production of almost all fine sediment sampled within the stream system. The results are consistent both for event and aggregated samples and for large and small events. Evaluations of uncertainty of the results using Monte Carlo simulation and regrouping of samples to increase sample size in the fingerprinting analysis support the conclusion that grazed floodplains are the primary source of fine sediment in the stream system.

Figure 2.8: (Left) Eroded bank in a grazed area. (Right) Cantilever failure at the outer bank of a meander bend in a grazed area.

The tracing results are consistent with visible and historical evidence of active erosion of grazed areas of floodplains upstream from the in-stream sampling location. Within the grazed areas, channel banks are sparsely vegetated and root penetration of grasses growing on the floodplain extends only a few tens of centimeters below the surface, offering little protection against erosion (Figure 2.8). Large sections of the channels banks have detached from the adjacent floodplain through the basal undercutting, the development of tension cracks, and subsequent cantilever failures. From a historical perspective, sections of the Sangamon River within the grazed areas have exhibited substantial amounts of lateral migration over the past several decades. Analysis of historical aerial photography indicates the river channel has in some cases moved laterally by several channel widths (Figure 2.9). In contrast, sections of the river upstream of the grazed areas, which have been channelized for the purpose of land drainage, are relatively stable and show little or no sign of lateral movement over the last 70 yr (Rhoads et al., 2016). Although erosion at cut banks may over the long term be balanced by deposition of sandy deposits on point bars, fine sediment released by cutbank erosion during sub-bankfull flows likely does not become re-deposited within the channel or floodplain system, but is transported downstream as wash load. Whether or not floodplains within the grazed areas are undergoing net

erosion in not clear. Such an assessment would require a mass balance investigation of net floodplain erosion and deposition.

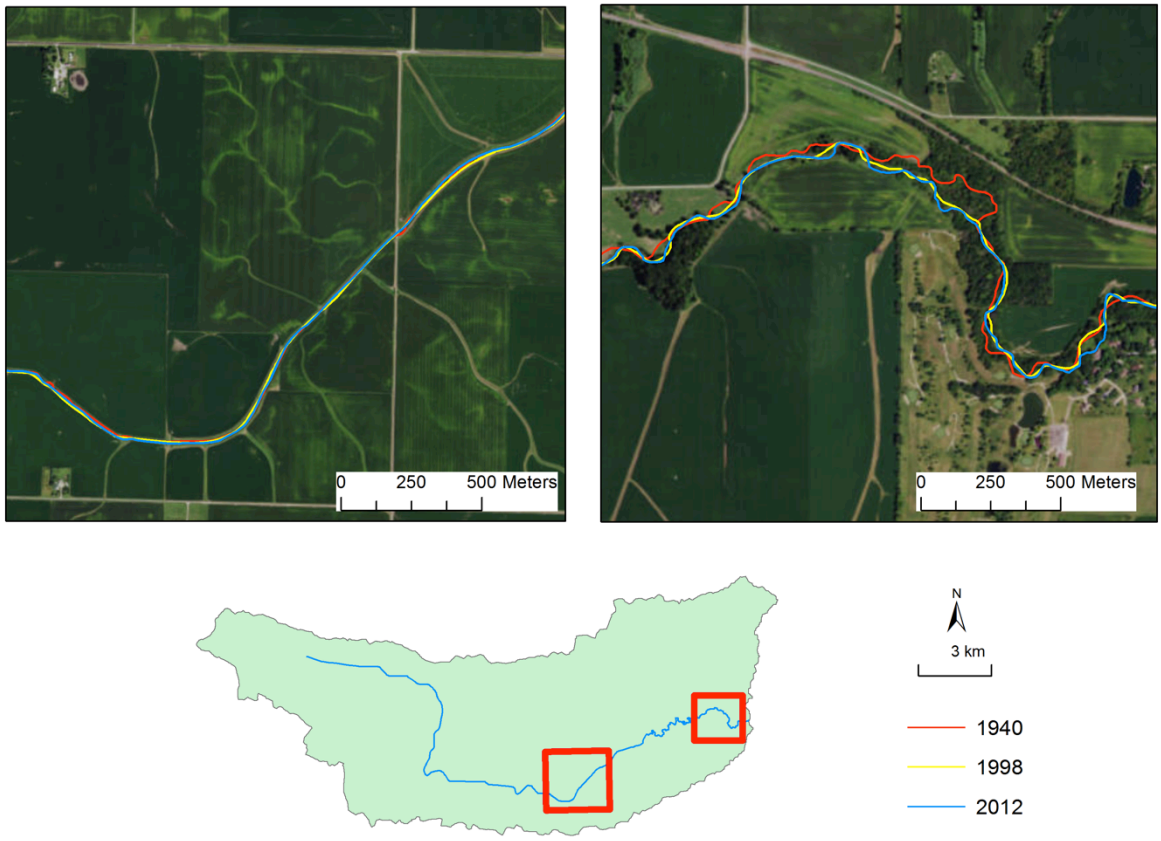

Figure 2.9: (Left) Lack of channel change over the same period upstream where the stream is channelized for the purpose of agricultural drainage. (Right) Historical changes in channel position due to channel migration in grazed area.

Evidence from field reconnaissance and inspection of aerial photography supports the conclusion that cattle grazing plays an important role in accelerating floodplain and streambank erosion. Analysis of airborne Lidar data indicates that the average slope of the grazed floodplain surface is about 3° toward the main channel. Bare exposed soil exists on cattle pathways and ramps into the stream, some of which have evolved into short, eroded gullies (Figure 2.10).

These exposed areas of soil contain abundant amounts of loose erodible fine material that can be introduced into the stream. Trampling on the floodplain weakens stream banks, increasing susceptibility to erosion. Hoof action both on stream banks and within the channel introduces sediment to the stream directly. Soils covered by short, shallowly rooted grasses on the floodplain surface are susceptible to erosion by runoff. A prominent gully was identified that appeared to be initiated by erosion where runoff entering the floodplain from a grassed waterway cascaded over the streambank and initiated a headcut that has progressively retreated across the floodplain toward the grassed waterway (Figure 2.11). Compared to the patches of bare, exposed soil and short grass on the grazed floodplain, soil in forested floodplains and grasslands adjacent to meandering reaches are protected from erosion by a thick, continuous cover of plants and grass.

Figure 2.10: (Left) Bare soil (foreground) from cattle trampling on a floodplain surface with unvegetated cattle ramp in background. (Right) Eroded streambank and unvegetated cattle pathway.

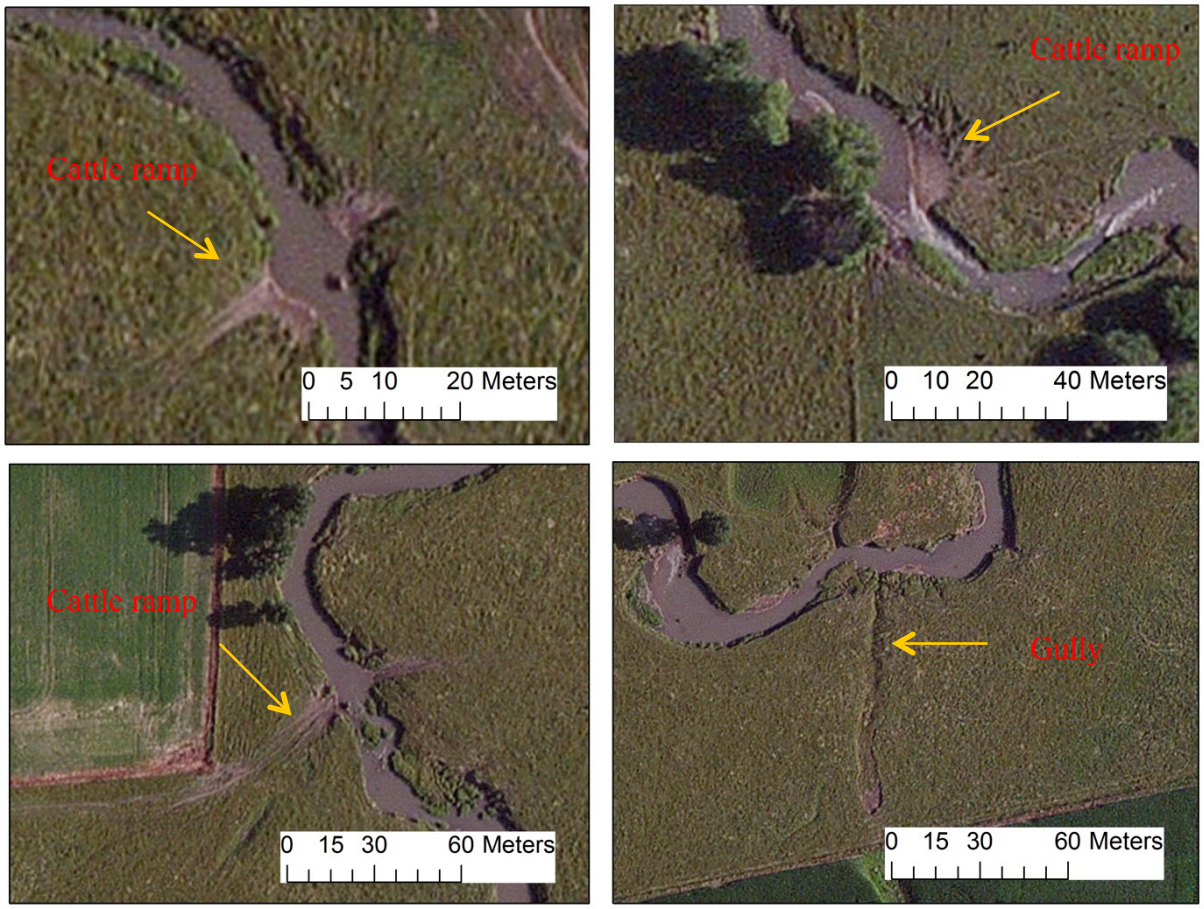

Figure 2.11: Channel migration, cattle pathways and gully scars on the grazed floodplain.

Conditions in the Saybrook watershed are consistent with past work that has shown cattle grazing can lead to exposure of bare soil and reduced soil porosity, permeability and infiltration through compaction. Together these conditions increase surface runoff and soil erosion, thereby increasing agricultural contributions to fine sediment production (Johnson, 1952; Knox, 2001; Lamba et al., 2015). Also, trampling of streambanks by cattle often leads to erosion rates in grazed areas that are substantially higher than rates in ungrazed areas (Trimble, 1994).

Grazed floodplains of the Saybrook watershed only account for 0.29% of the total watershed area, but contribute most of the suspended sediment to the stream system. Other tracing has produced similar results. In southcentral Wisconsin, grazed woodlands were identified as an important source of fine sediment (Lamba et al., 2015). Suspended sediment loss from cattle access paths and loafing areas within 15-m wide strips along the streams in Iowa accounted for up to 72% of the total loss, even though these features accounted for only 2.7% of the total area within 15-m wide riparian zones (Tufekcioglu et al., 2013). Grazed sites in semi-arid grasslands consistently produce 2.8 times more sediment than ungrazed sites (Belnap et al., 2009).

A recent tracing study within the Wildcat Slough watershed of the USRB found that most sediment sampled within the stream was derived from channel banks and forested areas adjacent to meandering reaches of the channel (Neal and Anders, 2015). A small amount of land in the Wildcat Slough watershed is grazed pasture (0.19%), but no signal of this source was found in the tracing results, nor was any material from the floodplain detected. The reason for the disparity in findings between that study and the present investigation is not entirely clear, but may be related to the smaller amount of grazed area in the Wildcat Slough watershed compared to the Saybrook watershed and to backwater effects in Wildcat Slough. The total area of grazed land in the Saybrook watershed is over twice the amount in the Wildcat Slough watershed. Moreover, the only area of grazing in the Wildcat Slough is located near the mouth of this tributary close to its confluence with the Sangamon River. Frequently, flow near the mouth is affected by backwater conditions that promote deposition, rather than erosion.

A common finding between Neal and Anders (2015) and the present study is that row crop agriculture does not constitute a dominant source of instream sediment, even though this

category accounts for over 90% of the land cover in both watersheds. The lack of large proportions of agricultural upland sediments in the stream seems to indicate weak connectivity between agricultural uplands and streams that impedes sediment delivery from this source. Channelized reaches of stream, or drainage ditches, in both watersheds are bounded by artificial levees that prevent surface runoff from directly entering the stream from adjacent hillslopes. Grazed pastures along the Sangamon River upstream from Saybrook also act as a buffer to keep sediment from entering the river from uplands. Low slopes in both watersheds also inhibit rapid downslope movement of soil material. Delivery of upland sediment most likely does occur in both watersheds, but may be threshold-driven and occur in abundance only during large runoff events that lead to enhanced connectivity between uplands and channels.

Other work elsewhere in the agricultural Midwest has shown that human influence on sediment dynamics has shifted or is shifting the main source of suspended sediment in the agricultural Midwest from agricultural land to streambanks and bluffs (Belmont et al., 2011; Stout et al, 2014). In particular, areas of the Midwest affected by the Wisconsin glacial episode, which tend to be characterized by relatively flat depositional uplands interspersed with incised stream valleys, seem to be characterized by the dominance of sources other than uplands. On older glacial landscapes, such those as in southern Iowa where upland slopes vary from 9 to 16%, contributions from uplands can dominate during some events, although contributions from streambanks also are substantial (Fox and Papanicolaou, 2007). Scale may also play a role in producing differences among studies as connectivity between uplands and channels is likely to be stronger in small watersheds, where travel distances of sediment between uplands and sampling locations are short, compared to large watersheds, where these distances are much longer. Although tracing studies in the agricultural Midwest have produced somewhat varied

findings, all of these studies, including the present investigation, indicate that human activities have affected sediment source apportionment. Moreover, this study and others (Belmont et al., 2011; Stout et al., 2014) emphasize the importance of considering floodplains in sediment source tracing.

The extent to which the results of this study can be generalized over time remains uncertain. Aggregated samples of instream sediment were collected only over a few months during spring and summer and only two events were sampled, both in the summer. Although the findings indicate that grazing of floodplains enhances sediment availability, the percentages identified by sediment fingerprinting may not be representative of long-term fluxes of sediment. Also, the results of the Monte Carlo analysis suggest that the delivery of sediment from cropland sources tends to increase with increasing amounts of runoff. Thus, in this low-relief landscape, connectivity of sediment flux across the landscape appears to be related to the magnitude of runoff. During large events runoff pathways from uplands to valley bottoms probably become better integrated, allowing sediment within these flows to be transported greater distances. This effect is enhanced by human-related modification of hillslopes, such as the creation and maintenance of grassed waterways that channel sediment-laden flows toward streams. The flux of sediment across hillslopes will also vary seasonally with movement likely highest from late fall to early spring when many fields are fallow and soils are exposed directly to runoff. Grazing generally is less intensive during winter months as feeding of cattle shifts from forage crops to hay or silage. Sediment fingerprinting conducted under these conditions may yield a different picture of the contributions of different sources to instream sediment flux.

2.6 Conclusion

This study has used sediment fingerprinting tracing techniques to examine the sources of in-stream fine sediment within a headwater agricultural watershed in a low-relief, intensively managed landscape of the midwestern United States. Results demonstrate that the suspended sediment loads are mainly derived both from streambank erosion along grazed areas of the floodplain and from erosion of the grazed floodplain by surface runoff. This study emphasizes the importance of grazed portions of the landscape in supplying suspended sediment to streams in agricultural environments. It highlights the role of humans in transforming the floodplain, a natural depositional environment, into a primary source of fine sediment. It also reinforces findings of previous studies that have demonstrated that relatively flat uplands in landscapes influenced by Wisconsin glaciation are not a major source of fine sediment to stream systems. Therefore, efforts to limit the production of fine sediment in midwestern landscapes should consider land management strategies targeted at grazed floodplains.

Future work should consider the impact of grazing on the sediment budget of the floodplain. Although erosion of the floodplain by failure of streambanks and by direct runoff introduces sediment to the stream system, overbank deposition most likely occurs during events that exceed bankfull flow, resulting in sediment retention. The extent to which human activity associated with floodplain grazing has influenced these erosional and depositional processes remains unclear. Estimates of bank erosion from historical photos (Lauer et al., 2017) or ground-based monitoring could provide a complementary constraint on the sediment budget to justify the fingerprinting results.

Upland soil erosion is a well-documented problem both currently and historically throughout the midwestern United States. This eroded material is eventually delivered to streams

and moves through the drainage network, ending up in reservoirs such as Lake Decatur. The results here indicate that upland material did not reach the stream system in abundance during the events sampled in this study. Additional research is needed to determine the conditions under which, and timescales over which upland sediment reaches streams in large amounts.

2.7 References

Asselman, N.E.M. (2000). Fitting and interpretation of sediment rating curves. *Journal of Hydrology, 234*(3–4), 228–248. http://doi.org/10.1016/S0022-1694(00)00253-5

Belmont, P., Gran, K.B., Schottler, S.P., Wilcock, P.R., Day, S.S., Jennings, C., … Parker, G. (2011). Large shift in source of fine sediment in the upper Mississippi River. *Environmental Science and Technology, 45*(20), 8804–8810. http://doi.org/10.1021/es2019109

Belmont, P., Willenbring, J.K., Schottler, S.P., Marquard, J., Kumarasamy, K., & Hemmis, J.M., (2014). Toward generalizable sediment fingerprinting with tracers that are conservative and nonconservative over sediment routing timescales. *Journal of Soils and Sediments, 14*(8), 1479–1492. http://doi.org/10.1007/s11368-014-0913-5

Belnap, J., Reynolds, R.L., Reheis, M.C., Phillips, S.L., Urban, F.E., & Goldstein, H.L. (2009). Sediment losses and gains across a gradient of livestock grazing and plant invasion in a cool, semi-arid grassland, Colorado Plateau, USA. *Aeolian Research, 1*(1–2), 27–43. http://doi.org/10.1016/j.aeolia.2009.03.001

Bogner, W.C. (2002). Sedimentation survey of Lake Decatur's Big and Sand Creek basins: Macon County, Illinois. Illinois State Water Survey contract report 2002-09.

Collins, A.L., & Walling, D.E. (2002). Selecting fingerprint properties for discriminating potential suspended sediment sources in river basins. *Journal of Hydrology, 261*, 218–244. http://doi.org/10.1016/S0022-1694(02)00011-2

Collins, A.L., Walling, D.E., & Leeks, G.J.L. (1996). Composite fingerprinting of the spatial source of fluvial suspended sediment : a case study of the Exe and Severn river basins, United Kingdom. *Géomorphologie : Relief, Processus, Environnement, 2*, 41–53.

Collins, A.L., Walling, D.E., & Leeks, G.J.L. (1997). Sediment sources in the Upper Severn

catchment: a fingerprint approach. *Hydrology and Earth System Sciences Discussions, 1*(3), 509-521. http://doi.org/10.5194/hess-1-509-1997

Collins, A.L, Walling, D.E., & Leeks, G. (1998). Use of composite fingerprints to determine the provenance of the contemporary suspended sediment load transported by rivers. *Earth Surface Processes, 23*(1), 31–52. http://doi.org/10.1002/(SICI)1096-9837(199801)23:1<31::AID-ESP816>3.0.CO;2-Z

Collins, A.L., Zhang,Y., Walling, D.E., Grenfell, S.E., & Smith, P. (2010). Tracing sediment loss from eroding farm tracks using a geochemical fingerprinting procedure combining local and genetic algorithm optimisation. *Science of the Total Environment, 408*(22), 5461–5471. http://doi.org/10.1016/j.scitotenv.2010.07.066

Collins, A.L., Pulley, S., Foster, I.D.L., Gellis, A., Porto, P., & Horowitz, A.J. (2017). Sediment source fingerprinting as an aid to catchment management: a review of the current state of knowledge and a methodological decision-tree for end-users. *Journal of Environmental Management, 194*, 86–108. http://doi.org/10.1016/j.jenvman.2016.09.075

D'Haen, K., Verstraeten, G., & Degryse, P. (2012). Fingerprinting historical fluvial sediment fluxes. *Progress in Physical Geography, 36*(2), 154–186. http://doi.org/10.1177/0309133311432581

Davis, C.M., & Fox, J.F. (2009). Sediment fingerprinting: review of the method and future improvements for allocating nonpoint source pollution. *Journal of Environmental Engineering, 135*(7), 490–504. http://doi.org/10.1061/(ASCE)0733-9372(2009)135:7(490)

Evrard, O., Navratil, O., Ayrault, S., Ahmadi, M., Némery, J., Legout, C., … Esteves, M. (2011). Combining suspended sediment monitoring and fingerprinting to determine the spatial origin of fine sediment in a mountainous river catchment. *Earth Surface Processes and*

Landforms, 36(8), 1072–1089. http://doi.org/10.1002/esp.2133

Evrard, O., Poulenard, J., Némery, J., Ayrault, S., Gratiot, N., Duvert, C., …. Esteves, M. (2013). Tracing sediment sources in a tropical highland catchment of central Mexico by using conventional and alternative fingerprinting methods. *Hydrological Processes, 27*(6), 911–922. http://doi.org/10.1002/hyp.9421

Fitzpatrick, W.P., Bogner, W.C., & Bhowmik N.G. (1987). Sedimentation and Hydrologic Processes in Lake Decatur and Its Watershed. Illinois State Water Survey Report of Investigation 107.

Fox, J. F., & Papanicolaou, A.N. (2007). The use of carbon and nitrogen isotopes to study watershed erosion processes. *Journal of the American Water Resources Association, 43*(4), 1047–1064. http://doi.org/10.1111/j.1752-1688.2007.00087.x

Fox, J. F., & Papanicolaou, A.N. (2008). Application of the spatial distribution of nitrogen stable isotopes for sediment tracing at the watershed scale. *Journal of Hydrology, 358*(1–2), 46–55. http://doi.org/10.1016/j.jhydrol.2008.05.032

Gao, P., & Josefson, M. (2012). Temporal variations of suspended sediment transport in Oneida Creek watershed, central New York. *Journal of Hydrology, 426*, 17–27. http://doi.org/10.1016/j.jhydrol.2012.01.012

Gellis, A.C., & Landwehr, J.M. (2006). Identifying sources of fine-grained suspended sediment in the Pocomoke River, an Eastern Shore tributary to the Chesapeake Bay. In Proceedings of the 8th Federal Interagency Sedimentation Conference (Vol. 2, p. e6).

Gellis, A.C., & Walling, D.E. (2011). Sediment source fingerprinting (tracing) and sediment budgets as tools in targeting river and watershed restoration programs. *Geophysical Monograph Series, 194*, 263–291. http://doi.org/10.1029/2010GM000960

Gellis, A.C., & Noe, G.B. (2013). Sediment source analysis in the Linganore Creek watershed, Maryland, USA, using the sediment fingerprinting approach: 2008 to 2010. *Journal of Soils and Sediments, 13*(10), 1735–1753. http://doi.org/10.1007/s11368-013-0771-6

Gingele, F.X., & De Deckker, P. (2005). Clay mineral, geochemical and Sr–Nd isotopic fingerprinting of sediments in the Murray–Darling fluvial system, southeast Australia. *Australian Journal of Earth Sciences, 52*(6), 965–974. http://doi.org/10.1080/08120090500302301

Gregory, K.J.. (2006). The human role in changing river channels. *Geomorphology, 79*(3), 172–191. http://doi.org/10.1016/j.geomorph.2006.06.018

Grimshaw, D.L., & Lewin, J. (1980). Source identification for suspended sediments. *Journal of Hydrology, 47*, 151–162.

Haan, M.M., Russell, J.R., Powers, W.J., Mickelson, S.K., Ahmed, S.I., Kovar, J.K., & Schultz, R.C. (2003). Effects of grazing management on sediment and phosphorus in runoff. *Rangeland Ecology & Management, 59*(6), 607-615. https://doi.org/10.2111/05-152R2.1

Hancock, G.J., Wilkinson, S.N., Hawdon, A.A., & Keen, R.J. (2014). Use of fallout tracers 7Be, 210Pb and 137Cs to distinguish the form of sub-surface soil erosion delivering sediment to rivers in large catchments. *Hydrological Processes, 28*(12), 3855–3874. http://doi.org/10.1002/hyp.9926

Horowitz, A.J. (2003). An evaluation of sediment rating curves for estimating suspended sediment concentrations for subsequent flux calculations. *Hydrological Processes, 17*(17), 3387–3409. http://doi.org/10.1002/hyp.1299

Johnson, E.A. (1952). Effect of farm woodland grazing on watershed values in the southern Appalachian mountains. *Journal of Forestry, 50*(2), 109–113.

http://doi.org/10.1007/s13398-014-0173-7.2

Kim, J.Y., & Sansalone, J. (2008). Event-based size distributions of particulate matter transported during urban rainfall-runoff events. *Water Research, 42*(10–11), 2756–2768. http://doi.org/10.1016/J.WATRES.2008.02.005

Knox, J.C. (2001). Agricultural influence on landscape sensitivity in the Upper Mississippi River Valley. *Catena, 42*(2–4), 193–224. http://doi.org/10.1016/S0341-8162(00)00138-7

Koiter, A.J., Owens, P.N., Petticrew, E.L., & Lobb, D.A. (2013). The behavioural characteristics of sediment properties and their implications for sediment fingerprinting as an approach for identifying sediment sources in river basins. *Earth-Science Reviews, 125*, 24–42. http://doi.org/10.1016/j.earscirev.2013.05.009

Lamba, J., Karthikeyan, K.G., & Thompson, A.M. (2015). Apportionment of suspended sediment sources in an agricultural watershed using sediment fingerprinting. *Geoderma, 239*, 25–33. http://doi.org/10.1016/j.geoderma.2014.09.024

Lauer, J.W., Echterling, C., Lenhart, C.F., Belmont, P., & Rausch, R. (2017). Air-photo based change in channel width in the Minnesota River basin: Modes of adjustment and implications for sediment budget. *Journal of the American Water Resources Association, 297*, 170–184. http://doi.org/10.1016/j.geomorph.2017.09.005

Martinez-Carreras, N., Gallart, F., Iffly, J.F., Pfister, L., Walling, D.E., & Krein, A. (2008). Uncertainty assessment in suspended sediment fingerprinting based on tracer mixing models : a case study from Luxembourg. Sediment Dynamics in Changing Environments, *IAHS Publication, 325*, 94–105.

Martínez-Carreras, N., Udelhoven, T., Krein, A., Gallart, F., Iffly, J.F., Ziebel, J., … Walling, D.E. (2010). The use of sediment colour measured by diffuse reflectance spectrometry to

determine sediment sources: Application to the Attert River catchment (Luxembourg). *Journal of Hydrology, 382*(1), 49–63. http://doi.org/10.1016/j.jhydrol.2009.12.017

Mukundan, R., Radcliffe, D.E., Ritchie, J.C., Risse, L.M., & McKinley, R.A. (2010). Sediment fingerprinting to determine the source of suspended sediment in a southern Piedmont Stream. *Journal of Environment Quality, 39*(4), 1328. http://doi.org/10.2134/jeq2009.0405

Neal, C.W.M., & Anders, A.M. (2015). Suspended sediment supply dominated by bank erosion in a low-gradient agricultural watershed, Wildcat Slough, Fisher, Illinois, United States. *Journal of Soil and Water Conservation, 70*(3), 145–155. http://doi.org/10.2489/jswc.70.3.145

Olley, J., & Caitcheon, G. (2000). Major element chemistry of sediments from the Darling–Barwon river and its tributaries: implications for sediment and phosphorus sources. *Hydrological Processes, 14*(7), 1159–1175. http://doi.org/10.1002/(SICI)1099-1085(200005)14:7<1159::AID-HYP6>3.0.CO;2-P

Peart, M., & Walling, D. (1986). Fingerprinting sediment source: the example of a drainage basin in Devon, UK. Hadley R.F. (Ed.), Drainage Basin Sediment Delivery, IAHS Publication, 159, IAHS Press, Wallingford, 41-55

Phillips, J. M., Russell, M.A., & Walling, D.E. (2000). Time-integrated sampling of fluvial suspended sediment: A simple methodology for small catchments. *Hydrological Processes, 14*, 2589–2602. http://doi.org/10.1002/1099-1085(20001015)14:14<2589::AID-HYP94>3.0.CO;2-D

Pimentel, D. (2012). Biofuels Causing Malnutrition in the World. In Global Economic and Environmental. Pimentel, David (Editor). Aspects of Biofuels. Taylor & Francis, Boca Raton, FL,1-13.

Rhoads, B., & Herricks, E. (1996). Naturalization of headwater streams in Illinois: challenges and possibilities. John Wiley & Sons: New York, 331-367.

Rhoads, B.L., Lewis, Q.W., & Andresen, W. (2016). Historical changes in channel network extent and channel planform in an intensively managed landscape: Natural versus human-induced effects. *Geomorphology, 252*, 17–31. http://doi.org/10.1016/j.geomorph.2015.04.021

Rhoton, F., Emmerich, W., & Nearing, M. (2006). Identification of sediment sources in a semiarid watershed using multiple diagnostic properties. In Proc., Federal Interagency Sedimentation Conf.

Ritchie, J., & Mchenry, J.R. (1990). Application of radioactive fallout Cesium-137 for measuring soil erosion and sediment accumulation rates and patterns : a review. *Journal of Environmental Quality, 19*, 215–233. http://doi.org/10.2134/jeq1990.00472425001900020006x

Seeger, M., Errea, M. P., Beguería, S., Arnáez, J., Martí, C., & García-Ruiz, J.M. (2004). Catchment soil moisture and rainfall characteristics as determinant factors for discharge/suspended sediment hysteretic loops in a small headwater catchment in the Spanish pyrenees. *Journal of Hydrology, 288*(3), 299–311. http://doi.org/10.1016/j.jhydrol.2003.10.012

Small, I.F., Rowan, M.C., & Franks, S.W. (2002). Quantitative sediment fingerprinting using a Bayesian uncertainty estimation framework. In: Dyer, F.J., Thoms, F.C., & Olley, J.M. (eds), Structure, Function, and Management Implications of Fluvial Sedimentary Systems, IAHS Publication 276, Wallingford, UK, 443-450.

Slattery, M.C., Burt, T.P., & Walden, J. (1995). The application of mineral magnetic

measurements to quantify within-storm variations in suspended sediment sources. Tracer Technologies for Hydrological Systems, Proceedings of a Boulder Symposium. IAHS Publication 229, 143-152.

Smith, H.G., & Blake, W.H. (2014). Sediment fingerprinting in agricultural catchments: A critical re-examination of source discrimination and data corrections. *Geomorphology, 204*, 177–191. http://doi.org/10.1016/j.geomorph.2013.08.003

Stout, J.C., Belmont, P., Schottler, S.P., & Willenbring, J.K. (2014). Identifying Sediment Sources and Sinks in the Root River, Southeastern Minnesota. *Annals of the Association of American Geographers, 104*(1), 20–39. http://doi.org/10.1080/00045608.2013.843434

Trimble, S.W. (1994). Erosional effects of cattle on streambanks in Tennessee, USA. *Earth surface processes and landforms, 19*(5), 451-464.

Tufekcioglu, M., Schultz, R.C., Zaimes, G.N., Isenhart, T.M., & Tufekcioglu, A. (2013). Riparian Grazing Impacts on Streambank Erosion and Phosphorus Loss Via Surface Runoff. *Journal of the American Water Resources Association, 49*(1), 103–113. http://doi.org/10.1111/jawr.12004

Urban, M.A., & Rhoads, B.L. (2003). Catastrophic human-induced change in stream-channel planform and geometry in an agricultural Watershed, Illinois, USA. *Annals of the Association of American Geographers, 93*(4), 783–796. http://doi.org/10.1111/j.1467-8306.2003.09304001.x

Vaughan, A., Belmont, P., Hawkins, C.P., & Wilcock, P. (2017). Near-channel versus watershed controls on sediment rating curves. *Journal of Geophysical Research: Earth Surface, 122*(10), 1901-1923. http://doi.org/10.1002/2016JF004180

Vercruysse, K., Grabowski, R.C., & Rickson, R.J. (2017). Suspended sediment transport

dynamics in rivers: Multi-scale drivers of temporal variation. *Earth-Science Reviews, 166*, 38–52. http://doi.org/10.1016/j.earscirev.2016.12.016

Walling, D.E. (2005). Tracing suspended sediment sources in catchments and river systems. *Science of The Total Environment, 344*(1–3), 159–184. http://doi.org/10.1016/j.scitotenv.2005.02.011

Walling, D.E., & Woodward, J.C. (1992). Use of radiometric fingerprints to derive information on suspended sediment sources. Erosion and Sediment Transport Monitoring Programmes in River Basins. Proceedings of the Oslo Symposium. IAHS, 210(210), 64–153.

Walling, D.E., Amos, C.M., 1999. Source , storage and mobilisation of fine sediment in a chalk stream system. Hydrological Processes 13(3), 323–340. http://doi.org/10.1002/(SICI)1099-1085(19990228)13:3<323::AID-HYP741>3.0.CO;2-K

Walling, D.E., & Collins, A.L. (2008). The catchment sediment budget as a management tool. *Environmental Science & Policy, 11*(2), 136–143. http://doi.org/10.1016/j.envsci.2007.10.004

Walling, D.E., Woodward, J.C., & Nicholas, A.P. (1993). A multi-parameter approach to fingerprinting suspended-sediment sources. *Tracers in Hydrology, 215*(215), 329–338. http://doi.org/10.2489/jswc.66.5.323

Warrick, J.A. (2015). Trend analyses with river sediment rating curves. *Hydrological processes, 29*(6), 936-949. http://doi.org/10.1002/hyp.10198

Wilkinson, S.N., Hancock, G.J., Bartley, R., Hawdon, A.A., & Keen, R.J. (2013). Using sediment tracing to assess processes and spatial patterns of erosion in grazed rangelands, Burdekin River basin, Australia. *Agriculture, Ecosystems and Environment, 180*, 90–102. http://doi.org/10.1016/j.agee.2012.02.002

Williams, G.P. (1989). Sediment concentration versus water discharge during single hydrologic events in rivers. *Journal of Hydrology, 111*(1–4), 89–106. http://doi.org/10.1016/0022-1694(89)90254-0

Williamson, T.N., Christensen, V.G., Richardson, W.B., Frey, J.W., Gellis, A.C., Kieta, K.A., & Fitzpatrick, F.A. (2014). Stream Sediment Sources in Midwest Agricultural Basins with Land Retirement along Channel. *Journal of Environment Quality, 43*(5), 1624. http://doi.org/10.2134/jeq2013.12.0521

Wilson, C.G., Matisoff, G., & Whiting, P.J. (2003). Short-term erosion rates from a7Be inventory balance. *Earth Surface Processes and Landforms, 28*(9), 967–977. http://doi.org/10.1002/esp.509

Wilson, C.G., Kuhnle, R.A., Bosch, D.D., Steiner, J.L., Starks, P.J., Tomer, M.D., & Wilson, G.V. (2008). Quantifying relative contributions from sediment sources in Conservation Effects Assessment Project watersheds. *Journal of Soil and Water Conservation, 63*(6), 523–532. http://doi.org/10.2489/jswc.63.6.523

Wilson, C.G., Papanicolaou, A.N.T., & Denn, K.D. (2012). Partitioning fine sediment loads in a headwater system with intensive agriculture. *Journal of Soils and Sediments, 12*, 966–981. http://doi.org/10.1007/s11368-012-0504-2

Yu, L., & Oldfield, F. (1989). A multivariate mixing model for identifying sediment source from magnetic measurements. *Quaternary Research, 32*(2), 168–181. http://doi.org/10.1016/0033-5894(89)90073-2

Zapata, F. (2012). Handbook for the assessment of soil erosion and sedimentation using environmental radionuclides (Vol. 219). Dordrecht: Kluwer Academic Publishers. http://doi.org/10.1007/s13398-014-0173-7.2

CHAPTER 3

ANALYSIS OF SUSPENDED SEDIMENT CONCENTRATIONS AT VARIOUS SCALES

Abstract

Transport of fine suspended sediment in streams is influenced by a wide range of factors. The precise link between upstream erosion, sediment mobilization and downstream sediment yield involves many uncertainties because of the nonlinear and discontinuous nature of sediment transfer processes at the watershed scale. To reveal the fundamental controls on sediment transport in intensively managed landscapes, the relationship between suspended sediment properties and the associated precipitation and discharge data of three sediment sampling sites along a lowland agricultural river in an intensively managed agricultural landscape are examined at annual, seasonal, intra-event, and event scales using the sediment rating curve method and hysteresis analysis. Results suggest that sediment rating curves developed for the three sites all show peaked patterns. Suspended sediment load in the stream is far below the stream transport capacity during high flows. The decrease of suspended sediment concentration during high flows might result from decreased sediment inputs to the stream systems or from increased deposition of sediment within the stream system. This study also suggests that the annual sediment load should be carefully estimated for different ranges of discharge based on magnitude-frequency analysis. This study enriches the research of sediment transport in low-gradient agricultural landscapes and highlights the importance of seasonality and drainage area in characterizing sediment dynamics at the watershed scale.

3.1 Introduction

Estimating suspended sediment flux in rivers is valuable for evaluating trends in river water quality and for managing and conserving water resources (Vaughan et al., 2017). Various

watershed models have been developed to estimate sediment loads in rivers (Wischmeier and Smith, 1965; Beasley et al., 1980; Nearing et al., 1989; Young et al., 1989; Morgan et al., 1998; Ewen et al., 2000; Prosser et al., 2001; Papanicolaou et al., 2008). Calibration and validation of these models depend on comparison of model predictions against measured sediment data. Properly estimating river suspended sediment loads involves selection of an appropriate sampling strategy for obtaining data on suspended sediment, a method of estimating suspended sediment load from measured data on sediment concentrations, and more importantly, an understanding of environmental and landscape factors influencing the generation and transport of suspended sediment, including land use and human activities (Gao and Josefson, 2012).

The rating curve methods provides the basis for establishing a relationship between discharge (Q) and suspended sediment concentration (SSC) (Walling and Webb, 1981; Phillips et al., 1999; Horowitz, 2003). Typically, rating curves are developed using regression analysis to fit a statistical function between Q (m^3/s) and SSC (mg/l) (Duan, 1983; Ferguson, 1986; Holtschlag, 2001; Horowitz, 2003; Kazama et al., 2005; Alexandrov et al., 2009). Most commonly, this relation is expressed in the form of a power function:

$$SSC = aQ^b \tag{3.1}$$

where a is a dimensional coefficient and b is a dimensionless exponent. Log-transformed discharge and suspended sediment concentration data are often fitted with a linear regression (Horowitz, 2003a). Using the SRC and continuous daily discharge data, daily suspended sediment load (Q_s) in metric tons per day can be estimated as:

$$Q_s = 0.0864Q(SSC) \tag{3.2}$$

Sediment load for a given time period can be computed by summing the estimated daily sediment loads (Asselman, 2000; Gao and Josefson, 2012).

The SRC for a watershed reflects the patterns of erosion and sediment delivery within a watershed and provides a useful starting point for interpreting important features of watershed sediment responses (Walling and Webb, 1982; Warrick, 2015). A SRC can be considered a "black box" model. Although the coefficients *a* and *b* in Eq. (3.1) have no physical meaning, they often reflect the alteration of sediment supply, the power of the stream to erode and transport sediment, and the spatial scale of the watershed (Asselman, 2000; Warrick, 2015). Rainfall, runoff and water and sediment routing through a landscape and channel network are the fundamental processes that influence sediment rating curves (Asselman, 2000; Warrick, 2015). Among those fundamental processes, the rate of sediment supply to a stream is the most obvious process. The rate of water discharge, which is related to the capacity of runoff to erode and transport sediment and also to dilution of the suspended sediment concentration in a stream, is another important variable that influence the sediment rating curve (Warrick, 2015; Warrick and Rubin, 2007). The alteration of sediment supply and water discharge can both influence the sediment rating curve.

Incorporating hysteresis analysis with SRC is a common approach for linking sediment sources to downstream sediment loads at the event-scale (Gao and Puckett, 2012). This analysis involves plotting SSC versus Q through time (Walling, 1974; Walling and Webb, 1982). Sediment at the event scale is controlled by rainfall patterns, seasonality, antecedent soil moisture, availability of erodible materials, the transport capacity of the flow, and the types of sediment sources (Walling, 1974; Walling and Webb, 1982; Asselman, 1999). If these controls influence SSC uniformly throughout an event, the relation between Q and SSC will be the same

during the early and later parts of the event. Under these conditions, the relation plotted in log-log space will be linear. However, if the influence of the controls varies over the event, the relation between SSC and Q will be looped; in other words, the SSC for a given Q will differ between the early and later parts of the event. Different types of hysteresis loops are associated different processes of runoff and sediment transport (Seeger et al., 2004). Williams (1989) concluded that there are five classes of hysteresis loops: single valued, clockwise, counter-clockwise, single valued plus a loop and figure-eight shaped. For most streams, the hysteresis is clockwise: given the same discharge, SSC is higher on rising limb than falling limb (Williams 1989; Gellis, 2013). The clockwise loop usually is interpreted as a first flush phenomenon, which means that sediment in stream is supplied from sources close to sampling locations (Williams, 1989; Seeger, 2004; Gao and Josefson, 2012; Gellis, 2013). It may also indicate source exhaustion during the falling limb, which causes the decrease of SSC (Williams, 1989; Kurashige, 1993; Wilson et sl., 2012). Counter-clockwise loops occur less frequent, but such loops are often prominent when sediment comes from distal sources and erosion is prolonged during flood (Williams, 1989; Asselman, 1999). Clockwise figure 8 type of hysteresis is often caused by ice breakup or initial sediment contribution from stream bed and banks, followed by a delayed contribution of sediment from distal sources (Williams, 1989; Eder et al., 2010).

The use of rating curves to predict sediment loads assumes constancy in the relation between Q and SSC. However, sediment transport across a watershed can be temporally and spatially variable in conjunction with variability in watershed variables such as climate, vegetation, topography, soil type, and human disturbances (de Vente and Poesen, 2005; Ali and De Boer, 2007; Fox and Papanicolaou, 2007; Nadal-Romero et al., 2008; Wilkinson et al., 2009). Changes in suspended sediment load in the stream with time may resulted not only from

variation in discharge but also with changes in climate, upstream sediment supply, landscape processes or human disturbance (Warrick and Rubin, 2007). The precise link between upstream erosion, sediment mobilization and downstream sediment load involves many uncertainties due to the nonlinearity and discontinuous nature of sediment processes. Therefore, the efficacy of sediment rating curve approach in characterizing sediment flux is related to amount of data for developing the rating curve, the statistical method used to fit the sediment rating curve, and the scatter about the regression line (Walling and Webb, 1981; Asselman 2000). (Asselman, 2000; Horowitz, 2003). Complex sediment dynamics often lead to considerable scatter around the best fit trend for Eq. (3.1) or even nonlinear trends that do not conform to power functions. Although various correction methods have been developed (Ferguson, 1986; Asselman, 2000) and more complex functions have been used to fit sediment rating curve (Horowitz, 2003), understanding the complex interaction between sediment transport and discharge and the fundamental controls on watershed-scale sediment dynamics are still needed. A fundamental difficulty of understanding sediment dynamics also lies in appropriately estimating sediment loads at different temporal (event, seasonal or annual) and spatial (reach, sub-watershed, watershed) scales (Walling and Zhang, 2004; Owens et al., 2005; Gao and Zhang, 2016). Moreover, a complete, predictive understanding of how water and sediment routed through a watershed and the interactions between water and suspended sediment has yet to be achieved (de Vente et al., 2013; Belmont et al., 2014).

The purpose of this study is to investigate spatial and temporal variability in watershed-scale sediment dynamics in an intensively managed agricultural landscape. It explores relationships among precipitation, discharge and suspended sediment concentrations at intra-event, event and seasonal scales. Analysis focuses on whether the Q-SSC relationship is constant

or varies in relation to the magnitude, seasonality, or spatial scale of runoff. By highlighting spatial and temporal variability in suspended sediment transport, the results provide insights into the sediment dynamics of low-gradient agricultural landscapes.

3.2 Study area

The study area is the Upper Sangamon River Basin (USRB), Illinois (Figure 3.1). The Upper Sangamon River Basin, a 3,690 km^2 watershed, is one of several Critical Zone Observatories in the US. It is characterized by low-relief, agricultural lands dominated by row-crop agriculture. The Upper Sangamon River Basin consists of natural, managed, and built environments (Winter, 2001). The diverse land-use pattern provides gradients in the landscape that should influence spatial patterns of sediment dynamics. The intensively managed landscape in the Upper Sangamon River Basin is representative of landscape transformations throughout the Midwest, which provides an opportunity to advance general understanding of sediment dynamics in IMLs.

Sediment samples for analysis in this study were collected during storm events at three sampling sites located throughout the watershed. The Saybook sediment sampling site is located in a headwater of USRB with a drainage area of 84.3 km^2. Mahomet sediment sampling site is located in the mainstem near the town of Mahomet, IL with a drainage area of 969.8 km^2. Monticello sediment sampling site is located in the downstream of mainstem near the city of Monticello, IL with a drainage area of 1400 km^2.

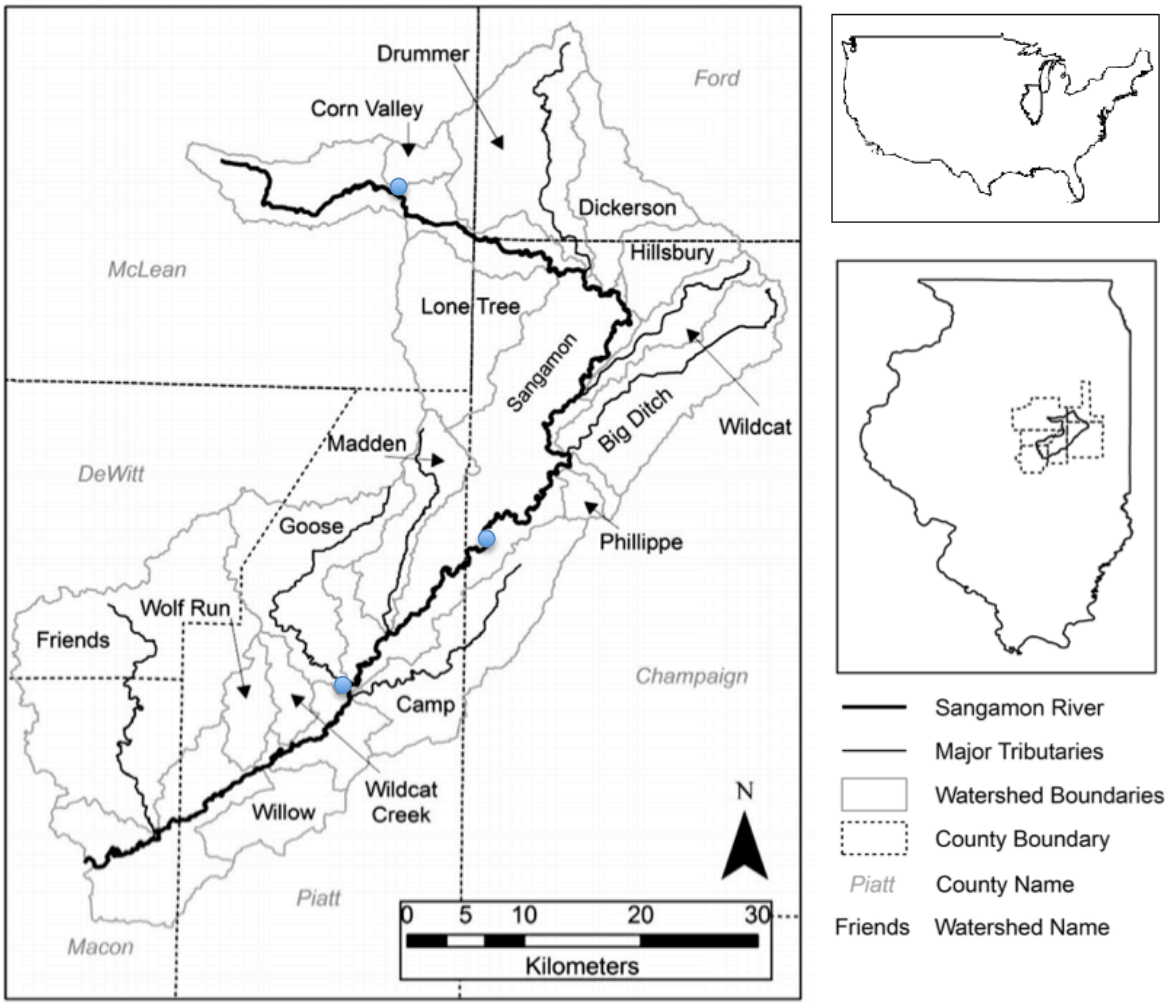

Figure 3.1: The Upper Sangamon River basin showing the location of the sediment sampling sites. Blue dots show the location of three sediment sampling sites from upstream to downstream: Saybrook, Mahomet, and Monticello.

3.3 Data and methods

Stage-discharge rating curves were constructed to determine the relationship between stage and discharge at three sediment sites. At Saybrook site, water discharge was measured using a Swoffer current meter during low, wadeable flows and an acoustic Doppler current profiler (ADCP) during high, unwadeable flows. Stage was monitored at 15-minute intervals

using pressure transducers installed within the rivers at the discharge-measurement locations. Discharge and stage date for Mahoment and Monticello sites are obtained from Illinois State Water Survey.

Daily rainfall data from 2013 to 2017 at Champaign 3S station were obtained from the Midwestern Regional Climate Center. Suspended sediment samples were collected throughout individual runoff events at all three sites using ISCO 6712 automatic pump samplers. The ISCO samplers were installed with intake tubes mounted above the normal flow heights. Samples of water and suspended sediment were obtained at specific time intervals when the water level exceeded a critical value, at irregular time intervals based on variations in the rate of change in water stage, or at regular time intervals. A total of 460 samples were collected from 2014 to 2016 at Saybrook with most samples obtained in spring and summer. No flood events were sampled in the winter because the ISCO samples had to be removed because of the danger of ice cover damaging the sampling equipment. A total of 392 samples were collected from 2014 to 2017 at Mahomet, and a total of 654 samples were collected at Monticello from 2013 to 2017. The threat of ice cover was not as great at these two sites and some winter samples were collected at these stations. After samples of water and sediment were transferred to the laboratory, suspended sediment concentrations were measured using the standard gravimetric method. Particle sizes of event samples were not determined; however, particle size analysis of suspended sediment collected at Monticello for Illinois State Water Survey Benchmark monitoring program shows that an average of 83.4% of suspended sediment was finer than 0.0625mm, which means suspended sediment samples mostly comprise silt, clay, and fine sand.

The statistical properties of discharge and suspended sediment concentration were examined to examine fundamental controls on sediment flux. SRCs for three sediment sites were

developed both for entire discharge-concentration datasets and for seasonal data to investigate temporal variations in patterns of fine sediment transport. To facilitate comparison between watersheds of different size and move the center of mass of the log-transformed Q data to the y intercept at y-axel, discharge data were normalized by the geometric mean of the sample discharges (Warrick, 2014; Vaughan et al., 2017). The power function SRC takes the form,

$$SSC = \hat{a}(\frac{Q}{Q_{GM}})^{\hat{b}} \tag{3.3}$$

where SSC is the suspended sediment concentration (mg/L), Q is the discharge (m^3/s), Q_{GM} is the geometric mean of the sample discharges (m^3/s), $\hat{a}$ is the vertical offset parameter (mg/L), and $\hat{b}$ is the slope between the log-transformed Q and SSC data.

To investigate the different processes of runoff and sediment transport at the three sites, classes of hysteresis loops for event samples are identified and interpreted. The hysteresis loops of event samples collected on April 5-19 and May 8-24, 2016 are compared to reveal the scaling of the relationships between discharge and suspended sediment load.

3.4 Results

3.4.1 Statistical properties of Q and C

Mean, maximum, minimum, standard deviation and coefficient of variation of daily rainfall totals for the Champaign 3S precipitation station were calculated for the complete dataset and also for each season (Table 3.1). Summer has the highest mean and maximum daily rainfall, whereas winter has the lowest mean daily rainfall and highest coefficient of variance.

Table 3.1: Statistical properties of daily rainfall.

	Spring	Summer	Fall	Winter	Total
Mean (mm/day)	3.1	3.9	2.7	1.7	2.9
Stdev (mm/day)	7.4	10.9	7.6	5.5	8.2
Max. (mm/day)	71.6	110.0	67.8	69.1	110.0
Min. (mm/day)	0.0	0.0	0.0	0.0	0.0
CV	2.4	2.8	2.8	3.3	2.8

The statistical properties of Q and SSC of event samples reflect the seasonality of runoff generation and sediment transport. Among the three seasons, summer had the highest mean discharge and fall had the highest mean SSC at Saybrook site. Spring had the highest maximum SSC and also largest coefficient of variation. Highest maximum SSC in spring was probably caused by the snowmelt and early spring floods that flushed the sediment from hillslopes and stream bed.

SSC does not follow the same seasonal pattern of discharge at Mahomet. The highest mean discharge occurred in winter and highest mean SSC occurred in summer. The highest mean discharge in winter is attributed to a relatively large flood event that occurred on December 30, 2015; other storm events in winter were relatively small. The influence of this single event on winter runoff is consistent with the high standard deviation and coefficient of variance of SSC in winter. The high mean SSC in summer may be attributable to intensive erosion by runoff during heavy rainfall events associated with convective storms.

The highest mean discharge and maximum SSC occurred in summer at Monticello – the season with the greatest rainfall and maximum rainfall. Mahomet had the highest mean and

maximum SSC in the summer, but the greatest mean and maximum discharge occurred in the winter. The highest maximum and mean SSC were in spring and fall respectively at Saybrook. These results suggest sediment concentrations tend to become more coincident with the seasonality of rainfall with increasing watershed size. Mean SSC, maximum SSC, and the variability of SSC are all greatest at Saybrook, the site with the smallest watershed area. Mean SSC and maximum SSC decrease downstream from Saybrook to Mahomet to Monticello.

Table 3.2: Statistical properties of Q and SSC.

		Spring			Summer			Fall			Winter			Year		
		Saybrook	Mahomet	Monticello	Saybrook	Mahomet	Monticello	Saybrook	Mahomet	Monticello	Saybrook	Mahomet	Monticello	Saybrook	Mahomet	Monticello
	Sample numbers	205	90	223	165	172	215	90	89	133	0	41	83	460	392	654
Q	Mean (m^3/s)	7.53	21.71	30.06	18.91	26.67	54.07	11.52	20.35	11.62	-	43.37	47.08	12.39	25.84	30.93
	Stdev.	2.12	14.6	24.23	14.55	21.2	44.91	5.23	11.71	11.69	-	42.96	76.78	10.43	22.54	40.15
	Max. (m^3/s)	14.96	59.95	210.27	64.3	125.58	200.08	22.9	46.08	48.11	-	182.9	379.22	64.3	182.9	379.22
	Min. (m^3/s)	5.2	3.49	4.08	4.07	2.03	0.49	2	3.69	0.08	-	4.99	0.22	2	2.03	0.08
	CV	0.28	0.67	0.81	0.77	0.79	0.83	0.45	0.58	1.01	-	0.99	1.63	0.84	0.87	1.3
SSC	Mean (mg/L)	179.94	110.02	111.07	300.87	143.78	103.31	431.19	98.65	98.25	-	110.34	81.57	272.48	122.29	103.79
	Stdev.	170.51	67.93	73.87	165.2	85.98	107.05	179.52	63.22	56.64	-	96.81	57.37	194.87	80.76	73.6
	Max. (mg/L)	1923.39	432.69	683.96	1230.52	658.7	904.85	732.46	291.81	428.44	-	431.39	269.69	1923.39	658.7	904.85
	Min. (mg/L)	105.2	26.28	15.37	105.55	42.5	17.18	35.34	16.39	9.32	-	32.36	6.67	35.34	16.39	6.67
	CV	0.95	0.62	0.67	0.55	0.6	1.04	0.42	0.64	0.58	-	0.88	0.7	0.72	0.66	0.71

3.4.2 Sediment rating curve analysis

Rating curves for all three sites exhibit considerable scatter. Despite this scatter, distinct segmentation of the three rating curves is evident with two distinct trends separated by a threshold value of geometric mean discharge Q_{GM}. To distinguish two sediment processes, linear regression equations were fitted separately for sediment data in ranges of $Q < Q_{GM}$ and $Q > Q_{GM}$. The slope of sediment rating curve (exponent $\hat{b}$ in Eq. (3.2)) for the samples in $Q < Q_{GM}$ is positive, while slope of sediment rating curve for samples in $Q > Q_{GM}$ is negative.

Table 3.3: Rating curves for three sites in low flow and high flow ranges.

	$Q < Q_{GM}$	$Q > Q_{GM}$
Saybrook	$\log(SSC) = 0.84 \log(Q) + 2.34$	$\log(SSC) = -0.17 \log(Q) + 2.58$
Mahomet	$\log(SSC) = 0.13 \log(Q) + 2.06$	$\log(SSC) = -0.12 \log(Q) + 2.03$
Monticello	$\log(SSC) = 0.18 \log(Q) + 2.07$	$\log(SSC) = -0.31 \log(Q) + 1.97$

Table 3.4: Mean SSC for rising limb and falling limb at three sites.

	Mean SSC for rising limb (mg/l)	Mean SSC for falling limb (mg/l)
Saybrook	299.53	271.44
Mahomet	151.92	100.52
Monticello	112.36	99.63

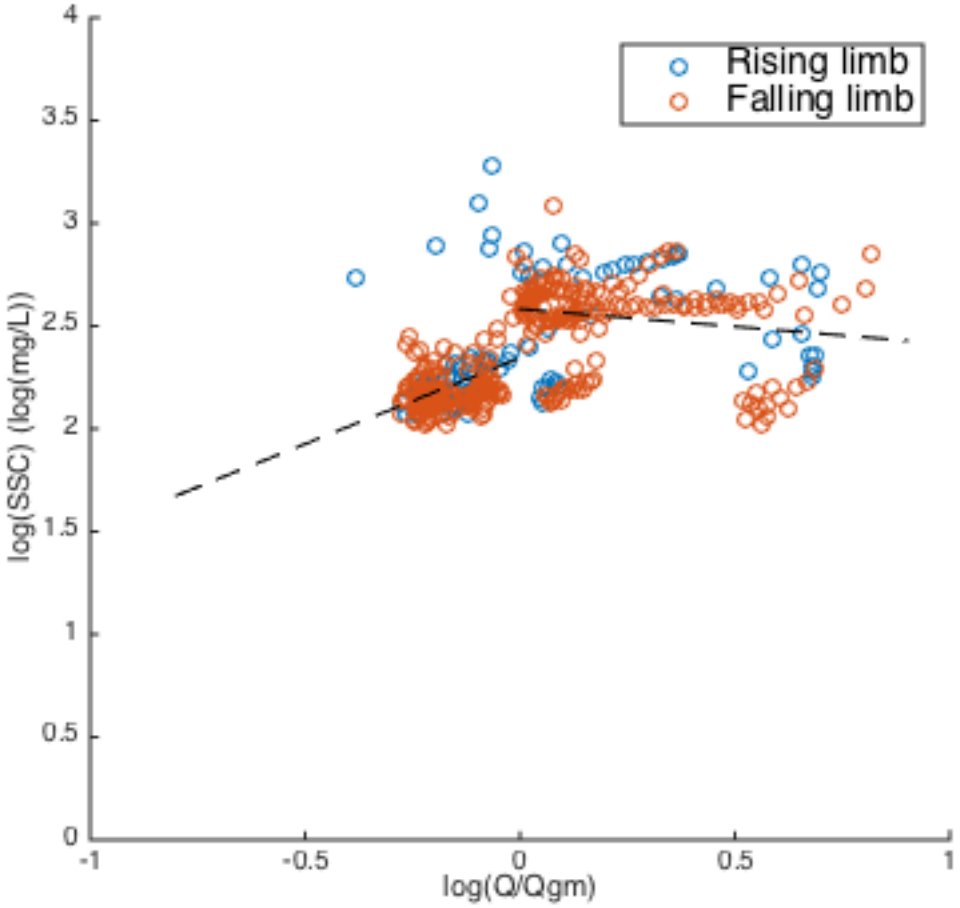

Figure 3.2: Sediment rating curve for Saybrook site.

The negative rate of increase in SSC with increasing discharge for large discharges ($Q > Q_{GM}$) indicates that the rate of increase in sediment load declines with increasing discharge. Moreover, differences exist between rising and falling limbs of hydrograph with SSCs for the rising limb exceeding slightly those for the falling limb (Table 3.4).

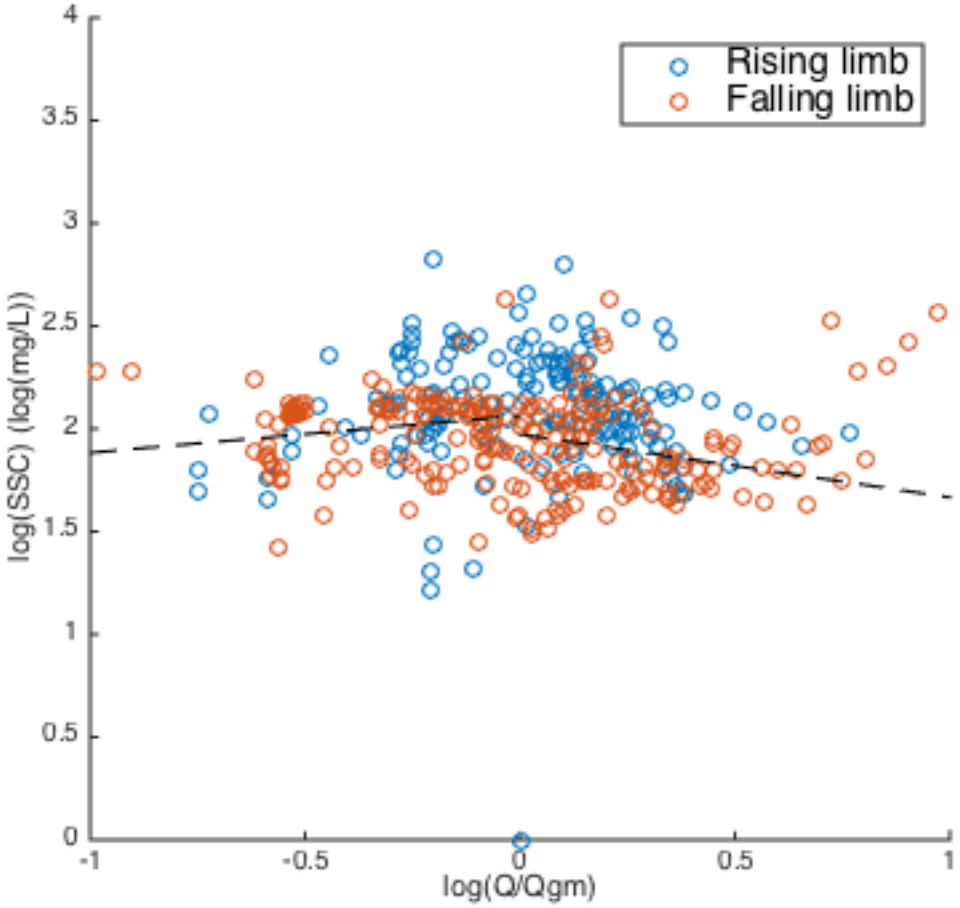

Figure 3.3: Sediment rating curve for Mahomet site.

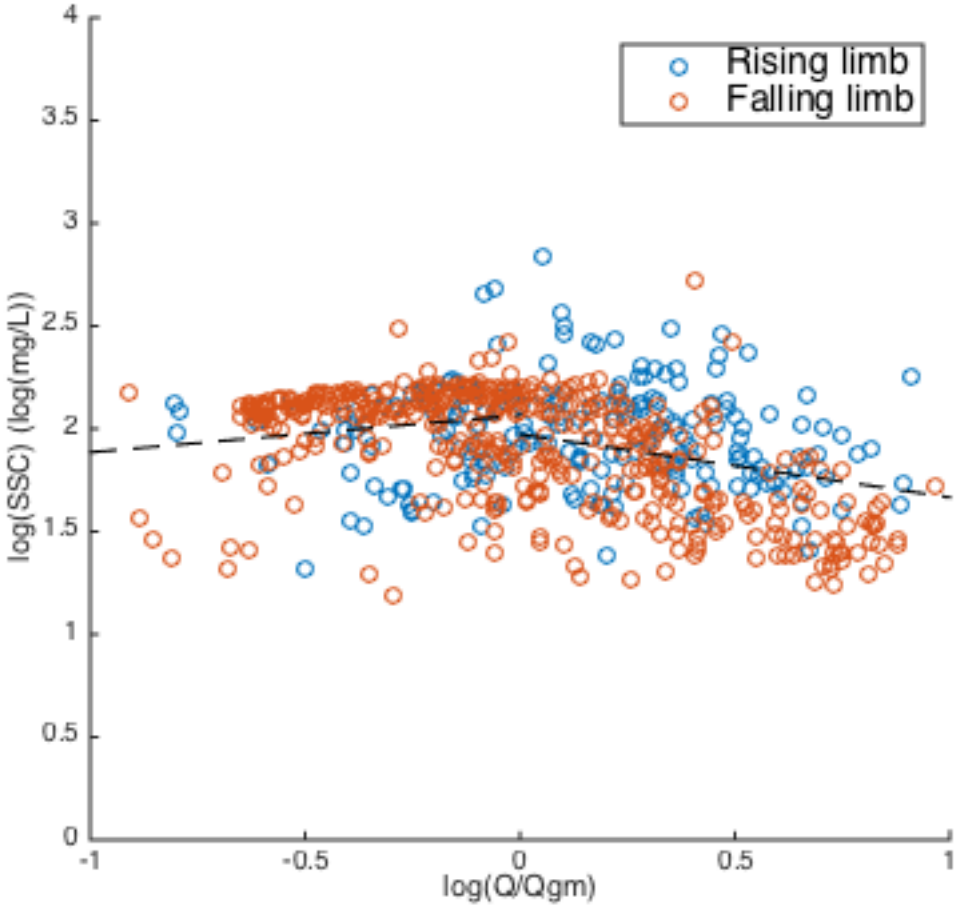

.

Figure 3.4: Sediment rating curve for Monticello site.

3.4.3 Seasonal patterns of sediment transport

Plots of SSC versus Q by season for the three gaging sites show that the patterns of data generally do not conform well to a log-log relation but in some cases exhibit patterns similar to the peaked pattern for entire datasets. Data generally are fairly scattered on these plots, even on a seasonal basis. At Saybrook the SSC-Q patterns for spring and summer are relatively flat, indicating little change in SSC with increasing Q. A strong positive relationship exists between Q and SSC for the fall, but SSC data are missing over a consider range of Q.

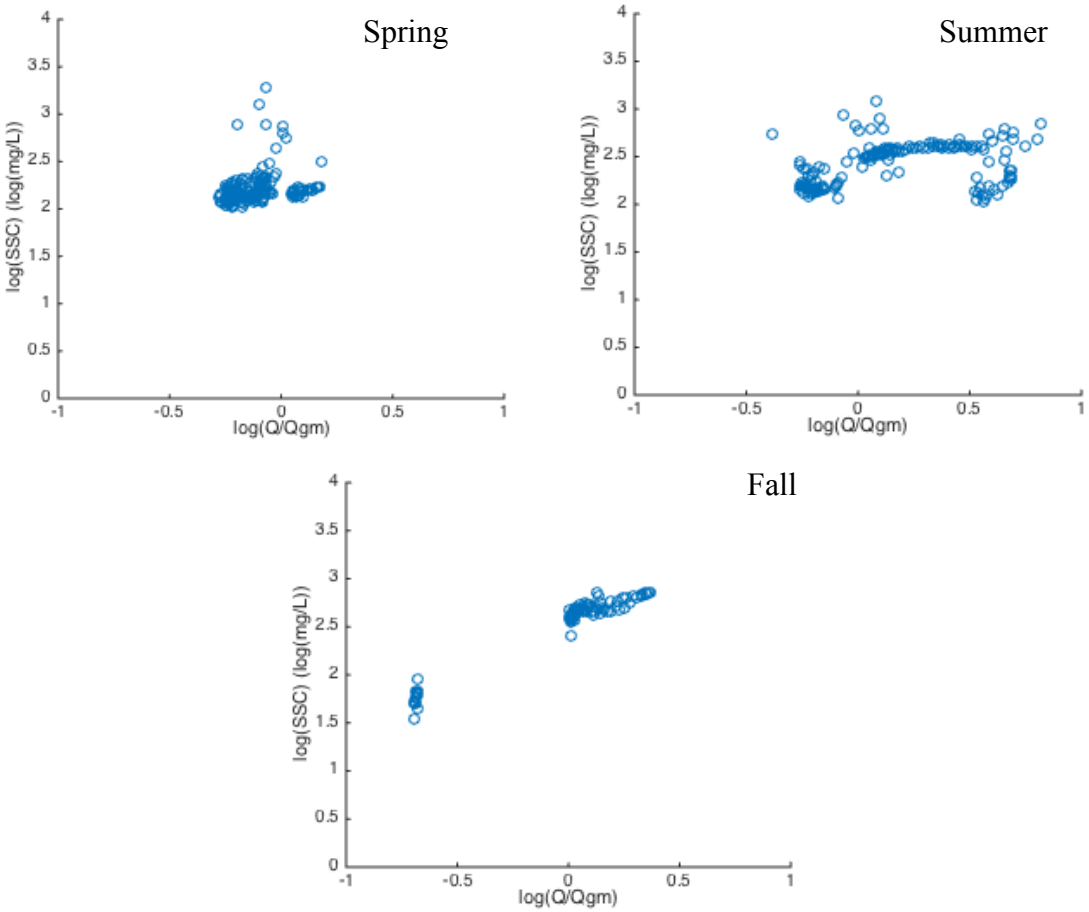

Figure 3.5: Seasonal sediment rating curve at Saybrook site.

Sediment data at Mahomet show an increasing trend as discharge increases in spring, whereas sediment data have a deceasing trend in summer. Because sediment samples were collected at Mahomet during relatively high flow events in summer and collected during low flow events in spring, the opposite trends in spring and summer coincide with the SRC trends in low flow and high flow ranges. The differences of sediment transport in spring and summer is

consistent with seasonal changes of land cover. Less vegetation cover and more exposed bare soils in spring than summer presumably provides more available material for erosion in the spring. Low values of R^2 (0.08) values suggest that power functions fail to accurately characterize the SSC-Q relation in fall and winter.

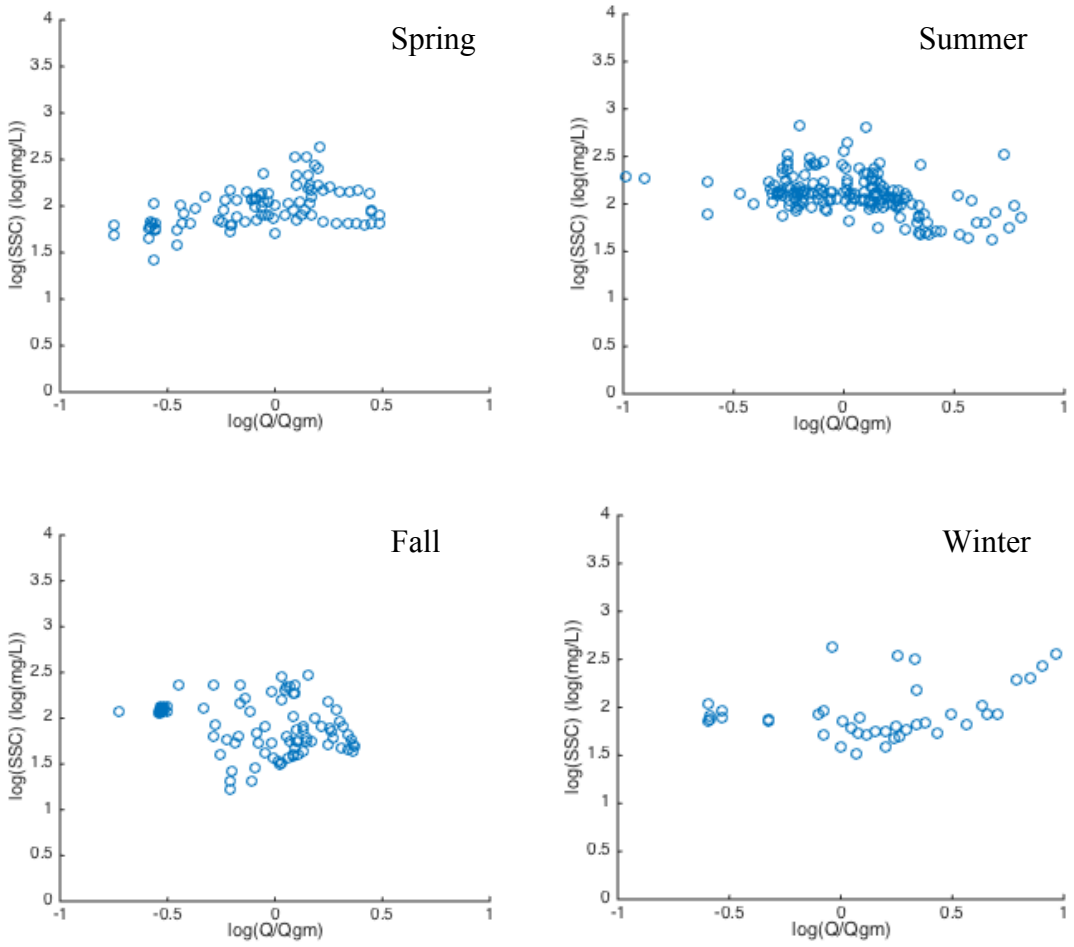

Figure 3.6: Seasonal sediment rating curve at Mahomet.

At Monticello site, the summer SSC-Q relation and to some extent the spring relation exhibit humped patterns similar to those for the entire data set. Data for fall and winter are scattered and do not exhibit any obvious trends.

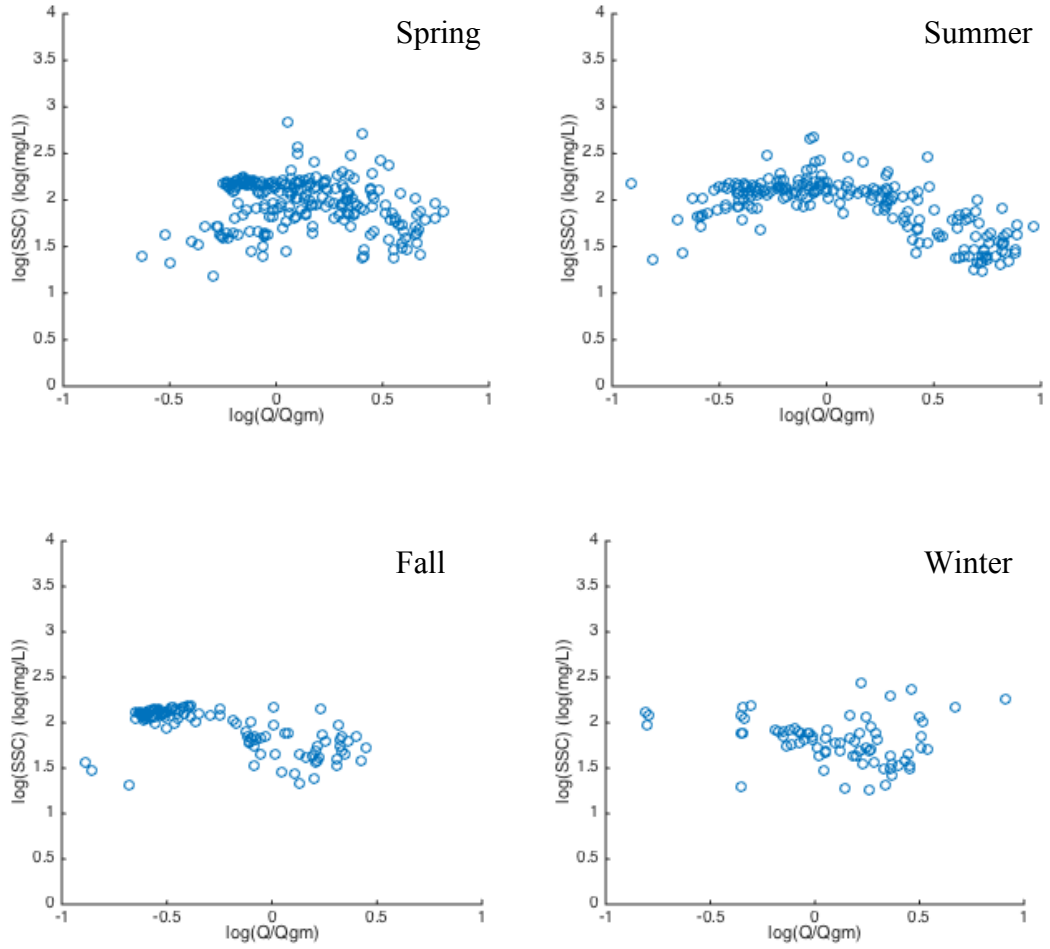

Figure 3.7: Seasonal sediment rating curve at Monticello.

3.4.4 Hysteresis analysis of flood events

Clockwise hysteresis loops are most common at three sites with SSC peaking earlier than discharge. A total of 15 flood events were captured at Saybrook site, among which 8 events had clockwise loops, one event had counter-clockwise loop and other 6 events had no hysteresis. The event with counter-clockwise hysteresis loop occurred in fall after a relatively long dry period (1 month). The reason for lagged peak of SSC is unclear. The thick vegetation in fall might impede sediment transporting from sources to the stream. Among the 6 events that have no hysteresis, 4 events occurred in spring. Snowmelt, early spring floods, and localized erosion might complicate

sediment supply and transport in spring. No figure 8/clockwise loop was presented in Saybrook sediment data, which means no distal sources contributed sediment to the stream.

Sediment samples were collected from 15 flood events at Mahomet site, of which 8 events had figure-8/clockwise loops and 5 events had clockwise loops, and 2 events had complex loops with no hysteresis. Despite the different types of hysteresis loops, suspended sediment concentrations peaked before discharge in all events. Clockwise loops indicate that erosion of available materials during floods resulted in high suspended sediment concentrations during the beginning of the flood event. The lower SSCs during the falling limb may reflect a decrease in the amount of available sediment delivered to the stream. The figure-8/clockwise loops indicate that distal sources contributed sediment to the stream.

At Monticello site, 28 flood events were sampled, among which 10 events had figure 8/ clockwise loops, one event had counter-clockwise loop, 9 events had clockwise hysteresis loops and the rests had no hysteresis. The event with counter-clockwise loop occurred in early summer just after the recession of preceding flood. The exhaustion of available surface materials may result in the delayed peak of suspended sediment.

Among all the events, samples of fine suspended sediment were collected at all three gaging stations in April 5-19, 2016 and May 9-22, 2016, providing the basis for comparison of how sediment dynamics within the USRB vary with watershed scale. The total rainfall for April 5-19 event and May 9-22 event are 37 mm and 46 mm respectively. In April event, suspended sediment concentrations and sediment fluxes at three sites all peaked before water discharge peaked (Figure 3.8 & 3.9). Temporal patterns of suspended sediment for Mahomet and Monticello exhibit figure8/clockwise loops, whereas no hysteresis is apparent for the Saybrook

station. The increases in SSC during the falling limb at Mahomet and Monticello were possibly contributed by distal sources from sub-watersheds.

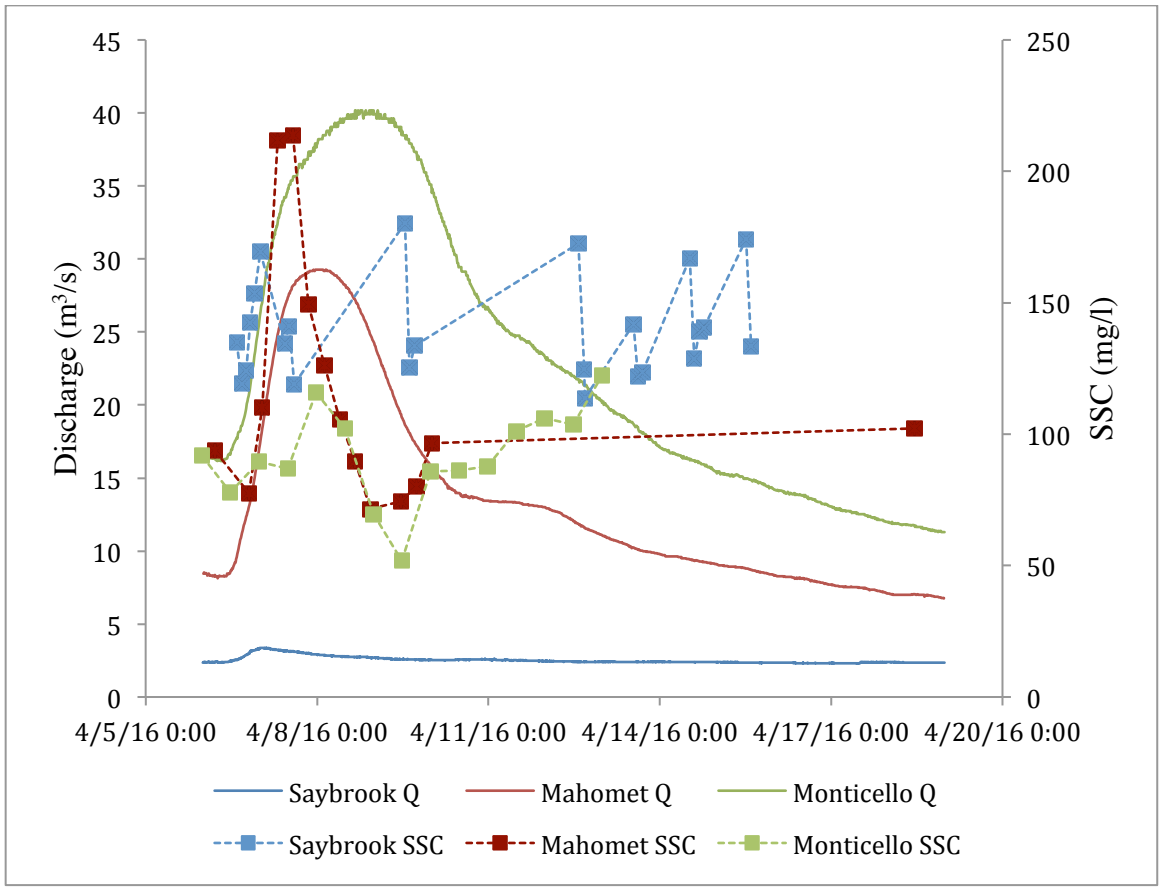

Figure 3.8: Q and SSC at three sites in April event, 2016.

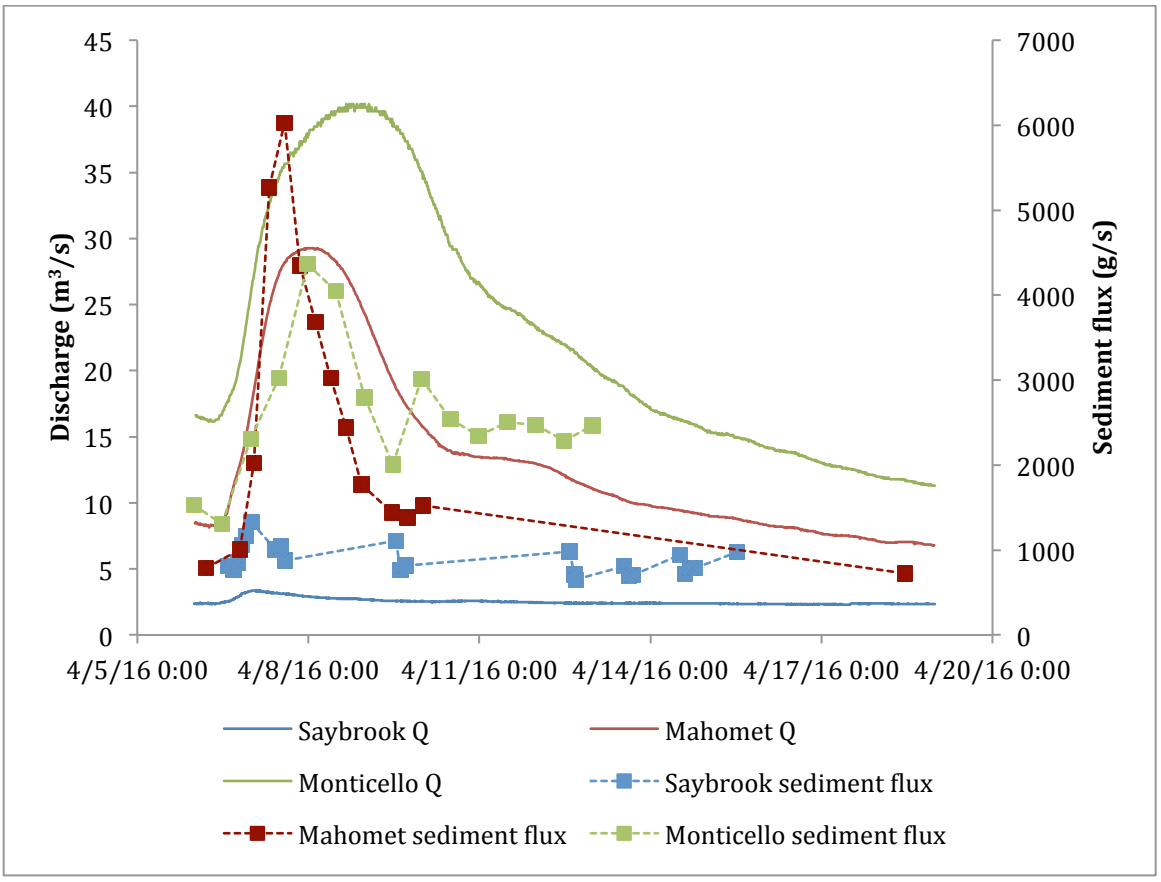

Figure 3.9: Q and sediment flux at three sites in April event, 2016.

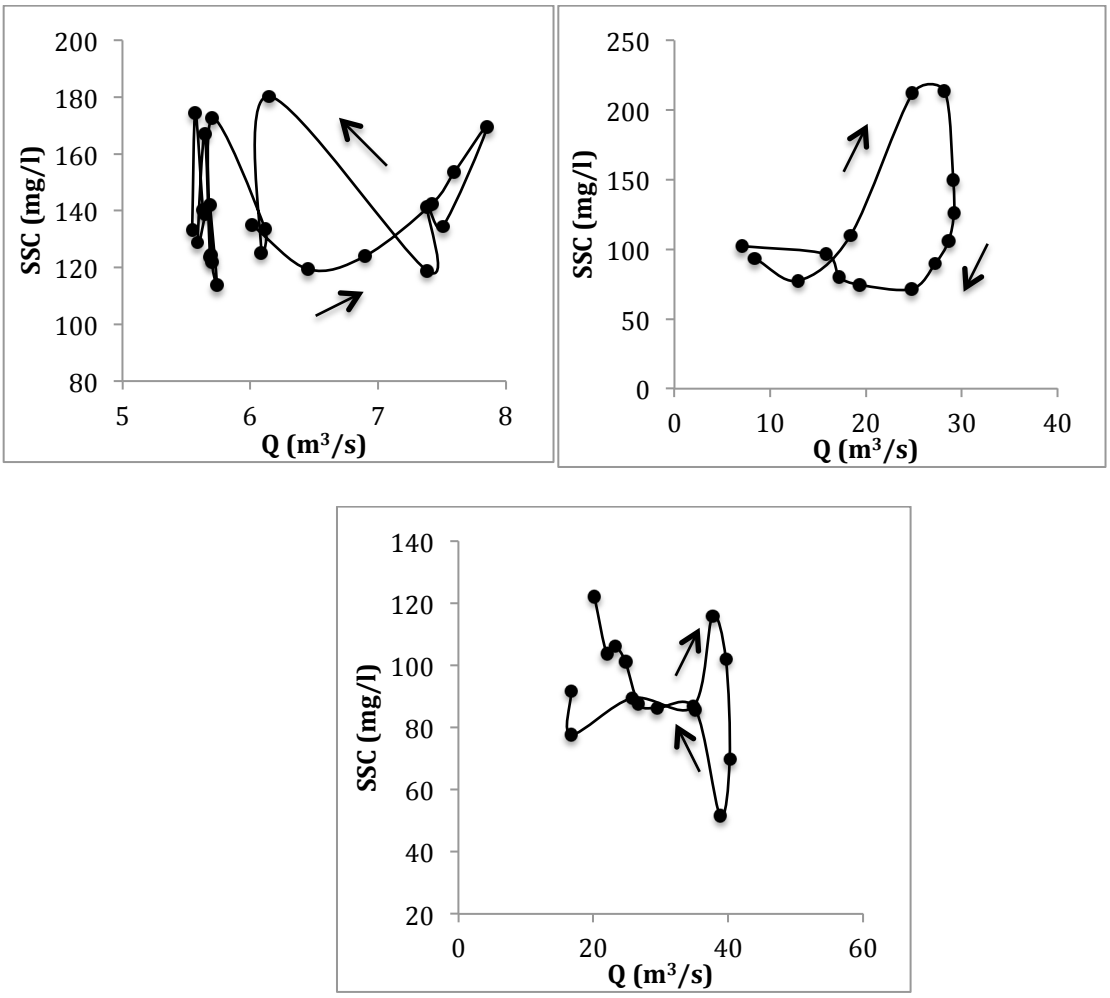

Figure 3.10: Hysteresis of three sites in April event, 2016.

In May event, suspended sediment concentration and sediment flux all peaked before water discharge reached peaks (Figure 3.11 & 3.12). Saybrook and Mahomet showed clockwise loops and Monticello showed figuere8/clockwise loops. A small storm event occurred during the falling limb at Saybrook, which is reflected as a secondary loop in the hysteresis loop. Suspended sediment concentrations and discharge at Saybrook reached peaks at the same time. The highest suspended sediment concentrations at Mahomet and Monticello were on rising limb, which indicated that sediment loads were mostly derived from near-channel sources at rising

limb. Contribution from distal sources from sub-watersheds or the decrease of discharge led to the increase of suspended sediment concentration on falling limb at Monticello.

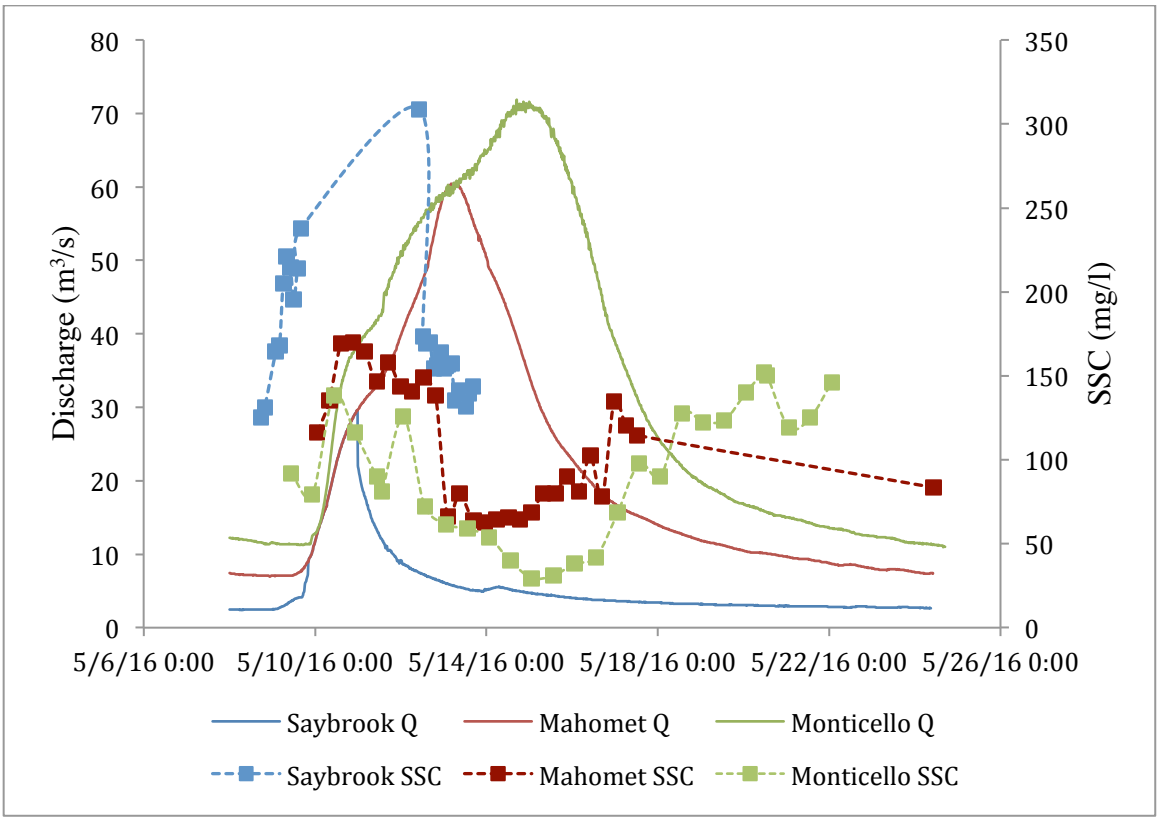

Figure 3.11: Q and SSC at three sites in May event, 2016.

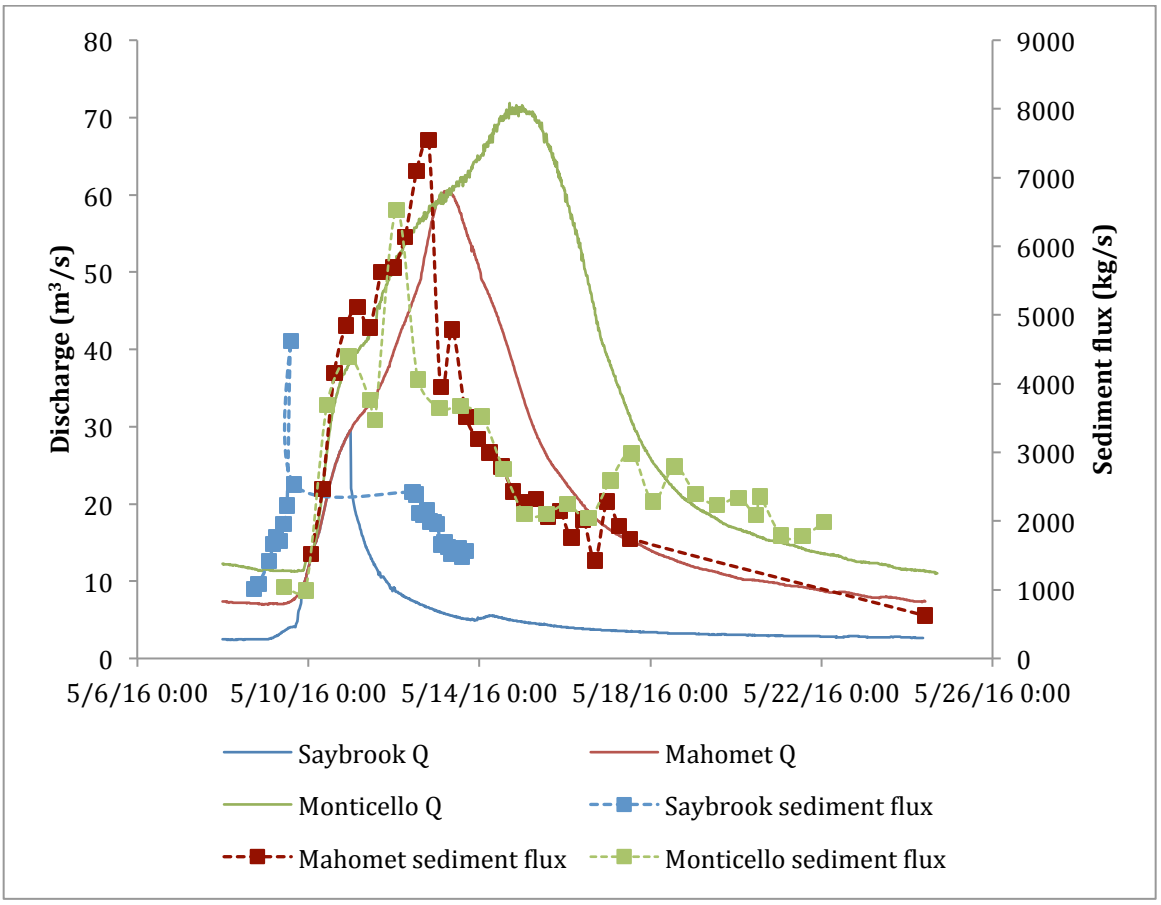

Figure 3.12: Q and sediment flux at three sites in May event, 2016.

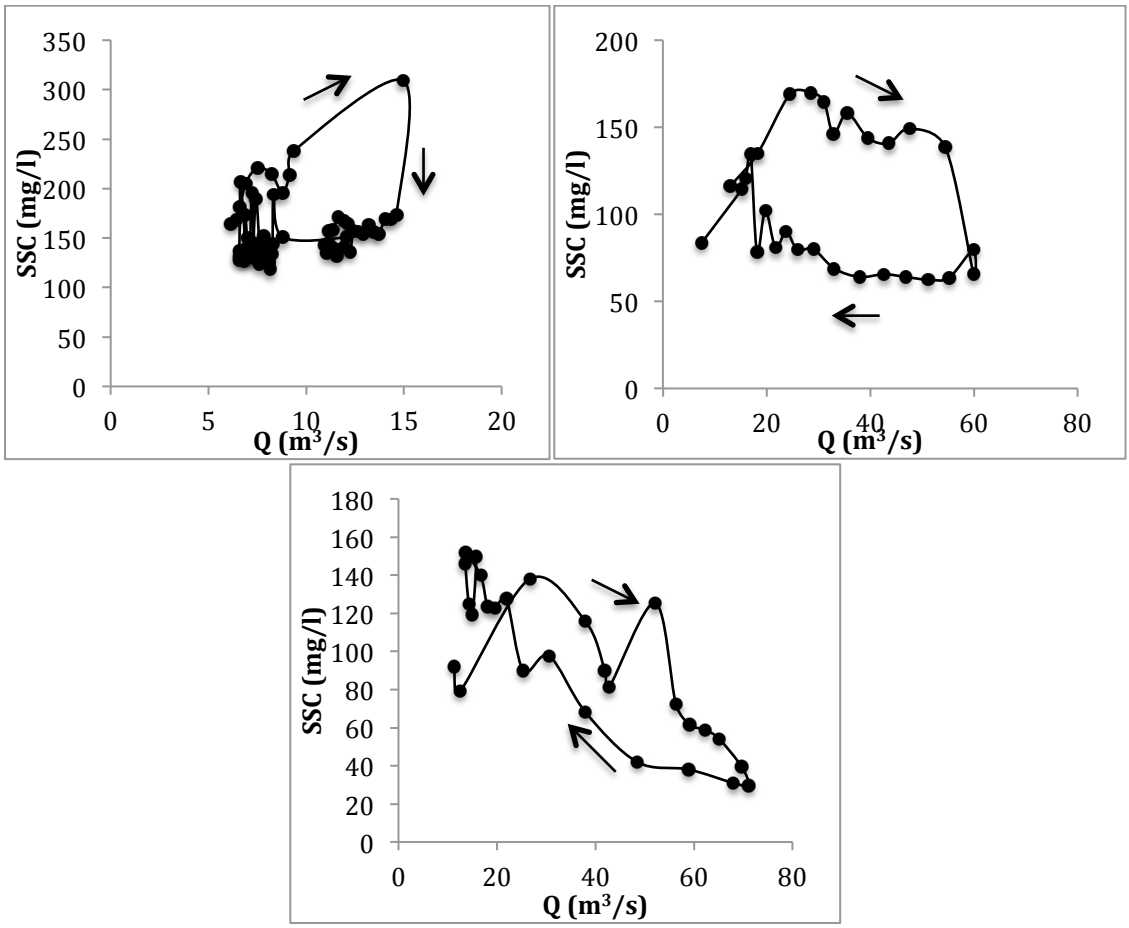

Figure 3.13: Hysteresis of three sites in May event, 2016.

3.5 Discussion

The results of this study suggest that suspended sediment load in the stream is far below the stream transport capacity during high flows. Sediment rating curves developed for three sites all have a peaked pattern with a transition point at geometric mean of discharge. This peaked pattern is most apparent in sediment rating curve developed on discharge and sediment data collected in summer. Decreased bank erosion and failure and increased deposition of sediment might lead to the decrease of suspended sediment concentration during high flows.

Rainfall is an important factor influencing sediment delivery to streams through runoff

generation and sediment transport on hillslopes. High overland flows generated by intensive summer rainfall can erode substantial amount of available materials from hillslopes and contributed to high water discharge, which can entrain and transport large amount of sediment from streambed and banks. High SSC is often observed in the first storm event in flood season, which is regarded as the first flush of sediment. However, high frequency of rainfall events in summer also limits the "recovery" for sediment supply after sediment is exhausted (Walling and Webb, 1982; Gellis, 2013). Soil moisture and sediment supply in one storm event is strongly relied on the antecedent storm events. If the "recovery time" of sediment supply is shorter than the storm intermittency, high concentration of suspended sediment is commonly expected in storm events. If sediment supply is not recovered during the storm intermittency, sediment sources are thereby limited in subsequent flood events.

Mean SSC decreases as drainage area increases, which is partly because of the deposition of sediment and dilution effect from the increases in groundwater flow to the stream (Walling and Webb, 1982). Mean SSCs estimated from the event samples were 272.48, 122.29 and 103.79 mg/l at Saybrook, Mahomet, and Monticello respectively (Figure 3.14), which exhibits a decrease trend as drainage area increases. The relationship between mean SSC and discharge is non-linear with the rate of increase in sediment load decreasing for discharges greater than the geometric mean. The decrease in SSC with increasing drainage area and discharge also indicates that either the delivery of sediment to the stream decreases with increasing drainage area or sediment storage within the river system increases with drainage area, or both. Sediment samples were mostly collected during storm events, less is known about the sediment concentration and loads at base flows. Proper estimation of annual sediment loads requires more information regarding the sediment transport at base flows.

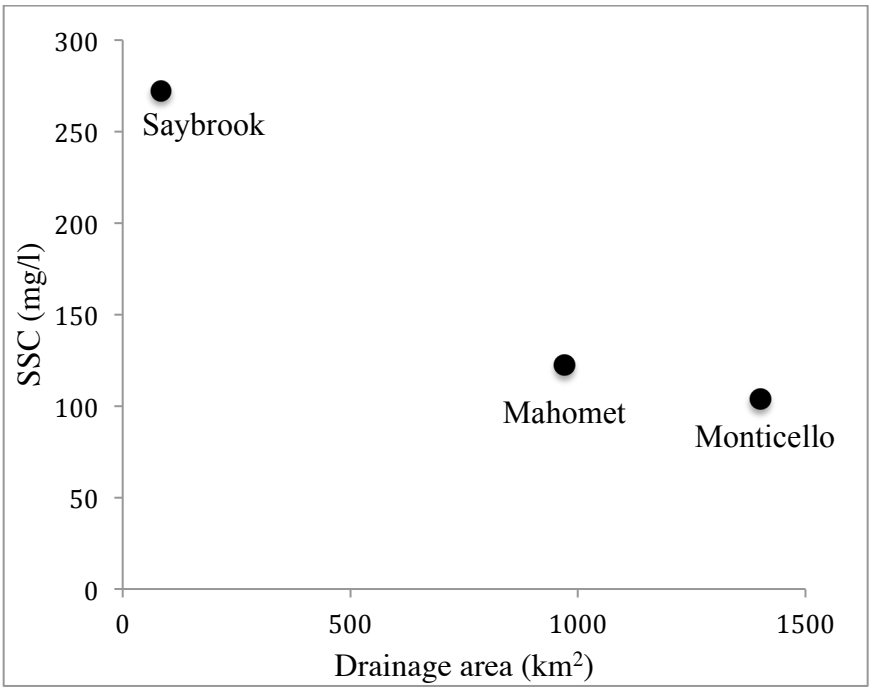

Figure 3.14: The relationship between mean event sediment load and drainage area.

The SRCs developed for the rising and falling limbs of hydrographs and the three sampling seasons also exhibit the same trends, which suggests that these trends are not scale-dependent. Although sediment supply during low flows was relatively small, the sediment load in the range of $Q < Q_{GM}$ might approach stream transport capacity, which is the maximum amount of sediment the stream can transport for a given Q. If sediment supply is abundant and readily available, intensive rainfall associated with high stream flows are expected to transport large amounts of sediment from hillslopes, streambed and banks. However, the decrease of SSC in the range of $Q > Q_{GM}$ indicates that sediment load in the range of $Q > Q_{GM}$ is less than the sediment transport capacity and therefore not sufficient enough to satisfy the increasing sediment transport capacity.

Exponents ($\hat{b}$) of SRCs for the three sediment sites in high flow ranges are negative, which indicates that the peaked pattern of SRCs is identified in this low gradient landscape. Vaughan et al. (2017) found that rivers with peaked SRCs are low-gradient and tend to lack the near-channel topography that characterizes rivers with steep power function relations. This peaked pattern is also observed in SRCs for both rising and falling limb data, which suggests that discharge, or total runoff volume, rather than phase of a hydrograph, is the major factor that controls the sediment transport patterns in this landscape.

The two trends of SRCs in low flows and high flows reveal sediment transport in this landscape during high flows is supply limited. The limited sediment supply to the stream during high flows is related to the decrease of erosion or increase of deposition. One explanation is that bank erosion and failures were more intensive during low flows. After the "first flush" of sediment or a sequence of events, the amount of materials available to be mobilized by overland flow was significantly reduced (Deletic, 1998; Stutter et al., 2008, Wilson et al., 2012). Thus the suspended load of closely-following, subsequent event is comprised mostly of in-channel sediments. The decrease of sediment from hillslopes will lead to a decrease of SSC in the stream at event scale. However, the discharge-related change of SSC is caused by the decrease of near-channel sediment supply. Alluvial deposits often have composite banks composed of lower non-cohesive materials deposits formed from relic channel bars and upper cohesive deposited by overbank flow (Thorne and Tovey, 1981). Materials from a lower, cohesionless bank is eroded by river flow at a much higher rate than material from the upper, cohesive bank. Basal undercutting and cantilever failures are expected to occur during low flows when flow erodes lower non-cohesive bank materials. Bank erosion and failures can contribute large amounts of sediment into the stream during low flows compared to high flows. The increase of discharge

might inhibit bank erosion and failures and lead to a decrease of sediment supply from banks during high flows.

Deposition of sediment might be another cause for the decease of SSC during high flows. The decreased event sediment concentrations from Saybrook upstream to Monticello downstream indicates that substantial amount of sediment was deposited and stored within the landscape and in the channel network. The threshold discharges that separated the trends at three sites are all below the bankfull discharge, and therefore floodplain inundation is not expected to occur at the threshold discharge at sampling sites. Although floodplain deposition processes do not generally prevail at the threshold discharge at the sampling sites, flooding may occur locally leading to some deposition and storage of sediment on the floodplain. Moreover, some storage of fine sediment may occur within the channel, behind log jams or other obstructions to flow, which are numerous within the part of the river system that includes Mahomet and Monticello. Analysis of the occurrence of floodplain inundation and bankfull discharge at the sampling site is needed to better understanding the floodplain sedimentation within this system.

In high flow ranges, SRCs developed for all three sites had negative exponents, and the decrease of exponents in high flow ranges also exhibits geographic trend: exponent of SRC developed for the downstream Monticello site is smaller than that of SRC developed for the upstream Saybrook site. This geographic trend reveals that the increase of sediment load per unit increase of discharge is slower when drainage area increases. The “sediment-starved” condition is more likely to occur in large watersheds than small watersheds under the same hydrological and meteorological conditions. Most of sediment is supplied from headwater areas where slopes area relatively steep (Lu et al., 2005). As drainage area increase, sediment supply per watershed area decreases and sediment sinks and storage increases with increasing flat valley bottoms and

floodplain. The increase of discharge from contributing areas is more significant than the increase of sediment load in large watershed, which increase the deficit between actual sediment load and sediment transport capacity of the stream.

The limitation of sediment supply is most significant in summer. The limited sediment supply in summer may be result from the intensive storms and short storm intermittency. Intensive summer storms may exhaust sediment sources quickly, leading to reduced sediment concentrations in a sequence of events. The relatively short "recovery time" for sediment sources results in a more significant "sediment-starved" condition of the stream in summer (Gellis, 2013).

3.6 Conclusion

Determining fundamental controls on suspended sediment transport is important for understanding the effect of sediment as a vector for pollutants and developing tools to control sediment transport (Horowitz, 2003; Gellis, 2013). This study analyzed sediment and discharge data from three sites along the channel network in low-gradient intensively managed agricultural watershed at event, intra-event and seasonal scales. Results suggest that suspended sediment load in the stream is far below the stream transport capacity during high flows. The sediment rating curves developed for three sediment sampling sites all exhibit peaked patterns. The peaked patterns are more significant in the watershed with large drainage area and in summer, which indicates seasonality and drainage area are important factors influencing the relationship between discharge and suspended sediment load. This peaked pattern of sediment rating curves also reflects a fundamental nature of sediment transport in the study area: suspended sediment transport is supply limited during high flow events. The limitation of sediment supply during

high flows might be resulted from increased sediment deposition caused by localized flooding within the system or decreased bank erosion and failure.

The non-linearity of sediment rating curves undermines the rationality of using one single sediment rating curve to estimate annual sediment load. Using one single sediment rating curve to characterize the relationship between suspended sediment concentration and discharge seems to be inappropriate in this low gradient watershed. The annual sediment load should be carefully estimated for different ranges of discharge based on magnitude-frequency analysis.

Further work is needed in using statistical methods to explain the factors influencing the variances of suspended sediment concentration (Walling, 1974; Seeger et al., 2004; Lana-Renault et al., 2007; Gellis, 2013). Incorporating information regarding sediment transport at base flow samples will enrich the sediment rating curve study. Investigation of the occurrence of localized flood events at sub-bankfull discharge is of great value to better understand the deposition processes of sediment. Additionally, further analysis is needed to reveal the underlying physical basis for the observation that transition points of sediment rating curves are at the geometric mean of discharges at three sites.

3.7 References

Alexandrov, Y., Cohen, H., Laronne, J. B., & Reid, I. (2009). Suspended sediment load, bed load, and dissolved load yields from a semiarid drainage basin: A 15-year study. *Water Resources Research*, *45*(8), 1–13. http://doi.org/10.1029/2008WR007314

Ali, K. F., & De Boer, D. H. (2007). Spatial patterns and variation of suspended sediment yield in the upper Indus River basin, northern Pakistan. *Journal of Hydrology*, *334*(3–4), 368–387. http://doi.org/10.1016/j.jhydrol.2006.10.013

Asselman, N. E. M. (2000). Fitting and interpretation of sediment rating curves. *Journal of Hydrology*, *234*(3–4), 228–248. http://doi.org/10.1016/S0022-1694(00)00253-5

Beasley, D. B., L. F. Huggins, and E. J. Monke (1980), ANSWERS: A model for watershed planning, Trans. ASAE, 23(4), 938–944.

Belmont, P., Willenbring, J. K., Schottler, S. P., Marquard, J., Kumarasamy, K., & Hemmis, J. M. (2014). Toward generalizable sediment fingerprinting with tracers that are conservative and nonconservative over sediment routing timescales. *Journal of Soils and Sediments*, *14*(8), 1479–1492. http://doi.org/10.1007/s11368-014-0913-5

de Vente, J., Poesen, J., Verstraeten, G., Govers, G., Vanmaercke, M., Van Rompaey, A., … Boix-Fayos, C. (2013). Predicting soil erosion and sediment yield at regional scales: Where do we stand? *Earth-Science Reviews*, *127*, 16–29. http://doi.org/10.1016/j.earscirev.2013.08.014

Deletic, A. (1998). The first flush load of urban surface runoff. *Water Research*, *32*(8), 2462–2470. http://doi.org/10.1016/S0043-1354(97)00470-3

Duan, N. (1983). Smearing Estimate: A Nonparametric Retransformation Method. *Journal of the American Statistical Association*, *78*(383), 605. http://doi.org/10.2307/2288126

Eder, A., Strauss, P., Krueger, T., & Quinton, J. N. (2010). Comparative calculation of suspended sediment loads with respect to hysteresis effects (in the Petzenkirchen catchment, Austria). *Journal of Hydrology*, *389*(1–2), 168–176. http://doi.org/10.1016/j.jhydrol.2010.05.043

Ewen, J., G. Parkin, and P. E. O'Connell (2000), SHETRAN: Distributed River Basin Flow and Transport Modeling System, J. Hydrol. Eng., 5(3), 250–258, doi:10.1061/(ASCE)1084-0699(2000)5:3(250).

Ferguson, R. I. (1986). River Loads Underestimated by Rating Curves. *Water Resources Research*, *22*(1), 74–76. http://doi.org/10.1029/WR022i001p00074

Gao, P., & Josefson, M. (2012). Temporal variations of suspended sediment transport in Oneida Creek watershed, central New York. *Journal of Hydrology*, *426–427*, 17–27. http://doi.org/10.1016/j.jhydrol.2012.01.012

Gao, P., & Puckett, J. (2012). A new approach for linking event-based upland sediment sources to downstream suspended sediment transport. *Earth Surface Processes and Landforms*, *37*(2), 169–179. http://doi.org/10.1002/esp.2229

Gao, P., & Zhang, Z. (2016). Spatial patterns of sediment dynamics within a medium-sized watershed over an extreme storm event. *Geomorphology*, *267*, 25–36. http://doi.org/10.1016/j.geomorph.2016.05.025

Gellis, A. C. (2013). Factors influencing storm-generated suspended-sediment concentrations and loads in four basins of contrasting land use, humid-tropical Puerto Rico. *Catena*, *104*, 39–57. http://doi.org/10.1016/j.catena.2012.10.018

Holtschlag, D. J. (2001). Optimal estimation of suspended-sediment concentrations in streams. *Hydrological Processes*, *15*(7), 1133–1155. http://doi.org/10.1002/hyp.207

Horowitz, A. J. (2003a). An evaluation of sediment rating curves for estimating suspended sediment concentrations for subsequent flux calculations. *Hydrological Processes*, *17*(17), 3387–3409. http://doi.org/10.1002/hyp.1299

Horowitz, A. J. (2003b). An evaluation of sediment rating curves for estimating suspended sediment concentrations for subsequent flux calculations. *Hydrological Processes*, *17*(17), 3387–3409. http://doi.org/10.1002/hyp.1299

Kazama, S., Suzuki, K., & Sawamoto, M. (2005). Estimation of rating-curve parameters for sedimentation using a physical model. *Hydrological Processes*, *19*(19), 3863–3871. http://doi.org/10.1002/hyp.5986

Kurashige, Y. (1993). Mechanism of Suspended Sediment Supply to Headwater Rivers and Its Seasonal Variation in West Central Hokkaido, Japan. *Japanese Journal of Limnology (Rikusuigaku Zasshi)*, *54*, 305–315. http://doi.org/10.3739/rikusui.54.305

Lana-Renault, N., Regüés, D., Martí-Bono, C., Beguería, S., Latron, J., Nadal, E., … García-Ruiz, J. M. (2007). Temporal variability in the relationships between precipitation, discharge and suspended sediment concentration in a small Mediterranean mountain catchment. *Nordic Hydrology*, *38*(2), 139–150. http://doi.org/10.2166/nh.2007.003

Lu, H., Moran, C. J., & Sivapalan, M. (2005). A theoretical exploration of catchment-scale sediment delivery. *Water Resources Research*, *41*(9), n/a-n/a. http://doi.org/10.1029/2005WR004018

Morgan, R. P. C., J. N. Quinton, R. E. Smith, G. Govers, J. W. A. Poesen, K. Auerswald, G. Chisci, D. Torri, and M. E. Styczen (1998), The Euro- pean Soil Erosion Model (EUROSEM): A dynamic approach for predicting sediment transport from fields and small catchments, Earth Surf. Processes Landforms, 23(6), 527–544, doi:10.1002/(SICI)1096-9837(199806)23:6<527::AID-ESP868>3.0.CO;2-5.

Nadal-Romero, E., Latron, J., Martí-Bono, C., & Regüés, D. (2008). Temporal distribution of suspended sediment transport in a humid Mediterranean badland area: The Araguás catchment, Central Pyrenees. *Geomorphology*, *97*(3–4), 601–616. http://doi.org/10.1016/j.geomorph.2007.09.009

Nearing, M. A., G. R. Foster, L. J. Lane, and S. C. Finkner (1989), A process- based soil erosion model for USDA - Water Erosion Prediction Project technology, Trans. ASAE, 32(5), 1587–1593.

Owens, P. N., Batalla, R. J., Collins, A. J., Gomez, B., Hicks, D. M., Horowitz, A. J., … Trustrum, N. A. (2005). Fine-grained sediment in river systems: environmental significance and management issues. *River Research and Applications*, *21*(7), 693–717. http://doi.org/10.1002/rra.878

Papanicolaou, A. N. T., Krallis, G., & Edinger, J. (2008). Sediment transport modeling review—current and future developments. Journal of Hydraulic Engineering, 134(1), 1-14.

Phillips, J. M., Webb, B. W., Walling, D. E., & Leeks, G. J. L. (1999). Estimating the suspended sediment loads of rivers in the LOIS study area using infrequent samples. *Hydrological Processes*, *13*(7), 1035–1050. http://doi.org/10.1002/(SICI)1099-1085(199905)13:7<1035::AID-HYP788>3.0.CO;2-K

Prosser, I. P., I. D. Rutherfurd, J. M. Olley, W. J. Young, P. J. Wallbrink, and C. J. Moran (2001), Large-scale patterns of erosion and sediment transport in river networks, with examples from Australia, Mar. Freshwa- ter Res., 52(1), 81–99, doi:10.1071/MF00033.

Seeger, M., Errea, M. P., Beguería, S., Arnáez, J., Martí, C., & García-Ruiz, J. M. (2004). Catchment soil moisture and rainfall characteristics as determinant factors for discharge/suspended sediment hysteretic loops in a small headwater catchment in the Spanish pyrenees. *Journal of Hydrology*, *288*(3–4), 299–311. http://doi.org/10.1016/j.jhydrol.2003.10.012

Sichingabula, H. M. (1998). Factors controlling variations in suspended sediment concentration for single-valued sediment rating curves, Fraser River, British Columbia, Canada. *Hydrological Processes*, *12*(12), 1869–1894. http://doi.org/10.1002/(SICI)1099-1085(19981015)12:12<1869::AID-HYP648>3.0.CO;2-G

Stutter, M.; Langan, S.; Cooper, R. (2008). Spatial contributions of diffuse inputs and within-channel processes to the form of stream water phosphorus over storm events. *Journal of Hydrology*, *350*(3–4), 203–214. http://doi.org/10.1016/J.JHYDROL.2007.10.045

Thorne, C. R., & Tovey, N. K. (1981). Stability of composite river banks. *Earth Surface Processes and Landforms*, *6*(5), 469–484. http://doi.org/10.1002/esp.3290060507

Vaughan, A., Belmont, P., Hawkins, C. P., & Wilcock, P. (2017). Near-channel versus watershed controls on sediment rating curves. *Journal of Geophysical Research: Earth Surface*, 1–23. http://doi.org/10.1002/2016JF004180

Walling, D. E. (1977). Limitations of the rating curve technique for estimating suspended sediment loads, with particular reference to British rivers. *Proc. Symp. on Erosion and Solid Matter Transport in Inland Waters*, 34–48.

Walling, D. E., & Webb, B. W. (1981). The reliability of suspended sediment load data [River Creedy, England]. International Association of Hydrological Sciences.

Walling, D. E., & Webb, B. W. (1982). Sediment availability and the prediction of storm-period sediment yields. *Recent Developments in the Explanation and Prediction of Erosion and Sediment Yield (Proceedings of the Exeter Symposium)*, *137*(137), 327–337.

Walling, D. E., & Zhang, Y. S. (2004). Predicting slope-channel connectivity: a national-scale approach. *IAHS Publication (International Association of Hydrological Sciences)*, (August), 107–114.

Warrick, J. A. (2015). Trend analyses with river sediment rating curves. *Hydrological Processes*, *29*(6), 936–949. http://doi.org/10.1002/hyp.10198

Warrick, J. A., & Rubin, D. M. (2007). Suspended-sediment rating curve response to urbanization and wildfire, Santa Ana River, California. *Journal of Geophysical Research: Earth Surface*, *112*(2), 1–15. http://doi.org/10.1029/2006JF000662

Wilkinson, S. N., Prosser, I. P., Rustomji, P., & Read, A. M. (2009). Modelling and testing

spatially distributed sediment budgets to relate erosion processes to sediment yields. *Environmental Modelling and Software*, *24*(4), 489–501. http://doi.org/10.1016/j.envsoft.2008.09.006

Williams, G. P. (1989). Sediment concentration versus water discharge during single hydrologic events in rivers. *Journal of Hydrology*, *111*(1–4), 89–106. http://doi.org/10.1016/0022-1694(89)90254-0

Wilson, C. G., Papanicolaou, a. N. T., & Denn, K. D. (2012). Partitioning fine sediment loads in a headwater system with intensive agriculture. *Journal of Soils and Sediments*, *12*, 966–981. http://doi.org/10.1007/s11368-012-0504-2

Winter, T. C. (2001). The concept of hydrologic landscapes'. *Journal Of The American Water Resources Association*, *37*(2), 335–349. http://doi.org/10.1111/j.1752-1688.2001.tb00973.x

Wischmeier, W. H., and D. D. Smith (1965), Predicting rainfall erosion losses from croplands east of the Rocky Mountains, USDA, Agric. Handb. 282, U.S. Gov. Print. Off., Washington, D. C.

Young, R. A., C. A. Onstad, D. D. Bosch, and W. P. Anderson (1989), AGNPS: A nonpoint-source pollution model for evaluating agricultural watersheds, J. Soil Water Conserv., 44(2), 168–173.

CHAPTER 4

UNDERSTANDING HUMAN IMPACTS ON SEDIMENT DYNAMICS IN AN INTENSIVELY MANAGED AGRICULTURAL LANDSCAPE USING A NETWORK SEDIMENT MODEL

Abstract

By altering hydrological and geomorphological processes at watershed scales, humans have substantially influenced the movement of sediment on Earth's surface. Despite widespread recognition of human impact on sediment dynamics, few studies have assessed the magnitude of change in stream sediment fluxes before and after human settlement of intensively managed agricultural landscapes and how agricultural development has altered the spatial distribution of sediment fluxes throughout stream networks. This study explores fluvial sediment dynamics before and after agricultural development in an intensively managed watershed in the midwestern United States using a coupled hydrologic and sediment model based on the representative elementary watershed approach. Comparison of model predictions with hydrological and sediment data and with information on floodplain sedimentation shows the model accurately captures contemporary fluxes of water and sediment. To assess human impact, land cover conditions prior to European settlement are used to estimate the magnitude and spatial distribution of before the landscape was transformed by agricultural production. Results indicate that sediment delivery from hillslopes to streams in this low-relief watershed has increased eleven-fold and the sediment load in streams has increased eight-fold since European settlement. Floodplain sedimentation has also increased dramatically, a finding consistent with recent estimates of post-settlement alluvium accumulation rates, but the proportion of sediment exported from the basin is now greater than it was in the 1800s. Artificial levees in headwater

channelized reaches impede sediment retention on the floodplain and promote deposition of sediment within channels. Overall, humans have greatly accelerated the sediment dynamics of this fluvial system.

4.1 Introduction

Humans are now major geomorphological agents effecting substantial change in the characteristics of Earth's physical landscapes. In some regions, such as the midwestern United States, the imprint of human agency is especially pervasive, producing what have become known as intensively managed landscapes (IMLs). It has been hypothesized that through human modification, IMLs, particularly those in the Midwest, have shifted from primarily a transformation-dominated system characterized by long residence times and substantial storage of water, nutrients, and sediment to a transport-dominated system characterized by rapid movement and limited storage of water, nutrients, and sediment (Rhoads et al., 2016; Kumar et al., 2018). The extent to which this hypothesis prevails have important implications for landscape sustainability.

A key issue of concern in IMLs is the influence of human activity on sediment dynamics. As the awareness of significant changes of sediment dynamics under human impact grows, the characterization and prediction of sediment transport processes is becoming a global issue attracting considerable attention. Human activity has a substantial impact on sediment dynamics by changing soil structure, exposing soils to erosion, and reducing sediment storage and residence times of stored sediment (Gregory, 2006; Nearing et al., 2017). Sediment generation and transport processes can be in a state of disequilibrium under profound human impact. This human-triggered disequilibrium affects the capacity of landscapes to adapt to ongoing human

activity or to extreme weather events associated with climate change. A broad range of sustainable ecosystem services, such as soil productivity and water quality, on which human populations depend are also threatened by enhanced sediment fluxes. Therefore, understanding and predicting the response of sediment dynamics to human impact is crucial to developing management strategies that enhance resilience and reduce vulnerability of IMLs to future changes in environmental conditions.

Human are capable of altering water and sediment fluxes in IMLs both directly and indirectly (Rhoads, 1995; Gregory, 2006). Indirect effects include changes related to transformations of land cover. Direct effects include physical modification of hillslope drainage and river channels. In the Midwest, extensive modification of surface and near-surface conditions, the part of the landscape system referred to as the Critical Zone, occurred in the 19th century with the advent of industrial agriculture (Rhoads and Herricks, 1996). The vast prairie was replaced almost wholly by cropland. Direct modification of hydrology occurred by installing subsurface tiles to improve the drainage of relatively flat farm fields. Also, headwater streams were channelized and extended headward to provide outlets for artificial subsurface drainage systems (Rhoads and Urban, 2003; Rhoads et al., 2016). Between 80 and 100 percent of the total length of headwater streams is now channelized in some areas (Mattingly et al., 1993).

Undoubtedly, human-induced change in landscapes of the midwestern United States has altered sediment dynamics, but the magnitude and spatial variability of change in these dynamics remain unknown. Most human-induced landscape modification occurred prior to the collection of scientific information on the effects of this modification and the degree of modification has been so profound and widespread that few, if any, undisturbed areas remain to provide a basis for comparison with disturbed areas (Rhoads and Herricks, 1996). As in most agricultural

landscapes, farming has increased rates of soil erosion (Montgomery, 2007), but quantification of the extent to which agricultural development in the Midwest has increased delivery of eroded soil to streams relative to presettlement rates of erosion is lacking (Nearing et al., 2017). Similarly, once this eroded material is delivered to streams, it can either move through the drainage network or be deposited on floodplains or within channels. This movement can be affected by human modification of river channels and the connection of these channels to floodplains (Noe and Hupp, 2005; Kroes and Hupp, 2010; Landwehr and Rhoads, 2003). Changes in hydrology and sediment delivery at the watershed scale can also influence channel erosion, another source of sediment in fluvial systems.

Human agency has become an important factor in sediment budgets (Reid and Dunne, 2013), enhancing sediment mobilization and morphodynamic change, but in many cases the extent to which this agency has altered modern sediment systems in relation to the state of these systems prior to human impact has yet to be determined. Sediment budgets for watersheds in the Midwest only include fluxes since the time of European settlement and agricultural production, rather than comparing these rates to estimates of rates under native vegetation cover (Trimble, 1983, 1999, 2009; Beach, 1994). Moreover, these budgets have been developed for moderately to highly dissected watersheds, rather than for relatively undissected, low-relief glacial depositional landscapes that characterize much of the farmland in the Midwest. Moreover, the effect of various human impacts on sediment dynamics at the watershed level is not well quantified (Maalim et al., 2013) and incorporating the influence of human activities on sediment dynamics into predictive models remains a challenging task. The characterization of sediment dynamics under human impact at the watershed scale requires an understanding of the connectivity between sediment generation on hillslopes and its delivery to and transport within

the river channel network (Verstraeten et al., 2007; Medeiros et al., 2010). Many natural and human factors cause mechanisms and rates of sediment generation and transport to vary in space and time. With the rapid development of numerical methods for fluid mechanics and sediment transport, computational modeling has become an effective tool for studying sediment supply, transport and load in various environments (Papanicolaou, et al., 2008). Over the past three decades, a large number of computational sediment transport models have been developed for diagnosing and predicting the sediment movement within watersheds (Fan, 1988; Papanicolaou et al., 2008), including: SEDNET (Prosser et al., 2001), USLE (Wischmeier and Smith, 1965), ANSWERS (Beasley et al., 1980), KINEROS (Smith, 1981), WEPP (Nearing et al., 1989), EUROSEM (Morgan et al., 1998), AGNPS (Young et al., 1989), and SHETRAN (Ewen et al., 2000). The choice of a certain model for solving a specific problem depends on the nature and complexity of the problem itself, model capabilities to simulate the problem adequately, data availability for model calibration, data availability for model verification, and the time and budget available for solving the problem. The majority of models have been used to determine upland erosion or to estimate in-channel processes. However, models that lack connectivity between hillslope erosion and in-channel processes often do not provide accurate estimates of watershed-scale water and sediment yields (Conroy et al., 2006; Dermisis et al., 2011). In particular, models for predicting sediment yield should account for the storage of eroded sediment on floodplains and other bottomland surfaces (Osterkamp and Toy, 1997).

This paper addresses two fundamental research questions related to human influence on sediment dynamics in intensively managed, low-relief agricultural landscapes of the midwestern United States: how has transformation of the presettlement landscape into the modern industrial agricultural landscape changed the magnitude of stream sediment fluxes and how has this

transformation influenced spatial variability of sediment fluxes, including source, storage, and export components of the fluvial sediment budget? To address these questions, the study applies a semi-distributed, coupled hydrological and sediment flux model to explore contemporary fluvial driven and human impacted sediment transport at the watershed scale in an agricultural watershed in Illinois and to estimate how alterations to this landscape since the time of European settlement have altered sediment dynamics. The results help to inform the hypothesis that agricultural activities have changed landscapes from a primarily transformational system to a transport-dominated system (Rhoads et al., 2016; Kumar et al., 2018)

4.2 Study area

The study area is the Upper Sangamon River Basin (USRB), Illinois, USA (Figure 4.1). This 3,690 km^2 watershed forms part of the Intensively Managed Landscapes Critical Zone Observatory (IML-CZO) (Kumar et al., 2018). The low-relief (< 50 m) landscape of the USRB consists mainly of agricultural lands dominated by row-crop agriculture (> 80% of total land use). Forested areas exist along a riparian corridor flanking the middle and downstream portions of the main river. A few small agricultural communities are scattered throughout the watershed. The areas of highest relief occur in headward portions of the watershed and along the main river, which has incised by about 25-30 m, forming a broad valley bottom bounded by adjacent bluffs.

Transformation of the landscape in this watershed is representative of that which has occurred throughout the Midwest. Since the time of European settlement in the 19^{th} century, the majority of this landscape has been converted from prairie and scattered forest to agriculture. The transformation has presumably had substantial impacts on water and sediment fluxes (Rhoads et al., 2016), but the magnitude of these impacts is poorly understood. For the purposes of improving land drainage by subsurface tiles and facilitating the use of large farm equipment

near streams, many channels throughout this region have been channelized (Rhoads and Herricks, 1996; Urban and Rhoads, 2003). Channelized sections of the main channel and tributaries show little or no evidence of recovery to human modification. The analysis of channel changes indicates that the modern channel network is nearly three times more extensive than the channel network in the 1820s (Rhoads et al., 2016).

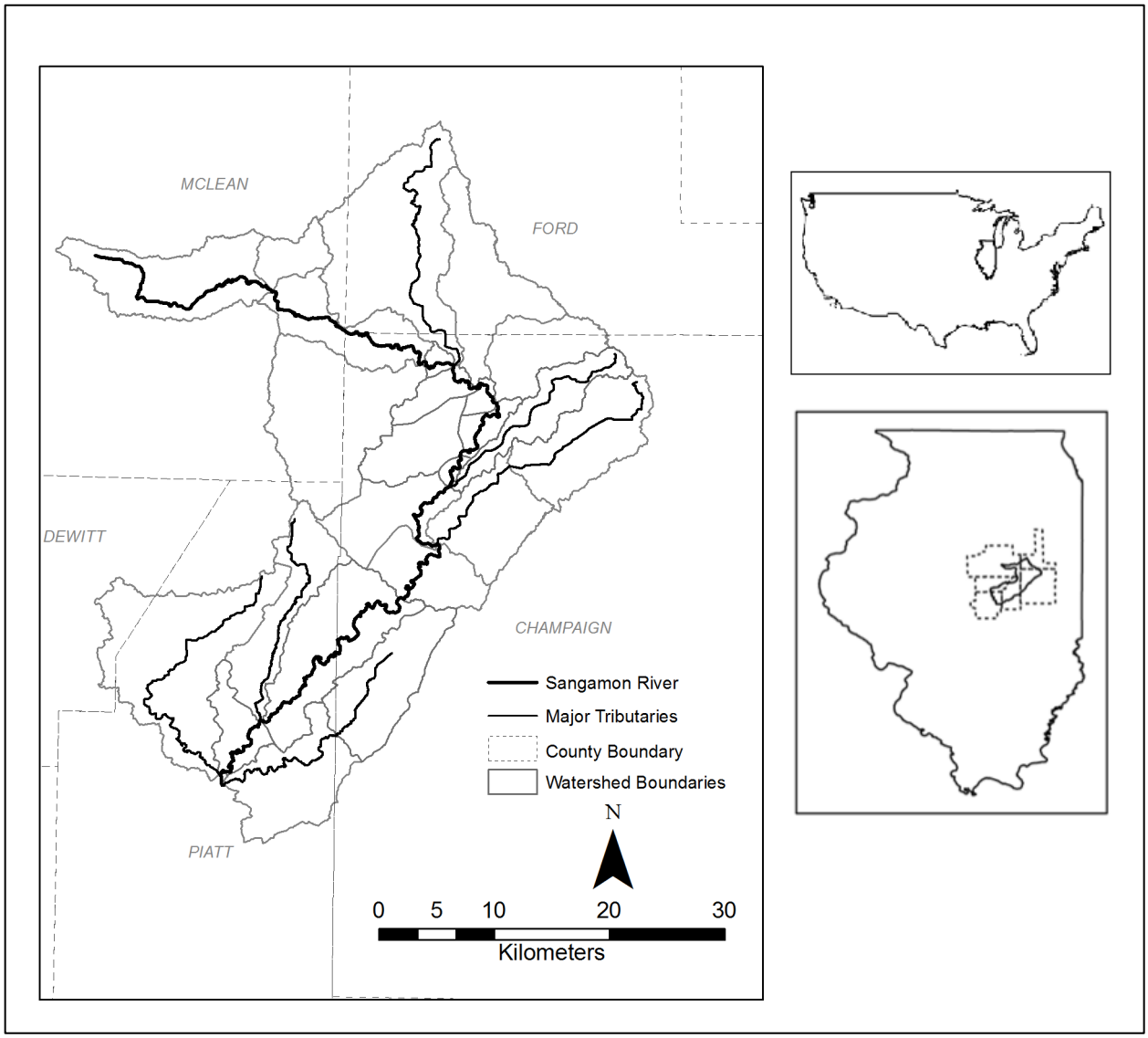

Figure 4.1*:* The Upper Sangamon River Basin with Representative Elementary Watershed delineation used in the model.

4.3 Model description

The modeling framework used in this study combines a network hydrology model based on the representative elementary watershed (REW) theory (Reggiani et al., 2001) with a network sediment transport model based on LASCAM model (Viney and Sivapalan, 1999). The network hydrology TsingHua Representative Elementary Watershed (THREW) model (Tian et al. 2008) builds on balance equations for mass and momentum for a hierarchical river network, whereas the network sediment transport model captures sediment delivery from hillslopes to streams, sediment propagation through the streams, and sedimentation on floodplains. The semi-distributed THREW model operates at fine temporal scale (sub-daily), and can also be applied at the spatial scale of coarse models (>1000 km^2) (Li et al., 2010; Patil et al., 2012; Ye et al., 2012). It is also capable of continuously simulating hydrological response over long periods (multiple years) with reasonable computational expenditure.

4.3.1 Representative Elementary Watershed (REW) theory

The network hydrology model is based on the Representative Elementary Watershed (REW) theory. In this scheme, a watershed is conceptualized as a collection of representative elementary watersheds (REWs) that constitute the smallest functional units of the model. REWs are connected to each other through the river network (Figure 4.2), and each REW consists of hillslope and channel components (Reggiani et al., 1998). The hillslope component comprises a surface layer and a sub-surface layer (Tian et al., 2008). Surface layers are classified into three types, or zones: bare soil (b-zone), vegetated areas (v-zone), and sub-stream-network zone (t-zone). The subsurface layers are categorized as zones of saturation (s-zone) and unsaturation (u-zone). Mass and energy are exchanged between surface and subsurface zones.

Every reach receives water from upstream REWs and the sub-stream-network zone in adjacent hillslopes. Sediment inputs originate from upstream REWs and erosion of adjacent hillslopes and the channel bed. Besides the hillslope and channel components built into the basic THREW model, a floodplain zone was added to the model in this study to simulate floodplain sedimentation.

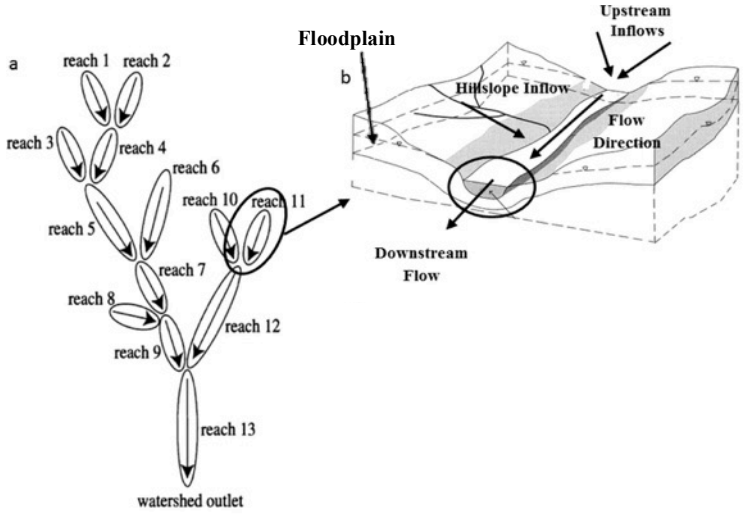

Figure 4.2: Schematic of the coupled hydrological-solute-transport model: (a) Watershed discretization into several REWs organized around the river network; and (b) each REW includes a hillslope and a channel reach (modified from Ye et al., 2012).

4.3.2 Network hydrology model

4.3.2.1 Hillslope process

Hillslope hydrological processes in the model include ground-surface depression storage, canopy interception, saturation and infiltration excess runoff, and routing of overland and channel flow. A set of ordinary differential equations account for conservation of mass, momentum, and energy (Tian et al. (2008). Only key processes are described here for the sake of brevity. Tian et al. (2008) provide a detailed description of hydrological processes in the model.

Surface runoff contributed from the hillslopes to channels consists of infiltration excess runoff from the bare soil zone (b-zone) and the vegetated zone (v-zone), saturation excess runoff from the sub-stream-network zone (t-zone), and baseflow from the saturation zone (s-zone). Infiltration rates in the unsaturated zone (u-zone) are related to rainfall intensity and the infiltration capacity. The latter is determined by soil properties and moisture. A spatially averaged infiltration capacity model based on the Green-Ampt model (Rogers 1992) is adopted in THREW model:

$$\overline{f_i} = K_s^u \times \left[1 + \alpha^{IFL} \frac{|\psi|(1-s^u)\varepsilon^u}{s^u y^u}\right] \tag{4.1}$$

where $\overline{f_i}$ is the spatially averaged infiltration capacity, K_s^u is the averaged saturated hydraulic conductivity of u-zone, ψ is the averaged matrix potential of u-zone, s^u is the saturation degree of u-zone, y^u is the soil depth of u-zone, ε^u is the soil porosity of u-zone, and α^{IFL} is the coefficient which represents the spatial heterogeneity. The t-zone includes saturated area of land surface and water bodies other than the main channel and can be regarded as a variable contribution area. The area of t-zone is calculated using Xin'anjiang model (Zhao, 1992). Baseflow is the water flowing from s-zone to channel. It is calculated as,

$$Q_{t,b} = \alpha \overline{K_t} \left(\frac{y_t}{Z}\right)^{\beta} \tag{4.2}$$

where α and β are coefficients, $\overline{K_t}$ is the averaged saturated hydraulic conductivity of s-zone, Z is the total soil depth defined in the input, and y_t, the depth of the s-zone, is calculated as,

$$y_t = \frac{ws_s}{A_s \cdot \phi} \tag{4.3}$$

where ws_s is the water storage (m^3) in s-zone, A_s is the area of s-zone (m^2), and ϕ is the soil porosity.

4.3.2.2 Channel process

The water balance equation for the r-zone in REW i, with inflows from the hillslope and two upstream nodes, is,

$$\frac{dS_w^i}{dt} = Q_h^i + \sum Q_{up}^j - Q_{out}^i \tag{4.4}$$

where S_w^i is water storage of the r-zone in REW i, Q_h^i is water flow that enters the r-zone from the t-zone in REW i, Q_{up}^j is inflows from upstream REW j, and Q_{out}^i is the outflow from the r-zone to the downstream node. Q_{up}^j and Q_{out}^i are calculated as,

$$Q_{up}^j = v^j \times A_{mc}^j \tag{4.5}$$

$$Q_{out}^i = v^i \times A_{mc}^i \tag{4.6}$$

where A_{mc}^j and A_{mc}^i are the cross-sectional areas of the r-zones in REWs i and j, and v^j and v^i are the velocities of the r-zones in REWs i and j. The cross-sectional area of the flow (A_{mc}^i) at the beginning of any time step is estimated by dividing the water storage (S_w^i) at the end of previous time step by the r-zone length (L^i). Velocity (v^i) is estimated through a simplified reach scale Saint-Venant momentum balance equation (Reggiani et al., 2001; Ye et al., 2012; Patil et al., 2012).

$$v^i = \frac{1}{n^i}\sqrt{\frac{(R_h^i)^{\frac{1}{3}}}{P_r^i L^i}\left(A_{mc}^i L^i sin\gamma^i \pm \sum_{j\neq i}\frac{1}{4}h^i\left(A_{mc}^i + A_{mc}^j\right) - \frac{1}{2}h^i A_{mc}^i\right)} \quad (4.7)$$

where n^i is a roughness coefficient, R_h^i is the hydaulic radius, P_r^i is the average slope of average wetted perimeter of local REW i, $sin\gamma^i$ is the mean slope of REW i, and h^i is the mean depth of REW i.

4.3.2.3 Floodplain process

The model calculates water storage (*wr*), cross-sectional area (*mr*), and water depth (*yr*) for each REW at each time step. When the water depth calculated by Eq. (4.7) exceeds the channel depth, overbank flow and floodplain inundation occur (Figure 4.3). The water storage at reach *i* is then re-distributed between the main channel and floodplain.

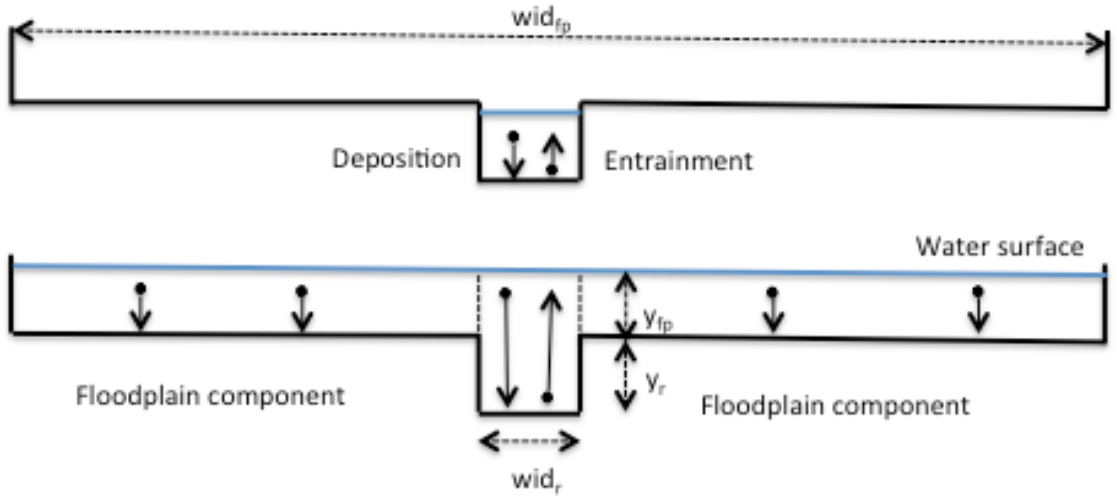

Figure 4.3: A sketch of floodplain and inundation.

The water depth and water storage in the floodplain is,

$$h_{fp}^{i} = \frac{mr_i - h_{mc}^{i} \times w_{top}^{i}}{w_{fp}^{i} + w_{top}^{i}} \tag{4.8}$$

$$wr_{fp}^{i} = h_{fp}^{i} \times w_{fp}^{i} \tag{4.9}$$

where h_{fp}^{i} is the water depth in the floodplain, mr_i is the cross-sectional area in REW i, h_{mc}^{i} is the bankfull water depth in the channel, w_{top}^{i} is the top channel width, w_{fp}^{i} is the floodplain width, and wr_{fp}^{i} is the water storage in the floodplain.

Flow velocity in the floodplain is calculated based on Eq. (4.7) with a roughness coefficient appropriate for vegetation cover on the floodplain. The model calculates the outflow from REW i as the summation of water flow from the channel and floodplain, which is the inflow to the downstream reach.

4.3.3 Network sediment transport model

The sediment transport model simulates the sediment transport process in a watershed in three stages: sediment generation from hillslopes, sediment propagation through the river channel network, and sediment deposition on floodplains. The model simulates the behaviors of sand and mud transport processes separately, and assumes all sediment transported in the streams is in suspension.

4.3.3.1 Hillslope process

Sediment is generated on hillslopes and transported into river channels by surface runoff. The sediment erosion rate on hillslope is a conceptualization of the Modified Universal Soil Loss Equation (Viney and Sivapalan, 1999),

$$E_i = CS_{t,i}Q_{t,i}^{\delta} \tag{4.10}$$

where E_i is the sediment erosion rate (kg/s) on hillslope in REW i, C and δ are the empirical parameters, $S_{t,i}$ is the slope of hillslope in REW i, and $Q_{t,i}$ is the water discharge from the hillslope to main channel (m^3/s) in REW i.

4.3.3.2 Channel process

Modeling of deposition and entrainment in channels follows the conceptual model of water and sediment fluxes developed from the LASCAM model (Viney and Sivapalan, 1999). Viney and Sivapalan (1999) indicated that the sediment model should remain as conceptually simple as possible due to the incomplete understaing of sediment processes at watershed scale and overwhelming number of unresolvable factors involved.

Sediment entrainment in the channel is related to the stream carrying capacity and critical shear stress. Sediment transport capacity is calculated through a simplified Bagnold Equation used in SWAT model (Neitsch *et al*., 2005). Williams (1980) (SPNM model) used Bagnold's (1977) definition of stream power to develop a method for determining degradation as a function of channel slope and velocity. The maximum amount of sediment that can be transported from a reach is calculated as,

$$conc_{max,i} = c \times v_i^{spexp} \tag{4.11}$$

where $conc_{max}$ is the maximum concentration of sediment that can be transported by the water (kg/m^3), c is a coefficient defined by the user, v_i is the channel velocity (m/s). The exponent,

spexp, is 1.5, the value used in the original Bagnold stream power equation (Arnold et al., 1995).

The calculated sediment transport capacity is compared to the actual sediment load transported in the reach. If the actual sediment load is greater than the sediment transport capacity, the depostion rate is calculated as (Foster et al., 1980),

$$D_i = \alpha_{er}(q_{sed,i} - T_{c,i}) \tag{4.12}$$

where D_i is the deposition rate (kg/m^2/s) in REW i, α_{er} is a first order reaction coefficient (m^{-1}), $T_{c,i}$ is the stream transport capacity (kg/m/s) and $q_{sed,i}$ is the stream sediment load (kg/m/s) in REW i. α_{er} can be estimated from

$$\alpha_{er} = \frac{v_f}{q_w} \tag{4.13}$$

where v_f is the particle fall velocity (m/s), and q_w is the discharge per unit width (m^3/m/s). The fall velocity is estimated through Stokes' law (Foster et al., 1980).

$$v_f = \frac{(\rho_s - \rho_w) \times g \times d^2}{18 \rho_w \nu} \tag{4.14}$$

where ρ_s and ρ_w are the density of sediment and water (kg/m^3), g is the gravity acceleration (m/s^2), d is the sediment particle diameter (m), and ν is the kinematic viscosity coefficient of water (m^2/s) at 20 °C.

If the sediment load in the stream is smaller than the transport capacity and shear stress is larger than the critical shear streass, erosion will occur. The erosion rate in the reach is calculated as,

$$E_{ch,i} = w_{c,i} K_{ch,i} (\bar{\tau} - \tau_{cr}) \quad (4.15)$$

where, $E_{ch,i}$ is the soil loss per unit channel length (kg/m/s), $w_{c,i}$ is the stream width (m), $\bar{\tau}$ is the shear stress(N/m^2), τ_{cr} is a critical shear stress (N/m^2), $K_{ch,i}$ is the an erodibility factor (g^{-1}s^{-1}).

4.3.3.3 Floodplain process

The basic THREW model was expanded in this study to consider floodplain deposition, an important factor in watershed-scale sediment dynamics, by including a 1D floodplain sedimentation component in the model. When a floodplain is inundated, water and sediment enter the floodplain at upstream end of the REW. Part of the sediment transported by the flow is deposited, and flow with a reduced sediment load leaves the floodplain at the downstream end of REW. The modeling approach of floodplain sedimentation is based on the procedure Chen (1975) developed to estimate sedimentation in settling tanks as a function of the trapping efficiency of the tank (Asselman and Van Wijngaarden, 2002). The trapping efficiency is calculated as,

$$TE_i = 1 - \exp\left(-v_f \frac{A_{f,i}}{Q_{f,i}}\right) \quad (4.16)$$

where TE_i is the floodplain trapping efficiency in REW i, v_f is the settling velocity of the suspended sediment. $A_{f,i}$ is the surface area of the floodplain (m^2) and $Q_{f,i}$ is the discharge (kg/m^3) through the basin.

This efficiency is a function of the ratio between floodplain area and the discharge through it (Asselman and Van Wijngaarden, 2002), which reflects the residence time of water and sediment in the floodplain. The sedimentation rate is computed as,

$$S_i = Q_{s,i} \times TE_i \quad (4.17)$$

where S_i s the sedimentation rate (kg/s) and $Q_{s,i}$ is the suspended sediment load transported to the floodplain (kg/s). An assumption of application of this model is that convection rather than diffusion causes sedimentation (Chen, 1975; Asselman and Van Wijngaarden, 2002). Another assumption is that no re-suspension or erosion occurs on floodplain regardless of bed shear stress or potential sources on the floodplain (Asselman and Van Wijngaarden, 2002). Thus, floodplains are sinks for transported sediment.

4.4 Methods

4.4.1 Model application

This study uses the coupled, semi-distributed hydrological and sediment model to simulate sediment generation, transport and load for at the Upper Sangamon River Basin upstream of a U.S. Geological Survey stream gauging site at Monticello, IL. A key use of the model is to evaluate sediment scaling issues and the effect of channelization and floodplain effects on sediment fluxes. Two scenarios reflecting the different degrees of human impacts on the landscape are examined. Scenario 1, which is referred to as the 2000s scenario, represents the water and sediment fluxes in modern drainage network and intensive agricultural activities. Scenario 2, which is referred to as the 1840s scenario, represents the channel network and soil erosion before European settlement. The modeling time period for the 2000s scenario is from October 1, 1995 to September 30, 2005, and the calibration period is from October 1, 1995 to September 30, 1997. The model was first calibrated for the two-year calibration period to best match observed records of water discharge and sediment load. The calibrated model was then applied to the entire 10-year modeling period for the 2000s scenario. It was then used to simulate sediment fluxes for the 1840s scenario. Modeling results of the two scenarios were compared to reveal the human impacts on the watershed-scale sediment dynamics.

For computational efficiency, the Upper Sangamon River Basin upstream of Monticello gage site was divided into 21 REWs (Figure 4.1), which is appropriate based on previously REW modeling for this landscape (Li et al., 2010). The coupled model was run at a 1-h time step for ten year modeling periods. The Nash-Sutcliffe coefficient (Nash and Sutcliffe, 1970) was used to evaluate the parameters required to produce a best fit over the calibration period and to evaluate model performance over the modeling period for the 2000s scenario. This coefficient measures the goodness of fit to the line of perfect fit (the 1:1 line), and estimates how well the simulated and observed flows correspond. The coefficient can range from $-\infty$ to 1 with an efficiency of 1 corresponding to an exact agreement between predicted and observed data.

The model only accounts for suspended sediment transport and does not consider transport of sediment as bedload in part because no bedload data are available for model calibration. Moreover, problems with reservoir sedimentation in Lake Decatur downstream of the Monticello gauging station indicate that the vast majority of sediment transported by the Sangamon River consists of fine sand, silt, and clay (Blair et al., 2018). The transport of two sizes of material, sand (0.0625 mm) and mud (0.0325 mm), are treated separately in the model. It is assumed that mud supply comes from hillslope erosion and that no mud fraction is deposited within the channel system, but that mud can be deposited on floodplains. Deposition of sand on the other hand occurs both within the channel system and on floodplains.

4.4.2 Data on Climate, Land Use, Soils, and Watershed Characteristics

Model inputs include data on climate, land use, soil order, and watershed characteristics. The climate conditions for two scenarios are assumed to be the same. Although temperature and precipitation have been altered at a global scale by human activities, this factor is not considered in this study; temperature and precipitation are identical for the two scenarios to evaluate the

response of the watershed to matching conditions. Hourly precipitation data at Champaign, Illinois were obtained from National Climatic Data Center (NCDC) of NOAA. Data on soil characteristics were extracted from the STATSGO database. Land cover data for the 2000s scenario were obtained the National Land Cover Database 2011 (Figure 4.5). Digital maps produced by the Illinois Natural History Survey from original General Land Office (GLO) survey maps provided land cover data for the 1840s scenario. Watershed characteristics such as drainage area and watershed slope were extracted from DEM data available through the Illinois State Geological Survey with a spatial resolution of 30 m; channel length, floodplain width, channel top width, and floodplain width were extracted from airborne LiDAR with resolution of 1.2m. Historical channel length and width were measured from maps of the stream network in the USRB produced from General Land Office (GLO) surveys (Rhoads et al., 2016). Floodplain width, watershed slope, drainage area, and soil order inputs for the 1840s scenario are assumed to be the same for both the 1840s and 2000s scenarios.

Table 4.1: Differences in inputs and parameters for two scenarios.

Scenario	Land cover	Channel network	Levees	Hydraulic geometry of the channel
1840s	Mainly prairie and forests	General Land Office (GLO) surveys conducted in the early 1800s	Not present	Eq. (4.19), (4.20) and (4.21)
2000s	Mainly row crop agriculture	Airborne LiDAR data and the DEM with the resolution of 1 arc second	Present	Eq. (4.19) and (4.20)

USGS records of streamflow for the Sangamon River at Monticello, IL were used to calibrate the model to predict discharge for the 2000s scenarios, whereas suspended sediment records for the same station collected as part of the Illinois State Water Survey Sediment Benchmark monitoring program were used to calibrate predictions of sediment load in the 2000s scenario. Annual sediment loads at Monticello were estimated from a sediment-rating curve developed for this station:

$$SSC = aQ^b \tag{4.18}$$

where *SSC* is suspended sediment concentration (mg/l), Q is discharge (m^3/s), a is a dimensional coefficient, and b is a dimensionless exponent (Horowitz, 2003).

The floodplain sedimentation rates within the USRB estimated by Grimley et al. (2017) were compared to predicted values of floodplain sedimentation in the 1840s and 2000s. No information is available on fractions of sand and mud in sediment supplied from hillslopes to channels in this landscape. The sand fraction of sediment eroded from hillslopes is assumed to be 10% - a reasonable value given the fine-grained nature of soils in the watershed (silt loam and silty clay loam) and the lower mobility of sand relative to silt and clay.

4.4.3 Data on Channel Geometry

Sediment entrainment, deposition and transport processes are directly related to the depth and width of stream reach. It is necessary to represent hydraulic geometry of the channel to capture the space-time variations of flow velocity, which determines the sediment dynamics in the stream. Stall and Fok (1968) conducted a survey of at-a-site and downstream hydraulic geometry for streams in Illinois and obtained best fits between measured channel top width, cross-sectional area, flow velocity, flow depth, drainage area and flow frequency. The relations

for channel top width and flow depth for the Sangamon River are:

$$\ln w_{top}^{i} = 0.43 \ln A^{i} + 0.18 \ln A_{d}^{1} + 0.91 \tag{4.19}$$

$$\ln h_{mc}^{i} = \ln A^{i} - \ln w_{top}^{i} \tag{4.20}$$

where w_{top}^{i} is the channel top width (ft) in REW i, h_{mc}^{i} is the mean flow depth (ft) of REW i, A^{i} is the cross-sectional area(ft^2) of REW i. and A_{d}^{i} is the drainage area (mi^2) of REW i. There regionalized relations were adopted in this modeling study to characterize the channel geometry across the Upper Sangamon River Basin in 2000s.

Channel width measured from General Land Office (GLO) survey notes suggests that the downstream of modern drainage network is narrower than the pre-settlement channel, while upstream of modern drainage network was wider than pre-settlement drainage network. The transition point is the location where Big Ditch joins the Sangamon River. The relationship between channel widths in the 1840s determined from GLO surveyor notes and channels widths in the modern drainage network widths is,

$$\log(W_{2000}) = 0.43 \times \log(W_{1840}) + 0.78 \tag{4.21}$$

where W_{2000} and W_{1840} are channel width in the 2000s and 1840s respectively. Moreover, the relationship between channel width and drainage area (DA) for the 1840s is,

$$\log(W_{1840}) = 0.79 \times \log(DA) - 5.69 \tag{4.22}$$

Eqs. (20) and (22) were used in the model to characterize pre-settlement channel width and depth.

Characteristics of artificial levees along drainage ditches and channelized streams were determined from airborne LiDAR data. Ten to twenty stream cross sections derived from the LiDAR data were averaged to define the heights of levees and depths of channelized streams (Figure 4.4). In the 2000s scenario, the depths of channels are the sum of natural channel depths and levee depths. No artificial levees are expected in 1840s, and thus the depths of channels in 1840s scenario are natural channel depths estimated from hydraulic geometry relations. The measured channel depths are compared with the flow depth calculated in Eq. (4.20). When calculated flow depths exceed the measured channel depths, overbank flow occurs and water and sediment are redistributed to the channel and floodplain.

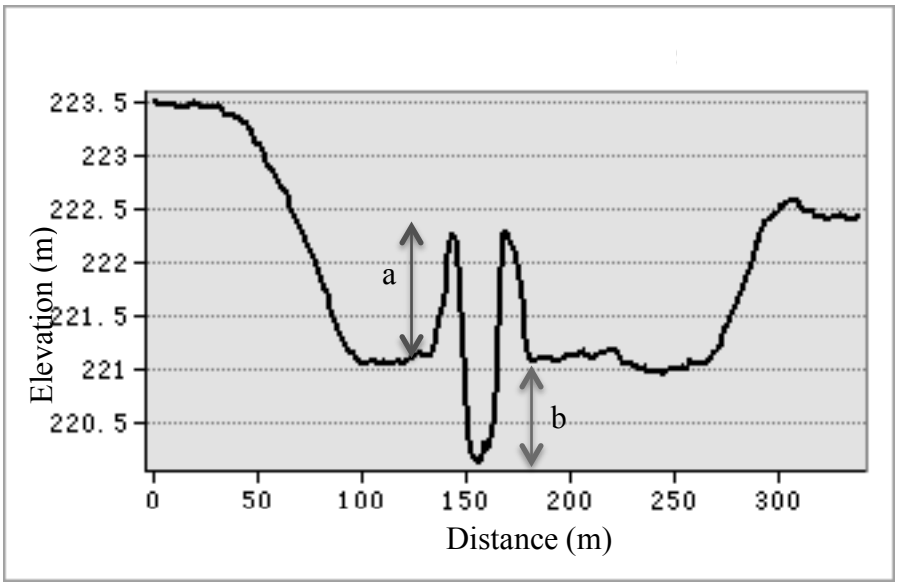

Figure 4.4: A sketch of stream cross-section measurements: (a) height of levee and (b) depth of natural channel.

4.5 Results

To evaluate the performance of the model of watershed-scale sediment dynamics, parameter calibration was first conducted for the two-year calibration period. The calibrated model was applied to simulate modern and pre-settlement sediment fluxes over 10-year periods with identical climatic inputs. The sediment dynamics of the 1840s and 2000s scenarios were compared at multiple scales.

4.5.1 Parameter Calibration and Model Performance

The model contains five calibration hydrological parameters (α, β, α^{IFL}, Manning's n for channel and Manning's n for floodplain) and five calibration sediment parameters (C, c, *spexp*, τ_{cr}, and $K_{ch,i}$). An automated parameter optimization procedure was not performed due to the high computational expenditure required for iterative simulation runs. Model parameters were adjusted manually within a predetermined parameter range based on previously reported values in the literature. Acceptability of parameter values and performance of the model were evaluated by comparing observed and simulated data using the Sutcliffe-Nash coefficient.

Parameter α^{IFL} controls infiltration capacity (Eq. (4.1)), and α and β control the baseflow (Eq. (4.2)). Hydrological parameters were adjusted by comparing predicted daily and monthly discharge with observed values (Table 4.2). The parameter inputs for each REW such as hydraulic conductivity, soil porosity, field capacity, air entry value, soil pore size distribution index, and ground surface depression capacity are estimated from soil order data and previously used values in Li et al. (2010). The hydraulic conductivity for u-zone ranges from 4.46×10^{-6} to 9.30×10^{-6} m/s and hydraulic conductivity for s-zone ranges from 2.41×10^{-6} to 7.48×10^{-6} m/s.

Table 4.2: Hydrological calibration parameters.

Parameters	Values
α	0.35
β	40
α^{IFL}	1.0
Manning's n for channel	0.01
Manning's n for floodplain	0.05

Parameter *C* in Eq. (4.10) controls the magnitude of sediment generated from hillslope. Direct measurements of hillslope erosion rate were not available; therefore the calibration of *C* is based on the comparisons between observed and predicted sediment loads at the watershed outlet. The parameter *C* is related to the vegetation type and crop management. In 1840s scenario, prairie and forests are two major land cover types, and prairie is viewed as grassland (Figure 4.5). Cultivated crops (i.e. corn), forests and grassland are the major land cover types in the 2000s (Figure 4.5). The vegetation and crop management factors of grassland, forests and corn are 0.02, 0.1 and 0.4 respectively (Renard et al., 1991). Parameter *C* in the 1840s scenario for each REW is adjusted as follows,

$$C_{1840s} = C_{2000s} \times \frac{\sum_{i=1}^{n} V_{i,2000s} \times A_i}{\sum_{j=1}^{m} V_{i.1840s} \times A_j} \tag{4.23}$$

where C_{1840s} and C_{2000s} are values of parameter *C* in the 1840s and 2000s scenarios respectively; *m* and *n* are the numbers of vegetation cover types in 1840s and 2000s scenarios

respectively; $V_{i,1840s}$ and $V_{i,2000s}$ are vegetation and crop management factors for the 1840s and 2000s scenarios respectively, and A_i is the area of a specific vegetation cover to the total area of a REW.

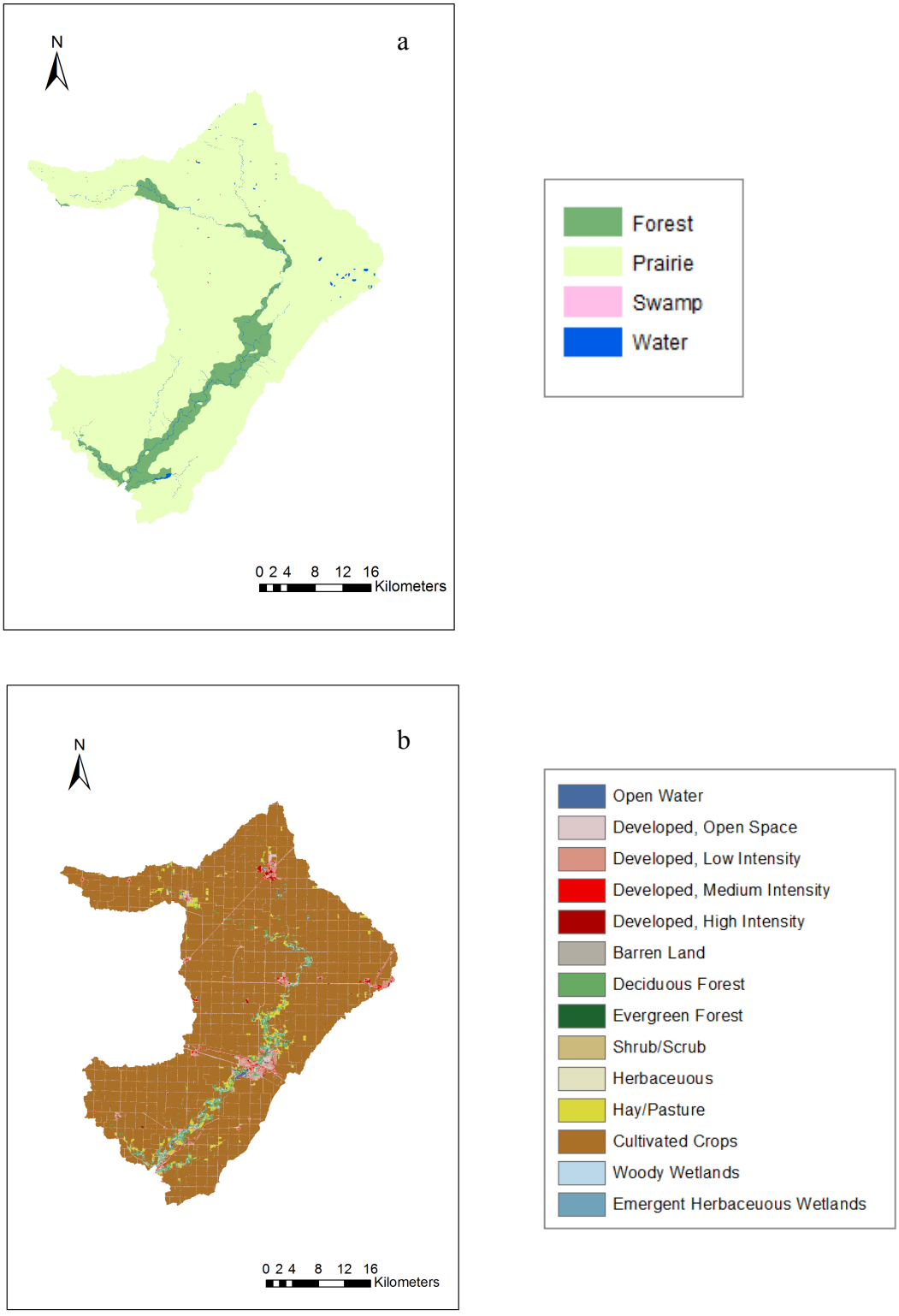

Figure 4.5: Land cover in the USRB upstream of Monticello: (a) 1840s land cover retrieved from Illinois State Natural History Survey and (b) 2000s land cover obtained from the National Land Cover Database 2011.

Parameter *c* and *spexp* in Eq. (4.11) control the stream carrying capacity. Analysis of the relationship between observed sediment load and discharge suggests the sediment transport during high flows in this low-gradient landscape is supply limited: suspended sediment concentration increases with discharge for small and medium discharges but then decreases as with increasing discharge increases after surpassing a threshold discharge. Through trial and error adjustments, values of 0.01 and 1.5 for parameters *c* and *spexp,* respectively, generated appropriate estimates of sediment transport capacity that reflected the supply-limited conditions during high flows and provided accurate estimates of the actual sediment load for the 2000s scenario. The stream erodibility and stream carrying capacity are assumed to be the same for the 1840s and 2000s scenarios, i.e. values of *c* and *spexp* are the same for 1840s and 2000s scenarios. Parameters τ_{cr} and $K_{ch,i}$ in Eq. (4.15) control the sediment erosion and deposition processes of sand fraction in the channel. Appropriate values of these two parameters were estimated that produced the best match between estimated sand fractions and the sand fraction in the suspended sediment load at the Monticello gauging station recorded by Illinois State Water Survey (Table 4.3).

Table 4.3: Sediment input parameters for 1840s and 2000s scenarios.

Scenarios	1840s	2000s
c	0.01	0.01
spexp	1.5	1.5
τ_{cr} (N/m^2)	0. 04	0. 04
$K_{ch,i}$ (g^{-1}s^{-1})	3×10^{-8}	3×10^{-8}

Calibration of model for the two-year calibration period was performed on daily and monthly bases. Calibrating the continuous simulation on an hourly basis is not efficient because of the immense amount of effort needed to match model predictions to patterns of observed data. The calibration on hourly basis also becomes difficult to accomplish because the model does not adequately capture the time lag between precipitation and discharge on hourly basis (Benaman et al., 2005; Abaci and Papanicolaou, 2009). The Nash-Sutcliffe coefficients for predicted daily water discharge and sediment load for the calibration period (from October 1, 1995 to September 30, 1997) are 0.70 and 0.68 respectively, indicating that the model captures reasonably well variability of water discharge and sediment fluxes.

Space-time variations of flow velocity determine the sediment dynamics in the stream. It is crucial to appropriately capture flow velocity both at-site and downstream (Ye et al., 2012). The predicted flow velocity at the basin out varies from nearly 0 to 1.62 m/s, which falls in a reasonable range based on field measurements of velocity at the Monticello gauging station and conforms closely to corresponding estimates of velocity from the Stall and Fok (1968) equations.

4.5.2 *Water and Sediment Dynamics of Modern Channel Network*

The calibrated model was applied to simulate water discharge and sediment loads for the 2000s scenario from October 1, 1995, to September 20, 2005. The Nash-Sutcliffe coefficient for hourly water discharge is 0.68, indicating a fair performance of the model for predicting hydrological response on an hourly basis. Seasonal variations in discharge over the ten years are captured by the model: discharge is highest in summer months and lowest in fall months (Figure 4.6). Predicted average water discharge for 12 months ranged from 0.74 to 25.27 m^3/s. The model predicts accurately the average discharges for 12 months during the ten-year period

(Figure 4.7). Slight under-estimation of discharge in early spring at both hourly and monthly scales may be related to snowmelt, which was not well represented in the model.

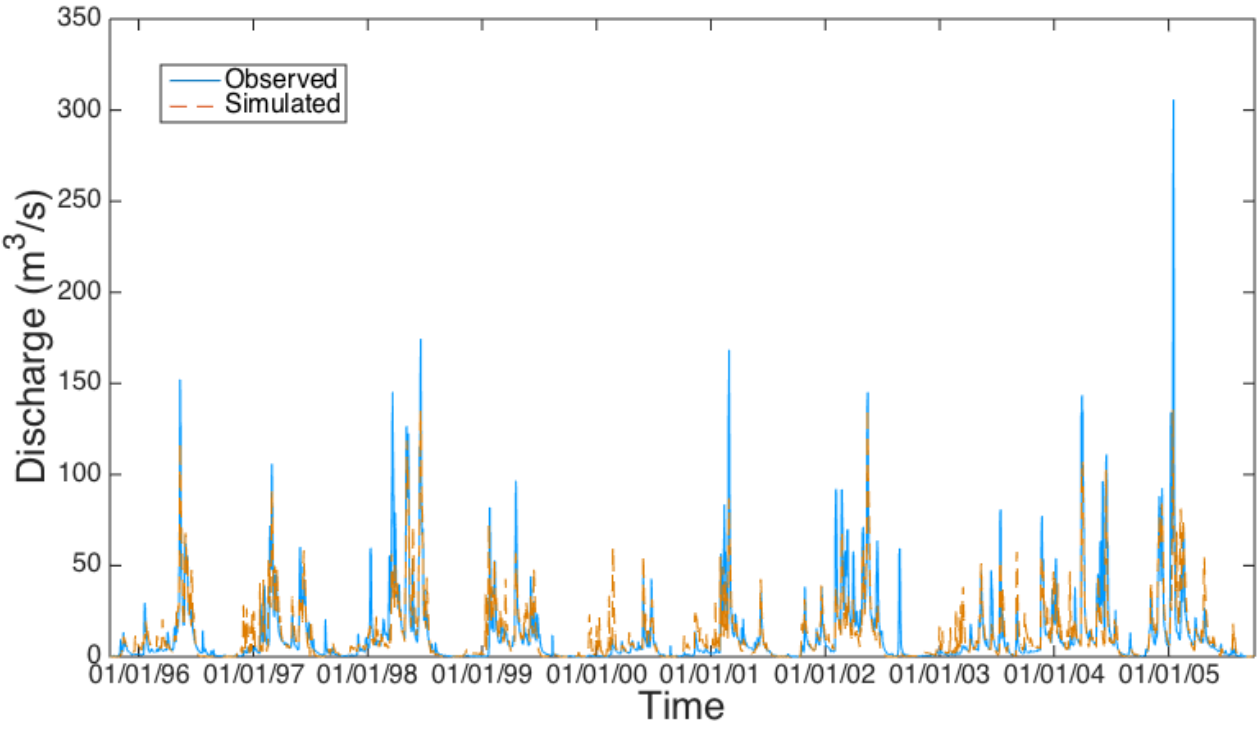

Figure 4.6: Observed and predicted hourly discharge.

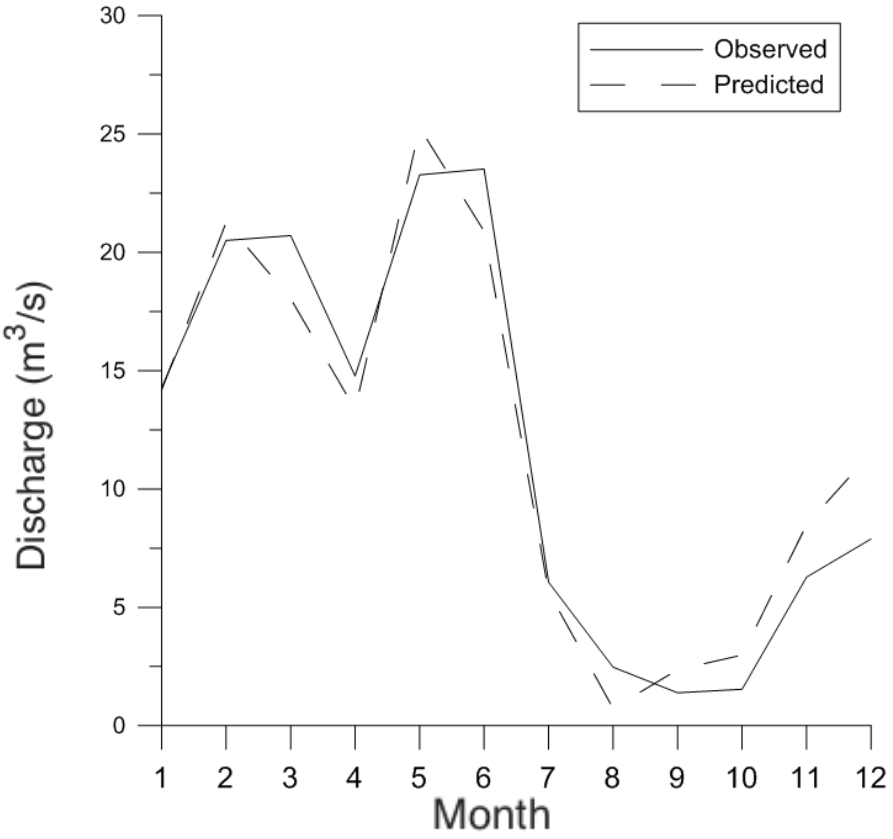

Figure 4.7: Observed and predicted discharge for 12 months.

Predicted sediment load at multiple scales and floodplain sedimentation rates in tributaries and mainstem were compared with observed values to evaluate the model performance in simulating sediment dynamics. The predicted hourly sediment load cannot be directly compared to observed sediment loads at Monticello gauge because the observed values are instantaneous loads. Predicted hourly sediment loads are of the same magnitude and exhibit the same patterns as the observed loads, suggesting reasonable modeling results and model performance on an hourly basis (Figure 4.8). The predicted peak sediment loads are generally higher than observed values in storm events because peak sediment loads might not be captured by periodic, instantaneous sampling.

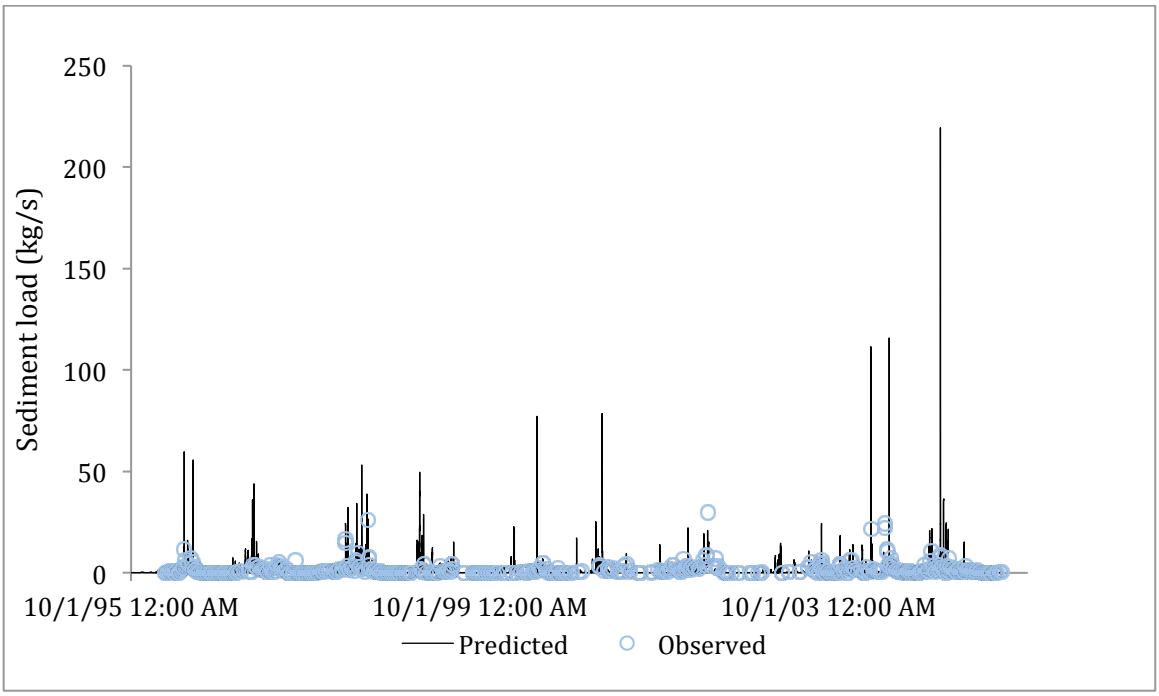

Figure 4.8: Observed and predicted hourly sediment load.

To facilitate the comparison of annual sediment loads, the observed annual sediment loads were calculated from the sediment rating curve for Monticello gauge site. The sediment rating curve developed for Monticello gauge site can be expressed as,

$$\log Q_s = 1.04 \times \log Q_w + 0.87 \tag{4.24}$$

where Q_w is water discharge (m^3/s) and Q_s is sediment load (tons/day).

Predicted annual sediment loads ranged from 17503.75 to 60106.21 tons/yr. The sand fraction of total suspended load at watershed outlet is 2.27%. Coarse sediment is more likely to be retained within the system than fine sediment. The Nash-Sutcliffe coefficient of annual suspended sediment load is 0.60. A 1:1 plot of observed and predicted annual sediment loads (Figure 4.9) indicates a relatively good estimation of annual sediment load. The model tends to

under estimate annual sediment load during high flow years (year 1997 and 2001) and over-estimate sediment load during low flow years (year 1999 and 2002) (Figure 4.10).

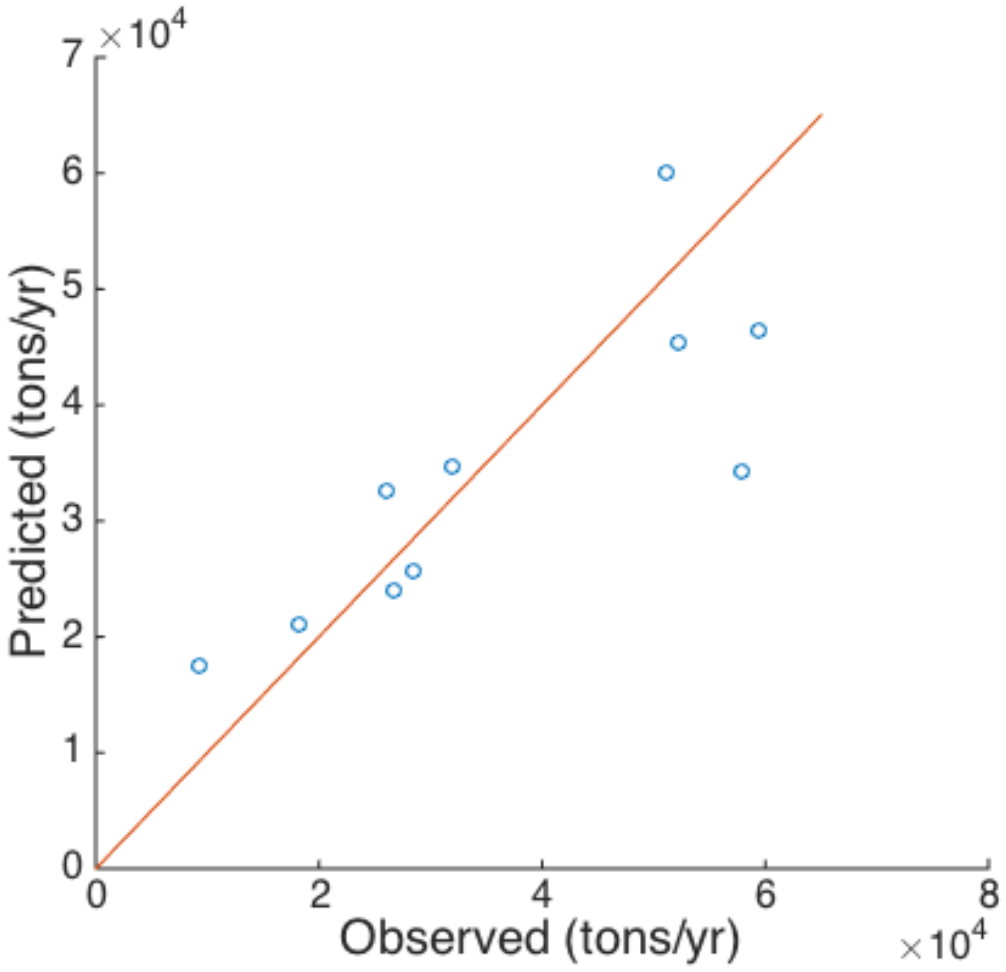

Figure 4.9: 1:1 plot of observed and predicted annual sediment load.

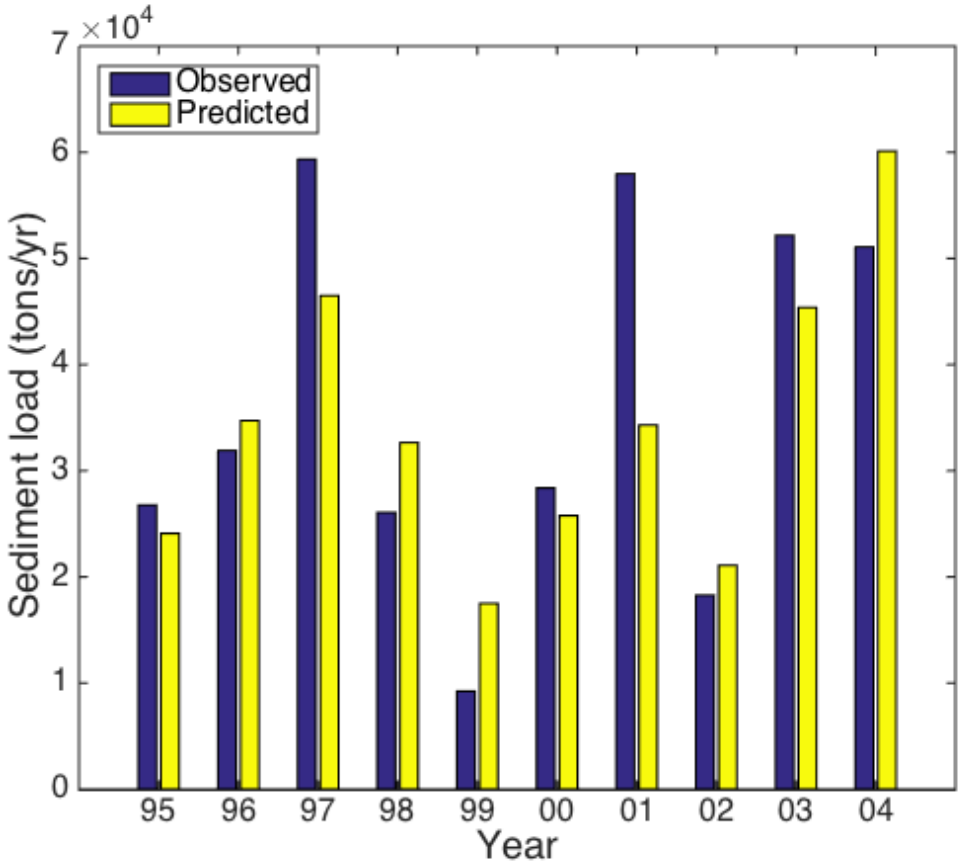

Figure 4.10: Observed and predicted annual sediment load.

The Nash-Sutcliffe coefficient for monthly sediment load is 0.67, which suggests the model performs better on a monthly basis than annual basis (Figure 4.11). The predicted sediment loads for 12 months ranged 10.54 from 225.19 tons/day. The Nash-Sutcliffe coefficient for the predicted sediment loads for 12 months is 0.91, suggesting this model adequately captures the seasonality of sediment load (Figure 4.12). The sediment loads are highest in February and May and lowest in September and October, which is consistent with the seasonality of observed water discharge (Figure 4.13). Snowmelt in February and intense storm events in May generate high sediment loads in the stream. The low sediment load in early fall might be attributed to the low water discharge and exhausted sediment supply after summer storms.

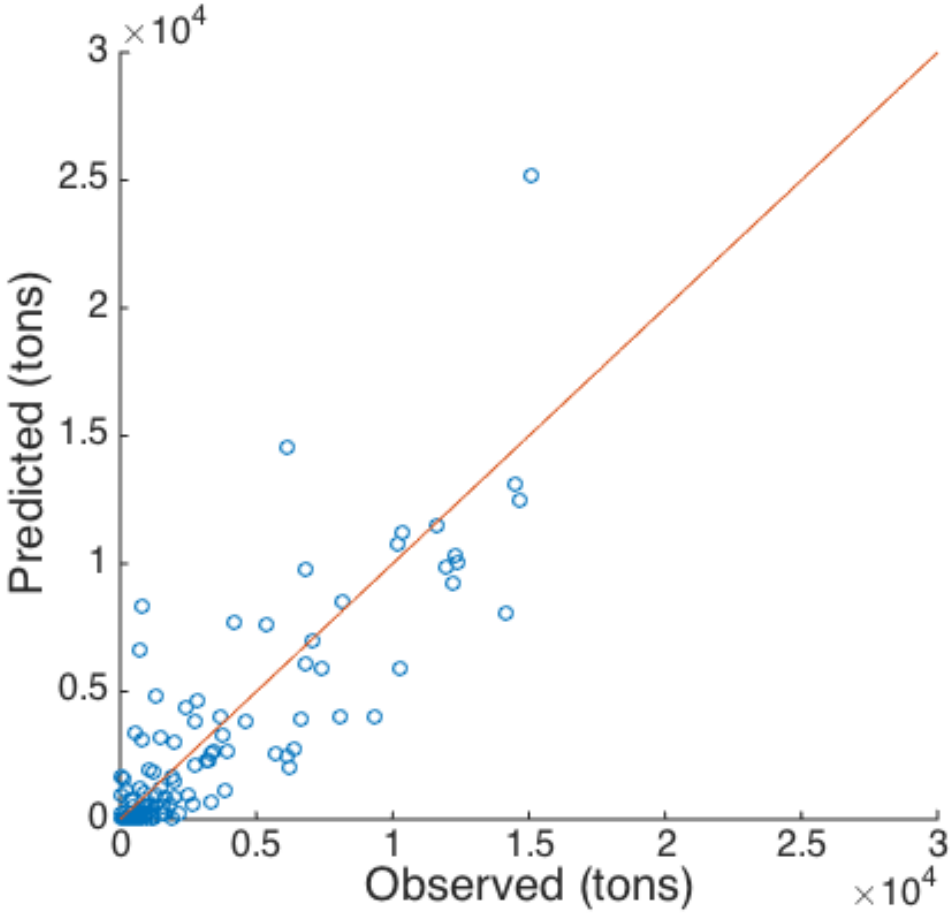

Figure 4.11: 1:1 plot of observed and predicted monthly sediment load.

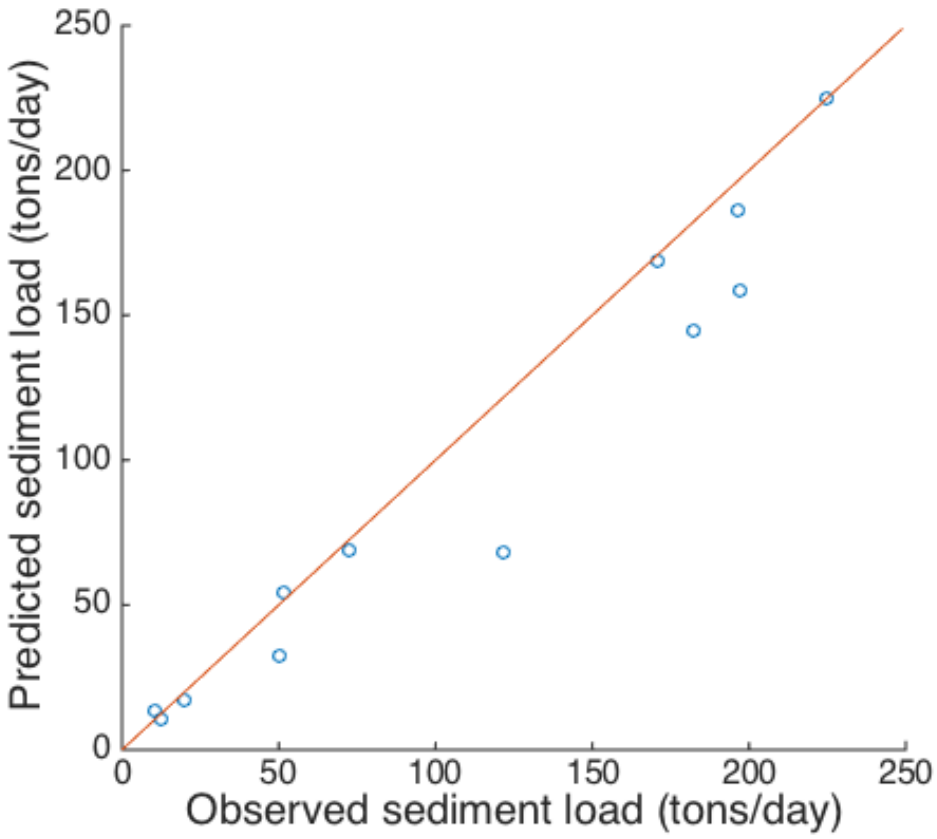

Figure 4.12: 1:1 plot of observed and predicted mean sediment load for 12 months.

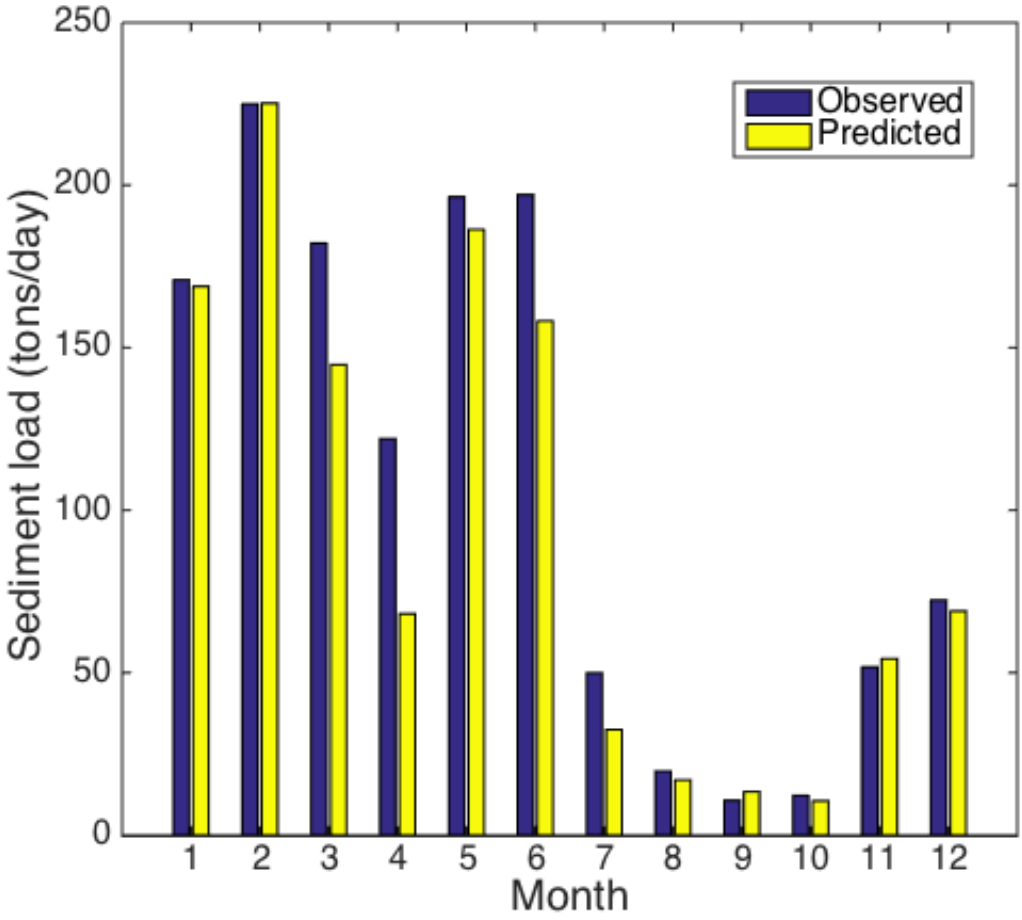

Figure 4.13: Observed and predicted sediment load for 12 months.

4.5.3 *Difference in Sediment Dynamics between Pre-settlement and Modern Conditions*

To understand how agricultural activities and channelization have impacted sediment dynamics, estimates of sediment delivery, storage, and export within the stream system were compared for the 1840s and 2000s. Spatial heterogeneity of the sediment supply sources is an important factor that controls sediment dynamics along the stream network. The sediment load in each headwater REW is controlled by its soil order, land cover and slope, which explains the scatter in plots of sediment load versus drainage area for REWs with drainage areas smaller than

200 km^2 (Figure 4.14). As sediment is transported through the channel network to higher order streams, sediment load increases within increasing drainage area. Sediment load in the 1840s increased slowly with increasing drainage area (A) in the headwaters (A < 500 km^2) compared to the 2000s scenario. This difference reflects the less extensive channel network and the abundant native vegetation cover on hillslopes in the 1840s. Overall, rates of increase in sediment load per unit increase in drainage area are much less for the 1840s than for the 2000s.

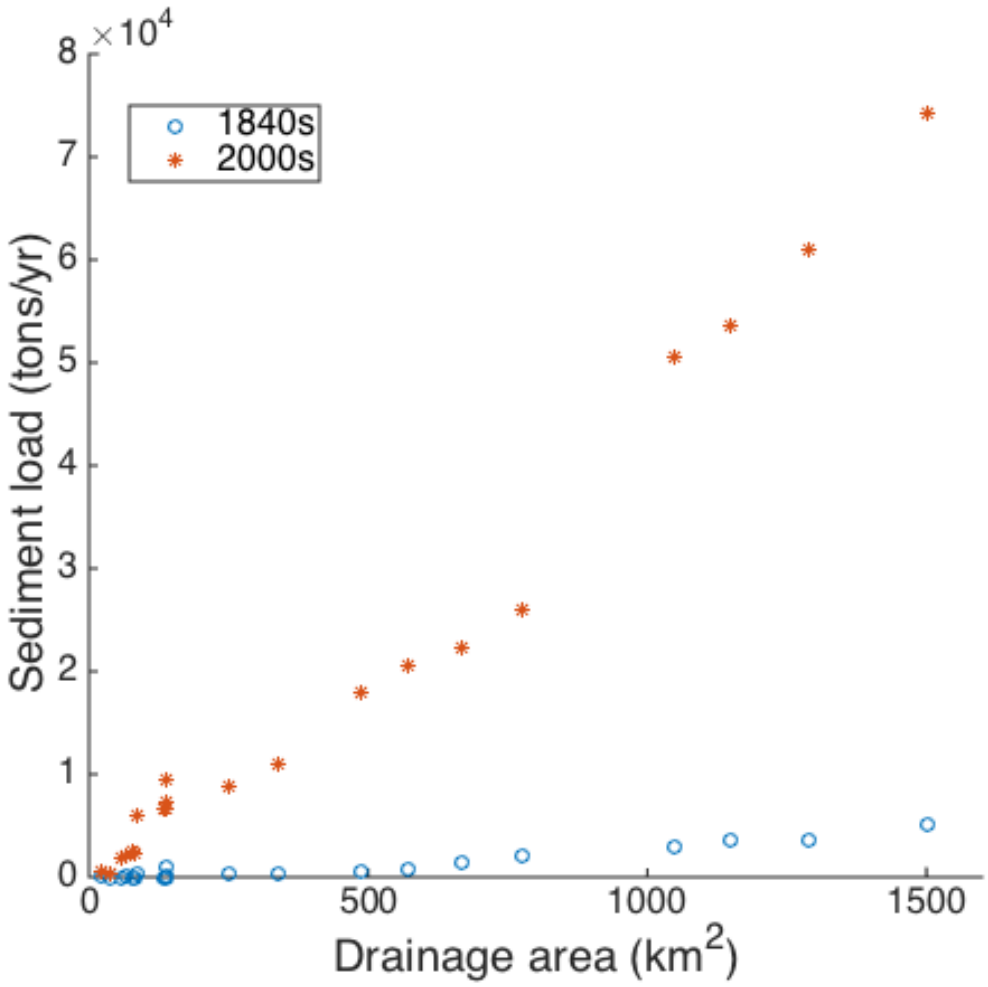

Figure 4.14: Sediment load versus drainage area for 1840s and 2000s.

The model predicts that all fluxes – delivery, storage, and export – are much greater today than in the 1840s for the exact same inputs of rainfall (Figure 4.15). Sediment delivery to

the streams from hillslope erosion has increased approximately eleven-fold, reflecting the enormous influence of change in land cover from prairie to row-crop agriculture on soil erodibility. The annual sediment load of the Sangamon River in the 2000s at the outlet of the watershed is eight times greater than the estimated load in the 1840s. The estimate of floodplain sedimentation is 6.5 times greater today than in the 1840s, whereas in-channel sediment deposition is predicted to have increased by a factor of 30. The only aspect of the sediment budget that is estimated to have been greater in the 1840s than today is channel erosion, which today constitutes about 63% of the 1840s value. The increase in stored sediment within the water column throughout the network during the simulations is similar for the two scenarios, with the 2000s value differing by only 8% from the 1840s value.

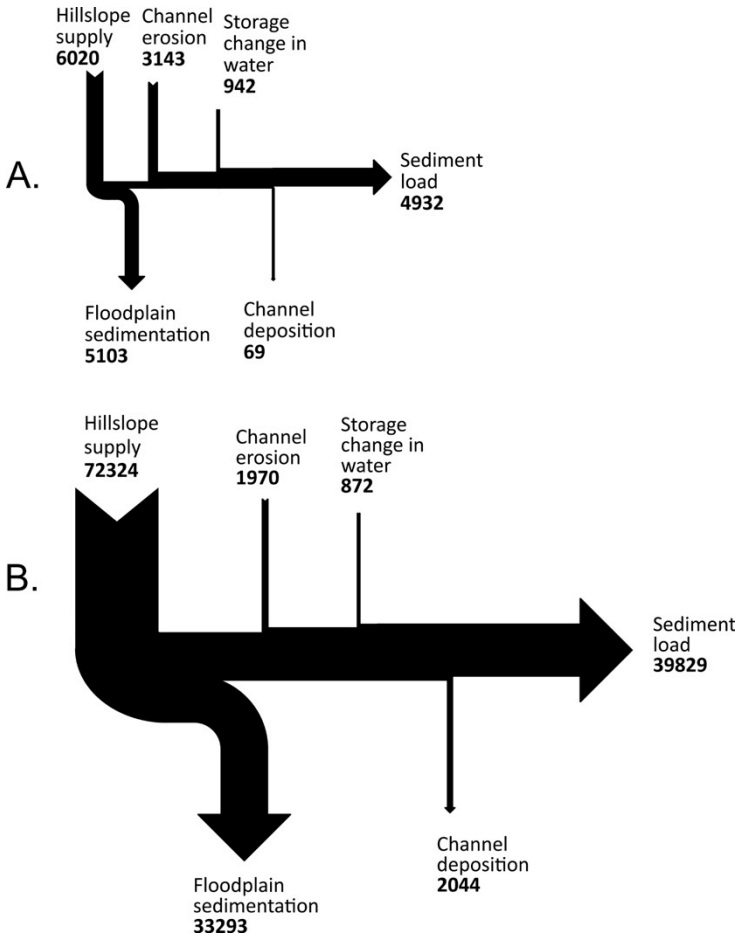

Figure 4.15: Estimated sediment fluxes in tons (Mg) yr^{-1} for A. 1840s and B. 2000s.

When considering the distribution of fluxes as percentages of the total sediment flux within the watershed, sediment supply from hillslopes increased from 60% to 96% from the 1840s to 2000s (Figure 4.16), indicating that hillslope erosion now dominates delivery of sediment to streams. In the 1840s erosion of channels constituted about 31% of the total sediment supply, but today this source represents only 3% of the supply. This change mainly reflects the enormous increase in hillslope supply, which now dwarfs channel erosion. Despite the large increase in total floodplain sedimentation between 1840 and today, the percentage of sediment deposited on the floodplain has decreased slightly from 50% to 44%. On the other

hand, slightly higher percentages of sediment are transported out of the system and deposited within channels in the 2000s than in the 1840s. Although the percentage of delivered sediment has shifted largely to hillslope-derived material, the percentage distribution of sediment deposited in sinks and exported from the basin today is not dramatically different from the distribution in the 1840s. Despite enormous changes in fluxes of sediment within the watershed, the percentage of sediment delivered to streams that leaves the watershed has increased only slightly because increased mobility has nearly been balanced by increased storage.

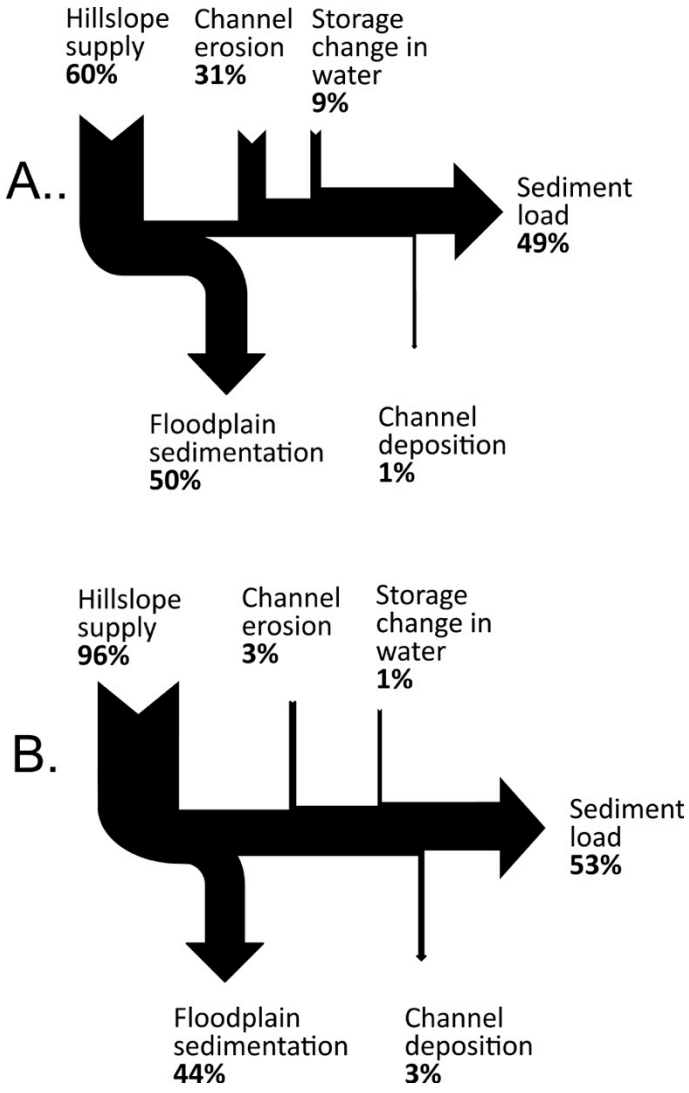

Figure 4.16: Percent of sediment sinks and load for (a) 1840s and (b) 2000s.

The sediment delivery ratios (SDR), which is the ratio of sediment load of a watershed to the total amount of soil detachment (Walling, 1983; Abaci and Papanicolaou, 2009), is often used to relate sediment load to gross erosion rates (Lu et al., 2005). SDRs calculated for the entire watershed for 1840s and 2000s are 49% and 53%, respectively. Because the model estimates sediment supply from hillslopes to streams in a lumped fashion and does not account for sediment deposition on hillslopes, calculated SDRs as calculated in this study represent the

ratio of sediment yield to sediment delivery to the stream network, rather than the total amount of soil erosion. These values of SDR reflect the efficiency by which streams transport sediment delivered to them by hillslope or channel erosion to the watershed outlet. Because redeposition of eroded soil on hillslopes is not accounted for by the model, SDR values in the present study are greater than SDR estimates that account for redeposition, which range from less than 10% to about 35% for watersheds in the midwestern United States (Trimble, 1983; Beach, 1994). In this flat landscape, the transport of sediment from hillslopes to streams is not expected to be efficient. The delivery ratios of suspended sediment load to detached sediment within the watershed, the typical way in which the SDR is expressed, undoubtedly is much lower than the SDRs estimated by the model. When budgets from past studies are expressed in terms of net hillslope erosion, the SDR values from increase to 30 to 60% (Beach, 1994; Trimble, 2009), results consistent with those in the present study. The delivery ratio of the sand fraction is 0.17 for 1840s and 2000s. This low delivery ratio of sand suggests that coarse sediment tends to be stored within the system.

Sediment generation and transport within a year is a temporally variable process. To examine the dynamics of sediment fluxes within a year, the sediment loads in the two scenarios are estimated over the course of the year for identical inputs. The model generated a highly accurate estimate of the sediment load in the year 2000 so inputs for this year were selected as the basis for comparison between contemporary and historical conditions. The plot of accumulated sediment loads in the year 2000 and the corresponding year with identical climate inputs in 1840s scenario (Figure 4.17) shows that accumulated sediment load has increased substantially for five major storm events under modern conditions.

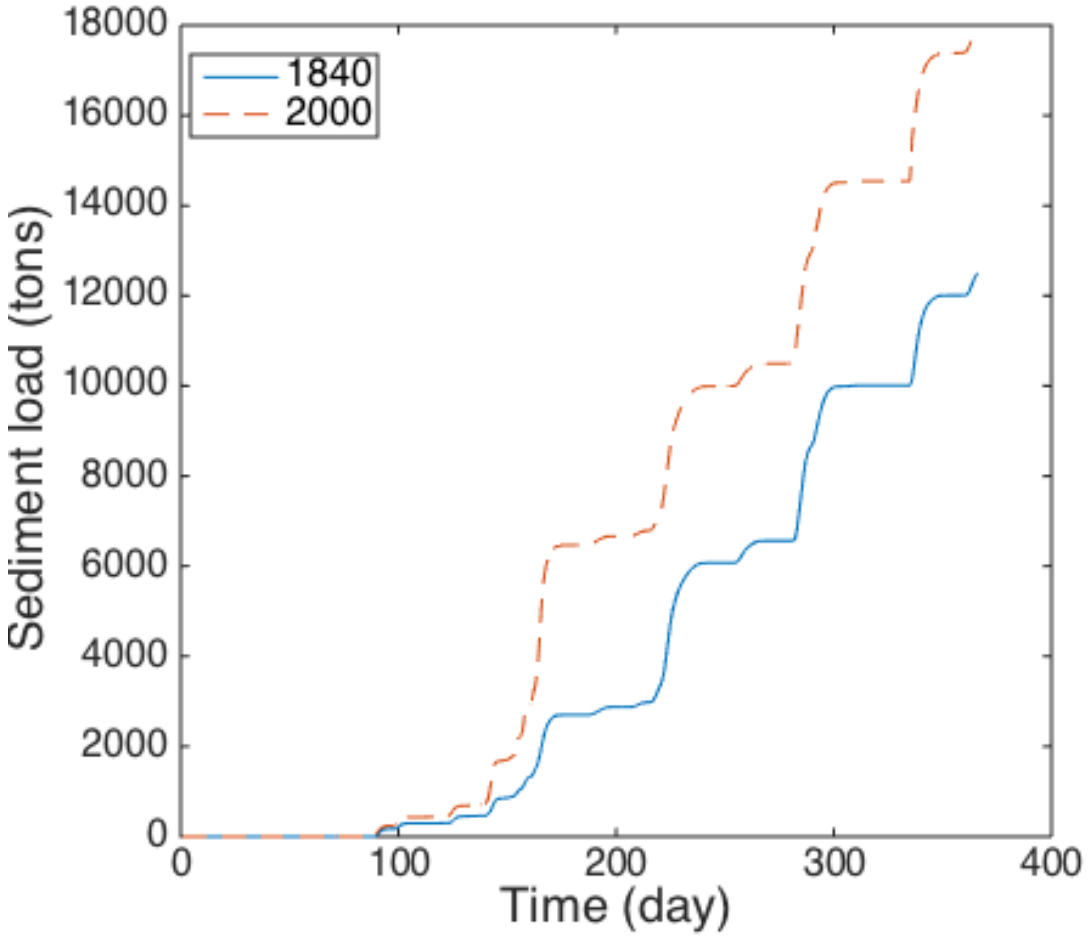

Figure 4.17: Accumulated sediment load in the year 2000 and corresponding conditions in 1840s scenario.

The delivery of sediment from streams to the watershed outlet exhibits an inverse relationship with drainage area (Figure 4.18). SDRs of small headwater REWs approach unity and SDR decreases with increasing drainage area. This inverse relationship is probably reflects increased sediment storage within increasing watershed size (Walling, 1983; Lu et al., 2005; Abaci and Papanicolaou, 2009). The SDRs in 1840s and 2000s do not differ markedly. SDRs of relatively medium-sized sub-watersheds are slightly lower in 2000s than that in 1840s,

suggesting that a higher percentage of sediment is stored in medium-sized sub-watersheds in 2000s than in 1840s.

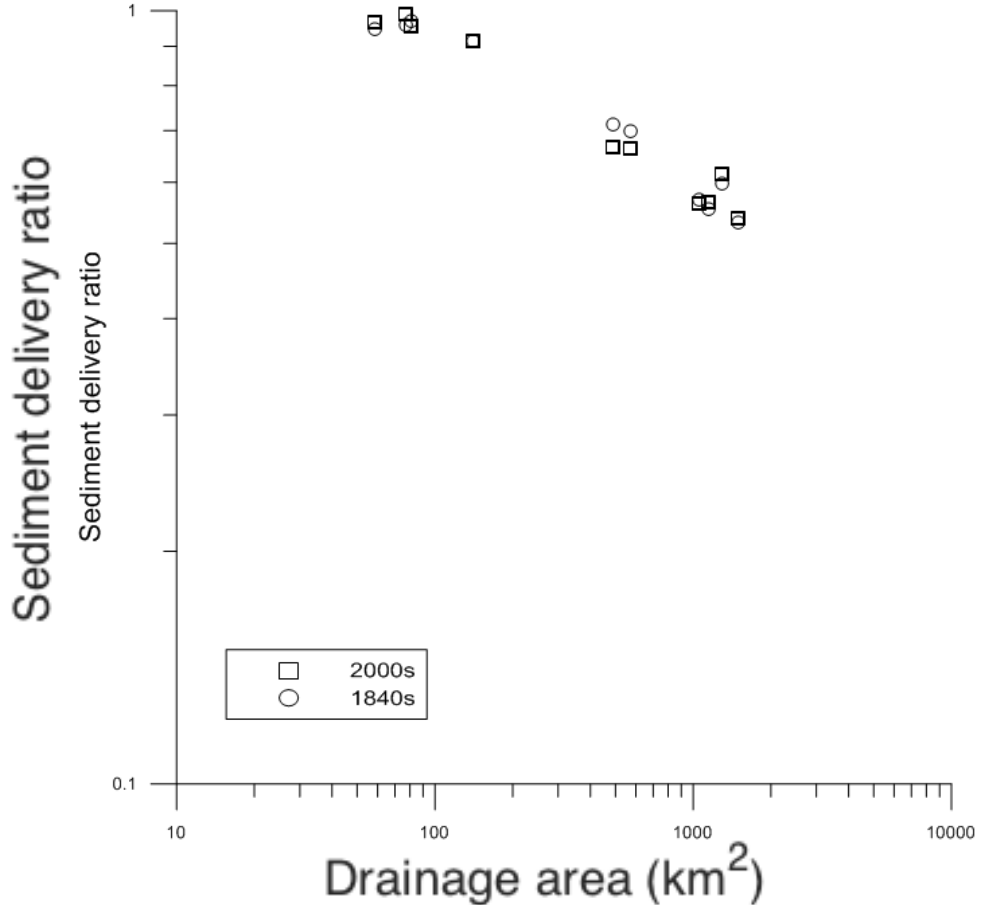

Figure 4.18: Relationship of sediment delivery ratio with drainage area.

Floodplain sedimentation rates in the 2000s are a magnitude higher than those in the 1840s, which is consistent with the average alluvial sediment rates in the USRB estimated by Grimley et al. (2017) using fly ash dating of floodplain sediments (Table 4.4). Floodplain sedimentation rates increased from 0.06 to 0.58 mm/yr in tributaries and from 0.22 to 1.19 mm/yr in mainstem. Tributaries have lower floodplain sedimentation rates than the mainstem in both scenarios. The model predicts somewhat lower floodplain sedimentation rates than those estimated by Grimley et al. (2017). Materials deposited on the floodplain are assumed to be

evenly distributed across the entire floodplain in the model, whereas the floodplain sedimentation rates estimated through using fly ash were based on the measurements on 17 sample sites. Considerable variations in floodplain sedimentation rates exist between sampling sites on the floodplain of the Sangamon River (Arnott, 2015). Spatial heterogeneity of floodplain sedimentation rates might explain the difference between point estimations of floodplain sedimentation rates by Grimley et al. (2017) and the floodplain sedimentation rates estimated by the model.

Table 4.4: Floodplain sedimentation rates estimated by the model and through using fly ash

	Time period	Tributaries (mm/yr)	Mainstem (mm/yr)
Grimley et al., 2017	Pre-settlement	0.09	0.70
	1960–2015 CE	2.00	6.00
Model estimation	1840s	0.06	0.22
	2000s	0.58	1.19

The influence of levees in channelized reaches is examined by comparing sediment-rating curves of three REWs with contrasting channel characteristics. REW 35 is a first order stream with levees in the 2000s, REW 50 is a first order stream without levees in the 2000s, and REW 16 is a reach on the mainstem of the Sangamon River without levees in the 2000s. Given the same discharge, sediment loads for the three REWs are all higher in 2000s than in 1840s due to increased sediment erosion from agricultural uplands; however, the increase of sediment load for channelized REW 35 greatly exceeds the increases for the unleveed reaches (Figure 4.19). The large increase of sediment load in REW 35 is related to the decreased sediment retention on the floodplain, which is caused by the presence of artificial levees.

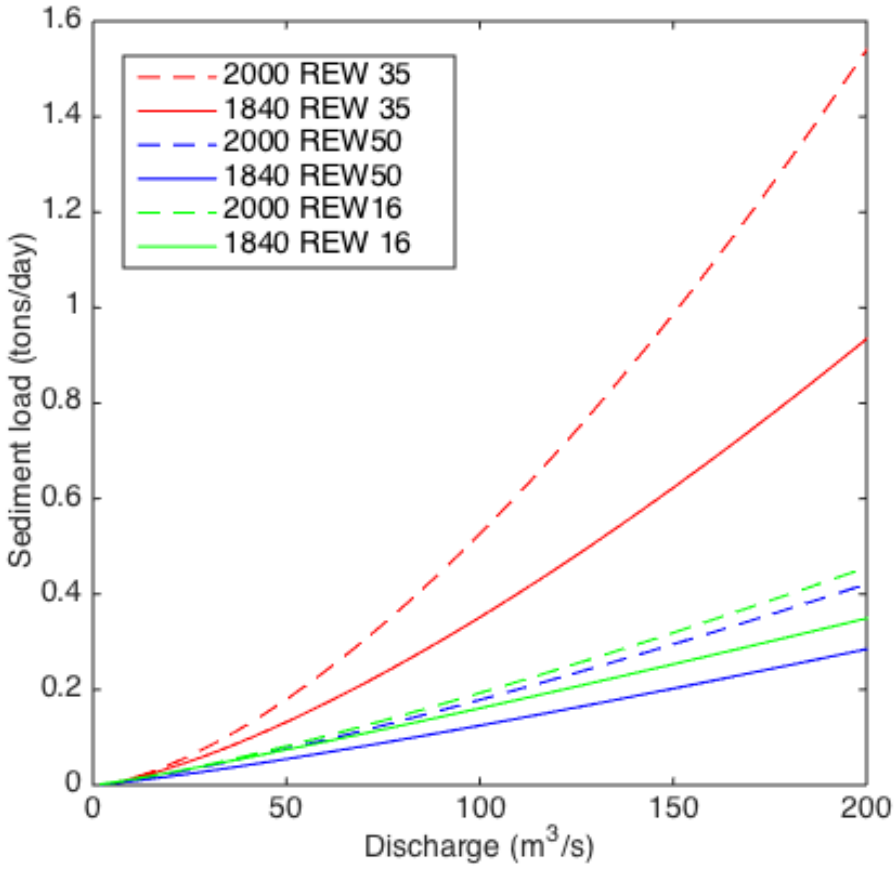

Figure 4.19: Sediment rating curves for REW 35, REW 50 and REW 16.

4.6 Discussion

The semi-distributed, coupled hydrologic and sediment model developed in this study yields accurate estimates of modern water and sediment fluxes across multiple scales in the Upper Sangamon River basin – an intensively managed agricultural watershed in East Central Illinois. This outcome implies that the calibrated model should provide reasonable estimates of water and sediment fluxes within this watershed prior to the implementation of agriculture. Results of the simulations suggest that intensive agricultural activities have greatly increased sediment loads and sediment storage within stream systems of intensively managed agricultural

landscapes of the Midwest. Relatively flat, low relief agricultural uplands now introduce large amounts of suspended sediment into streams. The model estimates that sediment supply from uplands increased 11-fold from the 1840s to 2000s. Estimates of presettlement hillslope erosion in the present study (0.04 Mg/ha/yr) are consistent with presettlement estimates of soil erosion rates in loess-coverd low-relief landscapes in the midwestern United States (0.035 to 0.06 Mg/ha/yr) (Norton, 1986; Nearing, 2017). Estimates of modern fluxes (0.48 Mg/ha/yr)) are relatively low compared to general estimates for cultivated cropland (6 to 9 Mg/ha/yr) (Nearing, 2017), but the estimates seem reasonable for the low-relief landscape of central Illinois. The estimated hillslopes fluxes do not correspond directly to soil-erosion rates, which should be higher than rates of delivery of sediment to streams from hillslopes. In any case, the comparison with published values suggests the model provides conservative estimates of modern hillslope erosion rates. The predicted increase in hillslope fluxes also conforms to results of experimental research on soil erosion rates in native grassland versus cropped land, which show that erosion rates range from eight times greater for cropland with no-till to as much as 170 times greater for cropland with conventional tillage (Zhang and Garbrecht, 2002).

With the transformation from prairie and forests to row crop agriculture, annual sediment load in 2000s is estimated to be eight times greater than the load in the 1840s. This dramatic increase in sediment load has important implications for water quality, river and stream habit, fluvial dynamics, and human water-resources infrastructure. As a result of enhanced sediment fluxes of fine sediment, the 12 km^2 Lake Decatur lost more than one-third of its original volume between the 1920s and early 2000s (Fitzpatrick et al., 1987; Bogner, 2002), necessitating dredging of the lake to maintain adequate capacity (Rhoads et al., 2016).

Present results are consistent with other sediment budget and modeling studies that suggest agricultural land use and associated management practices strongly influence the magnitude of soil erosion rates and increase stream sediment loads far above natural background levels (Meade and Trimble, 1974; Montgomery, 2007; Abaci et al., 2009; Gran et al., 2013; Maalim et al., 2013). Sediment budgeting studies in the midwestern United States have largely focused on the magnitude of sediment fluxes associated with agricultural activity and the response of those fluxes to agricultural conservation practices without considering the magnitude of pre-settlement fluxes (Trimble, 1983; Beach, 1994; Trimble, 2009). An exception is work in the Le Seuer basin in Minnesota where modeling suggest that transformation of land surface, vegetation and hydrology since European settlement has increased sediment load by a factor of four to five (Gran et al., 2009; Gran et al., 2011; Maalim et al., 2013). The results of this study therefore contribute to the understanding of the extent to which transformation of landscapes by industrial agriculture has accelerated fluxes of sediment delivery, storage, and transport within river networks.

The six-fold increase in floodplain sedimentation estimated by the model also is consistent with results of other studies that have examined rates of sediment accumulation pre- and post-settlement (James and Lecce, 2013); however, total thicknesses of accumulation are not as pronounced as in older glaciated or non-glaciated terrains in the Midwest with higher relief than the Sangamon basin, such as the Driftless Region of Wisconsin (Knox, 1987, 2006; Magilligan 1992, 1985; Lecce, 1997) and northeastern Iowa (Baker et al., 1993). The estimated impact of artificial levees and channelization on floodplain storage in headwater portions of the Sangamon River basin coincides with results of other work demonstrating that the smallest short-

term rates of floodplain deposition occur along channelized reaches of rivers, where the floodplain is essentially isolated from overbank deposition (Kroes and Hupp, 2010).

The net decrease in sediment supplied by channel erosion and net increase in sediment deposition within channels between the 1840s and 2000s suggests that channels were more active prior to settlement than at present. This result is consistent with the large increase in hillslope sediment supplied to the stream network. It also is consistent with analysis of channel change over the past 40 years in the upper Sangamon River basin, which indicates that most reaches of the main river and major tributaries have not moved laterally over the past 80 years (Rhoads et al., 2016). Although the present model does not simulate lateral erosion, net erosion of the channel bed in the model reflects excess energy available to change the channels via sediment transport. The same excess energy could generate lateral migration if such a component were included in the model. Thus, channel erosion in the model can be viewed as a general indicator of the tendency for channel dynamics. Despite the overall lateral stability of the Sangamon River and its tributaries since the 1930s, abundance evidence of past lateral migration is apparent in the form of scroll-bar topography and meander scars on floodplains. It appears the river was at one time more active in migrating laterally than at present. The predicted decrease in channel erosion and increase in channel deposition between the 1840s and 2000s may account for such a change.

Despite the dramatic increases in total sediment flux, the estimated sediment delivery ratio for the entire watershed increased from only 49% to 53% from the 1840s to the 2000s. The percentage of floodplain sedimentation and channel deposition only changed 2%~ 6%, indicating that the increased sediment supply does not have a substantial impact on the fate of mobilized sediment. Despite decreased retention of sediment on floodplain due to channelization, the

results agree with the general conclusion of other work that the majority of eroded material remains trapped in watersheds (Haggett, 1961; Walling, 1983; Trimble, 1999; Trimble and Crosson, 2000; Wilkinson and McElroy, 2007; Walter and Merritts, 2008, Reusser et al., 2015). Annual channel deposition under present conditions is 30 times of that under pre-settlement conditions – a result consistent with the three-fold increase in the density of headwater streams in the watershed and the persistent accumulation of sediment in headwater channels (Rhoads et al., 2016). Net deposition is a common fluvial response to stream channelization in agricultural drainage ditches, which motivates frequent excavation to remove accumulated sediment (Landwehr & Rhoads, 2003).

An important limitation of the current model is that it does not account for erosional processes affecting the floodplain. Recent tracing of fine sediment in the headwaters of the USRB suggests that active lateral migration of the Sangamon River channel along with erosion of the floodplain by surface runoff in areas of intensive cattle grazing locally contributes the majority of sediment to the instream load (Yu and Rhoads, 2018). While refinement of the model might incorporate mechanisms of floodplain erosion, it seems unlikely that this factor plays a major role in watershed-scale sediment fluxes given the limited amount of cattle grazing within the USRB (< 1% of total land use) and overall low rates of lateral migration of the Sangamon River and its tributaries (Rhoads et al., 2016).

4.7 Conclusion

Quantifying the impacts of humans on suspended sediment loads of watersheds is important to understand the extent to which humans have transformed the sediment dynamics of fluvial systems. This study developed and implemented a coupled, semi-distributed hydrologic and sediment model to simulate water and sediment fluxes in an intensively managed

agricultural watershed in the midwestern United States. Two scenarios were simulated to estimate sediment dynamics under contemporary conditions and sediment dynamics prior to European settlement. Sediment supply, floodplain sedimentation, sediment delivery ratio, and suspended sediment load for the two scenarios were compared across multiple scales. Results demonstrate that transformation of the landscape from prairie and forest to intensive agricultural has led to dramatic increases in upland erosion and river suspended sediment loads, which supports the argument that intensively managed landscapes have passed a threshold and have shifted from a transformation-dominated system, in which sediment delivery to stream systems was limited by dense vegetation cover, to a transport-dominated system, in which exposed soil is readily mobilized and redistributed throughout stream networks. The results of this study also indicate that channel network extension through the additional of channelized streams limits increases in floodplain storage, but enhances within-channel storage.

The coupled model is capable of accurately estimating sediment load and predicting the responses of sediment load to future changes in land management practices and the impact of climate change. It therefore provides a tool to examine how land and river management practices aimed as sediment management might influence watershed-scale sediment fluxes. The present modeling study focused mainly on the effects of human activities on delivery of upland sediment to streams and to the fate of sediment river-transported sediment. It did not characterize in detail erosional and depositional processes on the hillslope. The opportunity exists to link the present model with other models, such as GeoWepp (Renschler 2003), that explicitly account for soil detachment, movement, and deposition on hillslopes processes to fully account for linkages between hillslope and channel processes at the watershed scale.

4.8 References

Abaci, O., & Papanicolaou, A. N. (2009). Long-term effects of management practices on water-driven soil erosion in an intense agricultural sub-watershed: monitoring and modelling. *Hydrological Processes, 23*, 2818-2837. http://doi.org/10.1002/hyp.7380

Arnold, J. G., Williams, J. R., & Maidment, D. R. (1995). Continuous time water and sediment-routing model for large basins. *Journal of Hydraulic Engineering*, *121*, 171-183.

Arnott, D. R. (2015). Spatial and temporal variability in floodplain sedimentation during individual hydrologic events on a lowland, meandering river: Allerton park, Monticello, Illinois, (Master of Science thesis). Urbana, IL: University of Illinois at Urbana-Champaign.

Asselman, N. E. M., & Van Wijngaarden, M. (2002). Development and application of a 1D floodplain sedimentation model for the River Rhine in the Netherlands. *Journal of Hydrology*, *268*, 127-142. http://doi.org/10.1016/S0022-1694(02)00162-2

Bagnold, R. A. (1977). Bedload transport in natural rivers. *Water Resources Research, 13*(2), 303-312.

Baker, R. G., Schwert, D. P., Bettis, E. A., & Chumbley, C. A. (1993). Impact of Euro-American settlement on a riparian landscape in northeast Iowa, midwestem USA: an integrated approach based on historical evidence, floodplain sediments, fossil pollen, plant macrofossils and insects. *The Holocene*, *3*(4), 314-323.

Beach, T. (1994). The fate of eroded soil: sediment sinks and sediment budgets of Agrarian landscapes in southern Minnesota, 1851-1988. *Annals of the Association of American Geographer*, *84*(1), 5-28.

Beasley, D. B., Huggins, L. F., & Monke, E. J. (1980), ANSWERS: A model for watershed planning. *Transactions of the American Society of Agricultural Engineers, 23*, 938-944.

Benaman, J., Christine, A. S., & Douglas, A. H. (2005). Calibration and validation of soil and water assessment tool on an agricultural watershed in Upstate New York. *Journal of Hydrologic Engineering, 10*(5), 363-374.

Blair, N. E., Leithold, E. L., Papanicolaou, A. N., Wilson, C. G., Keefer, L., Kirton, E., et al. (2018). The C-biogeochemistry of a Midwestern USA agricultural impoundment in context: Lake Decatur in the intensively managed landscape critical zone observatory. *Biogeochemistry*, *138*, 171-195.

Bogner, W.C. (2002). *Sedimentation survey of Lake Decatur's Big and Sand Creek basins: Macon County, Illinois* (Contract Report 2002-09). Champaign, IL: Illinois State Water Survey.

Chen, C.-N. (1975). Design of sediment retention basins. *Proceedings of the National Symposium on Urban Hydrology and Sediment Control,* Lexington, Kentucky, 285-298.

Conroy, W. J., Hotchkiss, R. H., & Elliot, W. J. (2006). A coupled upland-erosion and instream hydrodynamic-sediment transport model for evaluating sediment transport in forested watersheds. *Transactions of the ASABE*, *49*(6), 1713-1722.

Dermisis, D. C., Papanicolaou, A. N., Abban, B., Flanagan, D. C., & Frankenberger, J. R. (2011). The coupling of WEPP and 3ST1D numerical models for improved estimation of runoff and sediment yield at watershed scales. *World Environmental and Water Resources Congress,* 4749-4758. http://doi.org/10.1061/41173(414)493

Ewen, J., Parkin G., & O'Connell, P. E. (2000). SHETRAN: Distributed River Basin Flow and Transport Modeling System. *Journal of Hydrologic Engineering*, *5*, 250–258. http://doi.org/10.1061/(ASCE)1084-0699(2000)5:3(250)

Fan, S.S. (1988). *Twelve selected computer stream sedimentation models developed in the*

United States. Proceedings of the Interagency Symposium on Computer Stream Sedimentation Model, Denver, Colorado.

Fitzpatrick, W. P., Bogner, W. C., & Bhowmik N. G. (1987). Sedimentation and hydrologic processes in Lake Decatur and its watershed (Report of Investigation 107). Champaign, IL: Illinois State Water Survey.

Foster, G. R., Lane, L. J., Asce, A. M., Knisel, W. G., & Asce, M. (1980). Estimating sediment yield from cultivated fields. *Proceedings of the Symposium on Wathershed Managment*. Boise, Idaho.

Gran, K. B., Belmont, P., Day, S., Jennings, C., Johnson, A., Perg, L., & Wilcock, P. R. (2009). Geomorphic evolution of the Le Sueur River, Minnesota, USA, and implications for current sediment loading. in James, L.A., Rathburn, S.L., and Whittecar, G.R., eds., *Management and Restoration of Fluvial Systems with Broad Historical Changes and Human Impacts: Geological Society of America Special Paper,* 451, 119–130. http://doi.org/10.1130/2009.2451(08)

Gran, K. B., Belmont, P., Day, S., Jennings, C., Lauer, J.W., Viparelli, E., et al. (2011). An integrated sediment budget for the Le Sueur River basin (Final Report to the Minnesota Pollution Control Agency).

Gran, K. B., Finnegan, N., Johnson, A. L., Belmont, P., Wittkop, C., & Rittenour, T. (2013). Landscape evolution, valley excavation, and terrace development following abrupt postglacial base-level fall. *Geological Society of America Bulletin*, *125*(11-12), 1851-1864. https://doi.org/10.1130/B30772.1

Gregory, K. J. (2006). The human role in changing river channels. *Geomorphology*, *79*, 172–191. http://doi.org/10.1016/j.geomorph.2006.06.018

Grimley, D. A., Anders, A. M., Bettis, E. A., Bates, B. L., Wang, J. J., Butler, S. K., et al. (2017). Using magnetic fly ash to identify post-settlement alluvium and its record of atmospheric pollution, central USA. *Anthropocene*, *17*, 84–98. http://doi.org/10.1016/j.ancene.2017.02.001

Haggett, P. (1961). Land use and sediment yield in an old plantation tract of the Serra Do Mar, Brazil. *The Geographical Journal*, *127*, 50–59. http://doi.org/10.2307/1793195

Horowitz, A. J. (2003). An evaluation of sediment rating curves for estimating suspended sediment concentrations for subsequent flux calculations. *Hydrological Processes*, *17*, 3387–3409. http://doi.org/10.1002/hyp.1299

Illinois Natural History Survey. *Pre-settlement vegetation for Illinois symbolized with categories used on the published map*. Retrieved from http://imperialis.inhs.illinois.edu/arcgis/rest/services/Land_Cover/Presettlement_Land_Cover_All/MapServer

James, L. A., & Lecce, S. A. (2013). Impacts of land-use and land-cover change on river systems. In Shroder, J. & Wohl, E. (Eds.), *Treatise on Geomorphology* (Vol. 71, pp. 768-793). San Diego, CA: Academic Press.

Knox, J. C. (1987). Historical valley floor development in the Upper Mississippi valley. *Annals of the Association of American Geographers*, *77*, 224- 244.

Knox, J. C. (2006). Floodplain sedimentation in the Upper Mississippi Valley: Natural versus human accelerated. *Geomorphology*, *79*, 286–310.

Kroes, D. E., & Hupp, C. R. (2010). The effect of channelization on floodplain sediment deposition and subsidence along the Pocomoke River, Maryland. *Journal of American Water Resources Association*, *46*(4), 686–699. http://doi.org/10.1111/ j.1752-

1688.2010.00440.x

Kumar, P., Le, P. V. V., Papanicolaou, A. N. T., Rhoads, B. L., Anders, A. M., Stumpf, A., et al. (2018). Critical transition in critical zone of intensively managed landscapes. *Anthropocene*, *22*, 10-19.

Landwehr, K., & Rhoads, B. L. (2003). Depositional response of a headwater stream to channelization, east central Illinois , USA. *River Research and Application*, *19*(1), 77–100. http://doi.org/10.1002/rra.699

Lecce, S. A. (1997). Spatial patterns of historical overbank sedimentation and floodplain evolution, Blue River, Wisconsin. *Geomorphology*, *18*, 265-277.

Li, H., Sivapalan, M., Tian, F., & Liu, D. (2010). Water and nutrient balances in a large tile-drained agricultural catchment: A distributed modeling study. *Hydrology and Earth System Sciences*, *14*, 2259–2275. http://doi.org/10.5194/hess-14-2259-2010

Lu, H., Moran, C. J., & Sivapalan, M. (2005). A theoretical exploration of catchment-scale sediment delivery. *Water Resources Research*, *41*, W09415. http://doi.org/10.1029/2005WR004018

Maalim, F. K., Melesse, A. M., Belmont, P., & Gran, K. B. (2013). Modeling the impact of land use changes on runoff and sediment yield in the Le Sueur watershed, minnesota using GeoWEPP. *Catena*, *107*, 35-45. http://doi.org/10.1016/j.catena.2013.03.004

Magilligan, F. J., (1992). Sedimentology of a fine-grained aggrading floodplain. *Geomorphology*, *4*, 393-408.

Mattingly, R. L., Herricks, E. E., & Johnston, D. M. (1993). Channelization and levee construction in Illinois: Review and implications for management. *Environmental Management*, *17*(6), 781–795.

Meade, R.H., & Trimble, S.W. (1974). Changes in sediment loads in rivers of the Atlantic drainage of the United States since 1900, in Effects of Man on the Interface of the Hydrological Cycle with the Physical Environment. I*nternational Association of Hydrological Sciences*, *113*, 99–104.

Medeiros, P. H. A., Güntner, A., Francke, T., Mamede, G. L., & Carlos de Araújo, J. (2010). Modelling spatio-temporal patterns of sediment yield and connectivity in a semi-arid catchment with the WASA-SED model. *Hydrological Sciences Journal*, *55*(4), 636–648. http://doi.org/10.1080/02626661003780409

Montgomery, D. R. (2007). Soil erosion and agricultural sustainability. *Proceedings of the National Academy of Sciences of the United States of America*, *104*(33), 13268–13272. http://doi.org/10.1073/pnas.0611508104

Morgan, R. P. C., Quinton, J. N., Smith, R. E., Govers, G., Poesen, J. W. A., Auerswald, K., et al. (1998). The European Soil Erosion Model (EUROSEM): A dynamic approach for predicting sediment transport from fields and small catchments. *Earth Surface Processes and Landforms*, *23*, 527–544. http://doi.org/10.1002/(SICI)1096-9837(199806)23:6<527::AID-ESP868>3.0.CO;2-5.

Nash, J. E., & Sutcliffe, J. V. (1970). River flow forecasting through conceptual models part i—a discussion of principles. *Journal of Hydrology*, *10*, 282–290. http://doi.org/10.1016/0022-1694(70)90255-6

Nearing, M. A., Xie, Y., Liu, B., & Ye, Y. (2017). Natural and anthropogenic rates of soil erosion. *International Soil and Water Conservation Research*, *5(2)*, 77-84. http://dx.doi.org/10.1016/j.iswcr.2017.04.001

Nearing, M. A., Foster, G. R., Lane, L. J., & Finkner, S. C. (1989). A process- based soil erosion

model for USDA - Water Erosion Prediction Project technology. *Transactions American Society of Agricultural Engineers*, *32*, 1587–1593.

Neitsch, S. L., Arnold, J. G., Kiniry, J. R., & Williams, J. R. (2005). Soil and water assessment tool - theoretical documentation - version 2005, Grassland, Soil and Water Research Laboratory, Agricultural Research Service and Blackland Research Center, Texas Agricultural Experiment Station, Temple, Tex.

Noe, G.B., & Hupp C.R. (2005). Carbon, Nitrogen, and Phosphorus Accumulation in Floodplains of Atlantic Coastal Plain Rivers, USA. *Ecological Applications*, *15*, 1178-1190.

Norton, S. A. (1986). A review of the chemical record in lake sediment of energy related air pollution and its effects on lakes. *Acidic Precipitation*. Springer, Dordrecht, 331-345

Osterkamp, W. R., & Toy, T. J. (1997). Geomorphic considerations for erosion prediction. *Environmental Geology*, *29*, 152–157. http://doi.org/10.1007/ s002540050113.

Papanicolaou, A. N., Krallis, G., & Edinger, J. (2008). Sediment transport modeling review—current and future developments. *Journal of Hydraulic Engineering*, *134*(1), 1-14.

Patil, S., Sivapalan, M., Hassan, M. A., Ye, S., Harman, C. J., & Xu, X. (2012). A network model for prediction and diagnosis of sediment dynamics at the watershed scale. *Journal of Geophysical Research*, *117*, F00A04. http://doi.org/10.1029/2012JF002400

Pizzuto, J. E. (1987). Sediment diffusion during overbank flows. *Sedimentology*, *34*, 301–317. http://doi.org/10.1111/j.1365-3091.1987.tb00779.x

Prosser, I. P., Rutherfurd, I. D., Olley, J. M., Young, W. J., Wallbrink, P. J., & Moran, C. J. (2001). Large-scale patterns of erosion and sediment transport in river networks, with examples from Australia, Mar. *Freshwater and Marin Research*, *52*, 81–99, http://doi.org/10.1071/MF00033

Reggiani, P., Sivapalan, M., Hassanizadeh, S. M., & Gray, W. G. (2001). Coupled equations for mass and momentum balance in a stream network: theoretical derivation and computational experiments. *Proceedings of the Royal Society A: Mathematical, Physical and Engineering Sciences*, *457*, 157–189. http://doi.org/10.1098/rspa.2000.0661

Reggiani, P., Sivapalan, M., & Hassanizadeh, S. M. (1998). A unifying framework for watershed thermodynamics: Balance equations for mass, momentum, energy and entropy, and the second law of thermodynamics. *Advances in Water Resources*, *22*, 367–398. http://doi.org/10.1016/S0309-1708(98)00012-8

Renard, K. G., Foster, G. R., Weesies, G. A., & Porter, J. P. (1991). RUSLE: Revised universal soil loss equation. *Journal of soil and Water Conservation*, *46*, 30-33.

Renschler, C. S. (2003). Designing geo-spatial interfaces to scale process models: The GeoWEPP approach. *Hydrological Processes*, *17*(5), 1005-1017.

Reid, L. M., and T. Dunne (2003). Sediment budgets as an organizing framework in fluvial geomorphology. In Kondolf G. M. and Piegay H. (Eds.), *Tools in Fluvial Geomorphology* (pp. 463–500). Chichester, U. K: John Wiley.

Reusser, L., Bierman, P., & Rood, D. (2015). Quantifying human impacts on rates of erosion and sediment transport at a landscape scale. *Geology, 43(2),* 171-174.

Rhoads, B. L., Lewis, Q. W., & Andresen, W. (2016). Historical changes in channel network extent and channel planform in an intensively managed landscape: Natural versus human-induced effects. *Geomorphology*, *252*, 17–31. http://doi.org/10.1016/j.geomorph.2015.04.021

Rhoads, B. L., & Herricks, E. E. (1996). Naturalization of headwater streams in Illinois: challenges and possibilities. In Brookes, A. & Shields, F. D. (Eds). *River Channel*

Restoration, Guiding Principles for Sustainable Projects (331–367). New York, NY: Wiley.

Rogers A. D. (1992). The development of a simple infiltration capacity equation for spatially variable soils, (Bachelor Thesis). Perth, Western Australia, Australia: The University of Western Australia.

Stall, J. B., & Fok, Y. S. (1968). Hydraulic Geometry of Illinois Streams (Water Resource Center Research Report, No. 15). Champaign, IL: Illinois State Water Survey.

Tian, F., Hu, H., & Lei, Z. (2008). Thermodynamic watershed hydrological model: Constitutive relationship. *Science in China Series E: Technological Sciences*, *51*(9), 1353–1369. http://doi.org/10.1007/s11431-008-0147-0

Trimble, S. W. (1983). A sediment budget for Coon Creek basin in the Driftless area, Wisconsin, 1853-1977. *American Journal of Science, 283*, 454-474.

Trimble, S. W. (1999). Decreased rates of alluvial sediment storage in the Coon Creek Basin, Wisconsin, 1975–93. *Science*, *285*, 1244-1246. http://doi.org/10.1126/science.285.5431.1244

Trimble, S. W. (2009). Fluvial processes, morphology and sediment budgets in the Coon Creek Basin, WI, USA, 1975–1993. *Geomorphology*, *108*, 8-23.

Trimble, S. W., & Crosson, P. (2000). U.S. soil erosion rates – myth and reality. *Science*, *289*, 248–250.

Urban, M. A., & Rhoads, B. L. (2003). Catastrophic human-induced change in stream-channel planform and geometry in an agricultural Watershed, Illinois, USA. *Annals of the Association of American Geographers*, *93*(4), 783–796. http://doi.org/10.1111/j.1467-8306.2003.09304001.x

Verstraeten, G., Prosser, I. P., & Fogarty, P. (2007). Predicting the spatial patterns of hillslope sediment delivery to river channels in the Murrumbidgee catchment, Australia. *Journal of*

Hydrology, *334*, 440–454. http://doi.org/10.1016/j.jhydrol.2006.10.025

Viney, N. R., & Sivapalan, M. (1999). A conceptual model of sediment transport : application to the Avon River basin in western Australia. *Hydrological Processes*, *13*, 727–743.

Walling, D. E. (1983). The sediment delivery problem. *Journal of Hydrology*, *65*, 209–237. http://doi.org/10.1016/0022-1694(83)90217-2

Walter, R.C., & Merritts, D.J. (2008). Natural streams and the legacy of water-powered mills. *Science*, *319*, 299–304, http://doi.org/10.1126/science.1151716

Wilkinson, B. H., & McElroy, B. J. (2007). The impact of humans on continental erosion and sedimentation. *Geological Society of America Bulletin*, *119*, 140–156, http://doi.org/10.1130/B25899.1

Williams, J. (1980). SPNM, a model for predicting sediment, phosphorus, and nitrogen yields from agricultural basins. *Water Resources Bulletin*, *16*, 843-848.

Wischmeier, W. H., & Smith D. D. (1965). Predicting rainfall erosion losses from croplands east of the Rocky Mountains: Guide for Selection of Practices for Soil and Water Conservation (Handbook No. 282). Washington DC: US Department of Agriculture.

Ye, S., Covino, T. P., Sivapalan, M., Basu, N. B., Li, H. Y., & Wang, S. W. (2012). Dissolved nutrient retention dynamics in river networks: A modeling investigation of transient flows and scale effects. *Water Resources Research*, *48*, W00J17. http://doi.org/10.1029/2011WR010508

Young, R. A., Onstad, C. A., Bosch, D. D., & Anderson, W. P. (1989). AGNPS: A nonpoint-source pollution model for evaluating agricultural watersheds. *Journal of Soil Water Conservation*, *44*(2), 168–173.

Yu, M., & Rhoads, B. L. (2018). Floodplains as a source of fine sediment in grazed landscapes:

Tracing the source of suspended sediment in the headwaters of an intensively managed agricultural landscape. *Geomorphology*, *308*, 278-292. https://doi.org/10.1016/j.geomorph.2018.01.022

Zhang, X. C., & Garbrecht, J. D. (2002). Precipitation retention and soil erosion under varying climate, land use, and tillage and cropping systems. *Journal of the American Water Resources Association*, *38*, 1241–1253. https://doi.org/10.1111/j.1752-1688.2002.tb04345.x

Zhao, R. J. (1992). The Xin'anjiang model applied in China. *Journal of Hydrology*, *135*, 371-381.

CHAPTER 5

CONCLUSIONS

5.1 Major findings of this dissertation

The flux of fine sediment within agricultural watersheds is an important factor determining the environmental quality of streams and rivers. Human activity has significantly altered the hydrological and biogeochemical cycles within terrestrial and aquatic environments through agricultural intensification, tile drainage installation, and urban development. The study of watershed-scale sediment dynamics is of great value for understanding and predicting the response of sediment dynamics to intensive human impact and is crucial to developing management strategies for reducing the vulnerability of the ecosystem to future changes. Thus, the primary objective of this dissertation was to investigate sediment sources, sediment transport, and sediment yield in an intensively managed agricultural landscape. This objective was accomplished by combining of field sampling and measurements, laboratory analysis, sediment fingerprinting study, statistical analysis and modeling exploration in the Upper Sangamon River Basin (USRB), IL. Chapter 2 estimated the relative contributions from potential sources to the suspended sediment of a headwater system of the USRB, Saybrook watershed, IL, by using sediment fingerprinting techniques. A Monte Carlo simulation approach was used to explore the uncertainty associated with results based on mean values of tracer properties. Chapter 3 explored the relationship between precipitation, discharge and suspended sediment concentration in three sediment sites along the Sangamon River by examining the patterns of sediment rating curves and hysteresis loops. The seasonal, inter-event and intra-event relationships between discharge and suspended sediment concentration were investigated to reveal the fundamental controls on the watershed-scale sediment transport. Chapter 4 developed and used a semi-distributed

hydrologic and sediment model to predict sediment fluxes in the USRB. It focused on comparing sediment generation on hillslope and channel, entrainment and deposition processes in channels, floodplain sedimentation, and suspended sediment yields between pre-settlement and modern times. This model-based evaluation of sediment flux was used to assess the impact of human activities, especially agricultural activities and channelization, on sediment dynamics at watershed scale.

The research was guided by key questions and objectives that are outlined in Chapter 1. These research questions are revisited here, along with summaries of the corresponding findings related to each question are given below.

R1) Where does fine (< 0.063 mm) suspended sediment in the headwater of IMLs come from, and how do land use and channel morphology influence the contributions from various sediment sources?

The grazed areas of the floodplain are the primary source of fine suspended sediment within the headwaters of the Sangamon River. Among cropland, forested floodplain, grassland, upper grazed floodplain, and lower grazed floodplain sources, upper grazed floodplain and lower grazed floodplain supplied 97% of suspended sediment in to the stream. Erosion of the floodplain both by surface runoff and by streambank erosion contribute to the production of almost all fine sediment sampled within the stream system. The results are consistent both for event and aggregated samples and for large and small events. Evaluations of uncertainty of the results using Monte Carlo simulation and regrouping of samples to increase sample size in the fingerprinting analysis support the conclusion that grazed floodplains are the primary source of fine sediment in the stream system.

The tracing results are consistent with visible and historical evidence of active erosion of grazed areas of floodplain upstream from the in-stream sampling location. Large sections of the channels banks have detached from the adjacent floodplain through the basal undercutting, the development of tension cracks, and subsequent cantilever failures. From a historical perspective, sections of the Sangamon River within the grazed areas have exhibited substantial amounts of lateral migration over the past several decades. Analysis of historical aerial photography indicates the river channel has in some cases moved laterally by several channel widths. Sections of the river upstream of the grazed areas, which have been channelized for the purpose of land drainage, by comparison are relatively stable and show little or no sign of lateral movement over the last 70 years (Rhoads et al., 2016).

Evidence from field reconnaissance and inspection of aerial photography supports the conclusion that cattle grazing plays an important role in accelerating floodplain and streambank erosion. Analysis of airborne Lidar data indicates that the average slope of the grazed floodplain surface is about 3 degrees toward the main channel. Bare, exposed soil exists on cattle pathways and ramps into the stream, some of which have evolved into short, eroded gullies. These exposed areas of soil contain abundant amounts of loose erodible fine material that can be introduced into the stream.

Although grazing occurs over only a small portion of the total watershed area, grazed floodplains, which lie in close proximity to the stream channel, are an important source of sediment in this headwater steam system. Efforts to reduce fluxes of fine sediment in this intensively managed landscape should focus on eroding floodplain surfaces and channel banks within heavily grazed reaches of the stream.

R2) How does the flux of fine sediment vary temporally and spatially within an IML watershed, and what factors control the spatial and temporal heterogeneity of fine-sediment export?

Suspended sediment load in the stream is far below the stream transport capacity during high flows. Sediment rating curves developed for three sites along the Sangamon River all have a peaked pattern with a transition point in the sediment concentration-discharge relation at geometric mean of discharge. Below this transition point concentration increases with increasing discharge, whereas below it concentration decreases with increasing discharge. The implication is that the rate of increase in sediment load diminishes with increasing discharge above the transition point.

Spatially, suspended sediment concentrations (SSC) tend to become more coincident with the seasonality of rainfall and discharge with increasing watershed size. Localized erosion and sediment delivery have more profound influence on the suspended sediment supply at the scale of small headwater subwatersheds than at the scale of the the entire watershed.

The mean SSC decreases as drainage area increases, which may be caused by deposition of sediment within the system and a dilution effect, perhaps from increases in groundwater flow to the stream (Walling and Webb, 1982). The decrease in SSC with increasing drainage area and discharge also indicates that either the delivery of sediment to the stream decreases with increasing drainage area or sediment storage within the river system increases with drainage area, or both. The decreased event sediment concentrations from Saybrook upstream to Monticello downstream indicate that substantial amounts of sediment may be deposited and stored within the channel network. However, the threshold discharges that separate the positive and negative trends in the rating curves at three sites are all below the bankfull discharge.

Therefore, this transition is not directly related to the stage at which the floodplain becomes inundated and deposition of sediment on the floodplain becomes a factor influencing instream SSC. Although floodplain deposition processes do not generally prevail at the threshold discharge at the sampling sites, flooding may occur locally leading to some deposition and storage of sediment on the floodplain. Moreover, some storage of fine sediment may occur within the channel, behind log jams or other obstructions to flow, which are numerous within the part of the river system that includes Mahomet and Monticello. Also, at stages well above the transition the floodplain does become inundated, leading to floodplain sediment storage.

In high flow ranges, SRCs developed for all three sites had negative exponents, and the decrease of exponents in high flow ranges exhibits a geographic trend: the exponent of SRC developed for the downstream Monticello site is smaller than the exponent for the upstream Saybrook site. This geographic trend reveals that the increase of sediment load per unit increase of discharge is slower when drainage area increases. The "sediment-starved" condition is more likely to occur in large watersheds than small watersheds under the same hydrological and meteorological conditions.

Temporally, the SRCs developed for the rising and falling limbs of hydrographs and the three sampling seasons also exhibit the same trends, which suggests that these trends are not timescale-dependent. The peaked pattern of sediment rating curve is most apparent in sediment rating curve developed on discharge and sediment data collected in summer, which means the limitation of sediment supply is most significant in summer. The limited sediment supply in summer may be result from the intensive storms and short storm intermittency. Intensive summer storms may exhaust sediment sources quickly, leading to reduced sediment concentrations in a sequence of events. The relatively short "recovery time" for sediment sources results in a more

significant "sediment-starved" condition of the stream in summer (Gellis, 2013).

R3) How did watershed-scale fine sediment dynamics change under human impact and how will watershed-scale fine sediment dynamics change under ongoing human impact?

Intensive agricultural activities since European settlement have increased sediment supply and enhanced suspended sediment load in stream, and also have influenced the re-distribution of detached sediment within the system.

The percent of sediment supplied from each source to the total amount of mobilized sediment significantly changed from 1840s to 2000s, and the agricultural uplands have become the major source of suspended sediment in the stream. In this intensively managed landscape, agricultural activities have introduced a substantial amount of sediment into the stream in 2000s. The amount of sediment supply in 2000s was 12 times of that in 1840. Sediment supply from hillslope increased from 60% to 96% from 1840s to 2000s, indicating hillslope sediment has become a major source of the suspended sediment in the steam. The channel bed contributed 31% of the suspended in 1840s. In 2000s, however, the channel bed contributed only 3% of the suspended sediment.

The rates of increase in sediment supply per unit increase in drainage area are much less for the 1840s than for the 2000s. Sediment supply in 1840s increased slowly with increasing drainage area (A) in the headwaters ($A < 500$ km^2) compared to the 2000s scenario. This difference likely reflects the less extensive channel network in the 1840s and the abundant vegetation cover on hillslopes.

The amount of sediment deposited within the watershed and transported out of the watershed in 2000s is 5 to 25 times higher than that in 1840s. The amount of sediment deposited

and stored within the watershed in 2000s is 7 times of that in 1840s, and the sediment yield in 2000s is 8 times of that in 1840s. A higher percent of sediment is transported out of the system and deposited in the channel in 2000s than in 1840s. The percentage of sediment deposited on the floodplain to the amount of sediment mobilized decreased from 50% to 44%.

Suspended sediment load has increased more rapidly than floodplain sedimentation. In this intensively managed landscape, the increase of sediment fluxes and stores due to agricultural activities is complicated by extension of channel network and channelization. Sediment supply increased 7 times from 1840s to 2000s, and floodplain sedimentation rates in 2000s are an order of magnitude higher than the floodplain sedimentation rates in 1840s. However, the floodplain sedimentation only increased 5.5 times.

The re-distribution of detached sediment is also influenced by the presence of built levees and extended channel network. Artificial levees in channelized reaches impede sediment retention on the floodplain and result in an increase of sediment deposition in the channel. The artificial levees, which disconnect the floodplain from the stream and increase bankfull height, have led to a smaller portion of sediment retained on the floodplain. Given the same discharge, the increase in sediment load between 1840 and the 2000s is greater in channelized REWs than in un-channelized REWs.

Extension of channel network also prevents sediment being transported onto the floodplain. Channel extension and the increase of channel width in headwaters in 2000s caused a lower water level for a given amount of flow in the channel. For the same hydrologic condition for 1840s and 2000s scenarios, the decreased water level, along with increased bankfull height caused by channelization, led to a decrease in frequency of floodplain inundation and floodplain sediment retention.

With the increased sediment supply and decreased percent of floodplain sedimentation, sediment delivery ratio for the entire watershed only increased by 4%. The percentage of floodplain sedimentation and channel deposition to the sum of sediment deposition within the watershed and export out of the system only changed 1%~ 3%, indicating that the increased sediment supply does not have a significant impact on the fate of mobilized sediment.

5.2 Future work

This dissertation has investigated the sediment dynamics in an intensively managed agricultural landscape and provided insight into the factors that control sediment generation, transport and yield at the watershed scale. Additional effort could be invested to further understand the sediment dynamics in intensively managed landscapes.

Future work should consider the extent to which grazing affects the sediment budget of the floodplain. Although erosion of the floodplain by failure of streambanks and by direct runoff introduces sediment to the stream system, overbank deposition most likely occurs during events that exceed bankfull flow, resulting in sediment retention. The extent to which human activity associated with floodplain grazing has influenced these erosional and depositional processes remains unclear. Estimates of bank erosion from historical photos (Lauer et al., 2017) or ground-based monitoring could provide a complementary constraint on the sediment budget to justify the fingerprinting results.

Efforts could be invested to develop method of sediment load estimation based on sediment rating curve approach for this low-gradient, supply-limited landscape. The non-linearity of sediment rating curves undermines the rationality of using one single sediment rating curve to estimate annual sediment load. Using one single sediment rating curve to characterize the relationship between suspended sediment concentration and discharge seems to be

inappropriate in this low gradient watershed. The annual sediment load can be estimated for different ranges of discharge or based on magnitude-frequency analysis. Additionally, further analysis is needed to reveal the underlying physical basis for the observation that transition points of sediment rating curves are at the geometric mean of discharges at three sites.

Using statistical methods to explain the factors influencing the variances of suspended sediment concentration will be beneficial to revealing the complex relationships between storm patterns, discharge, and suspended sediment concentrations (Walling, 1974; Seeger et al., 2004; Lana-Renault et al., 2007; Gellis, 2013). Evaluating the descriptive statistics of main factors (e.g. peak discharge, total rainfall, maximum rainfall intensity and mean discharge) using a stepwise regression and a cluster analysis could explain the variability of suspended sediment concentration at the intra-events and seasonal scales.

Future work should examine hillslope sediment dynamics in greater detail. In this low-gradient landscape, the delivery of sediment from upland sources to the stream is not expected to be efficient given that eroded sediment can readily be deposited or temporarily stored on the hillslope. Physical models can be applied to evaluate the delivery of sediment from hillslope to stream. Agricultural activities not only have impact on the erosion rate but also influence deposition processes on hillslope. Accounting for soil detachment and sediment deposition processes on hillslope is of great value to accurately estimate sediment delivery ratio for the entire watershed.

5.3 References

Gellis, A. C. (2013). Factors influencing storm-generated suspended-sediment concentrations and loads in four basins of contrasting land use, humid-tropical Puerto Rico. *Catena*, *104*, 39–57. http://doi.org/10.1016/j.catena.2012.10.018

Lana-Renault, N., Regüés, D., Martí-Bono, C., Beguería, S., Latron, J., Nadal, E., … García-Ruiz, J. M. (2007). Temporal variability in the relationships between precipitation, discharge and suspended sediment concentration in a small Mediterranean mountain catchment. *Nordic Hydrology*, *38*(2), 139–150. http://doi.org/10.2166/nh.2007.003

Lauer, J. W., Echterling, C., Lenhart, C. F., Belmont, P., & Rausch, R. (2017). Air-photo based change in channel width in the Minnesota River basin: Modes of adjustment and implications for sediment budget. *Journal of the American Water Resources Association*, *297*, 170–184. http://doi.org/10.1016/j.geomorph.2017.09.005

Rhoads, B. L., Lewis, Q. W., & Andresen, W. (2016). Historical changes in channel network extent and channel planform in an intensively managed landscape: Natural versus human-induced effects. *Geomorphology*, *252*, 17–31. http://doi.org/10.1016/j.geomorph.2015.04.021

Seeger, M., Errea, M. P., Beguería, S., Arnáez, J., Martí, C., & García-Ruiz, J. M. (2004). Catchment soil moisture and rainfall characteristics as determinant factors for discharge/suspended sediment hysteretic loops in a small headwater catchment in the Spanish pyrenees. *Journal of Hydrology*, *288*(3–4), 299–311. http://doi.org/10.1016/j.jhydrol.2003.10.012

Walling, D. E. (1974). Suspended sediment production and building activity in a small British basin. *Effects of Man on the Interface of the Hydrological Cycle with the Physical*

Environment, (113), 137.

Walling, D. E., & Webb, B. W. (1982). Sediment availability and the prediction of storm-period sediment yields. *Recent Developments in the Explanation and Prediction of Erosion and Sediment Yield (Proceedings of the Exeter Symposium)*, *137*(137), 327–337.